NASA CR-72716
R-8272

LOW-SPEED INDUCERS FOR A ROCKET ENGINE FEED SYSTEM

by

J. A. King

ROCKETDYNE
A DIVISION OF NORTH AMERICAN ROCKWELL CORPORATION

prepared for

NATIONAL AERONAUTICS AND SPACE ADMINISTRATION

NASA Lewis Research Center
Contract NAS3-10280
W. A. Rostafinski, Project Manager

Requests for copies of this report should be referred to

National Aeronautics and Space Administration
Scientific and Technical Information Facility
P.O. Box 33
College Park, Md. 20740

Attention: SAF/DL, ACQ Division

NASA CR-72716
R-8272

FINAL REPORT

LOW-SPEED INDUCERS FOR A ROCKET ENGINE FEED SYSTEM

Contract NAS3-10280

June 1970

Prepared for

National Aeronautics and Space Administration
NASA Lewis Research Center
Large Engine Technology Branch
Cleveland, Ohio

Prepared by

Rocketdyne
A Division of North American Rockwell Corporation
Canoga Park, California 91304

J. A. King
Principal Engineer
Advanced Turbomachinery

E. B. Monteath
Program Manager
Advanced Technology Programs

FOREWORD

The research described herein was done at Rocketdyne, a division of North American Rockwell Corporation, under NASA Contract NAS3-10280 with Mr. W. A. Rostafinski, Large Engine Technology Branch, NASA-Lewis Research Center, as Project Manager.

Acknowledgement is made to Mr. W. J. Mabe, Jr. for the hydrodynamic design of the low-speed inducers and to Mr. E. C. Farrell and Mr. D. R. Person for the oscillation studies.

ABSTRACT

The use of low-speed inducers in a rocket engine feed system was analytically investigated as a follow-on effort to Contract NAS3-10280, dynamics of a partial-flow, hydraulic-turbine-driven, low-speed inducer program. Analytical performance data for optimum low-speed inducers were developed, and analog and digital system simulation were used to evaluate the potential of using a low-speed inducer to simplify propellant tank pressurization and avoid resonant interaction of oscillations in the feed system and vehicle structure. Transient study results defined low-speed fuel inducer requirements for starting with zero suction pressure. Results of a study of LOX feed system oscillations indicated a low-speed inducer can significantly alter feed system-engine structure frequency response characteristics.

CONTENTS

ILLUSTRATIONS

TABLES

SUMMARY

The object of this contract was to investigate analytically the use of low-speed inducers in a rocket engine feed system to simplify propellant tank pressurization and to avoid resonant interaction of oscillations in the feed system and vehicle structure. Preliminary designs of low-speed inducers for the J-2S LOX and fuel feed systems were made. Performance curves developed for each inducer and turbine were used in conjunction with analog and digital system simulation to demonstrate the advantages of using low-speed inducers in rocket engine feed systems.

Task I - Hydrodynamic Design of Optimum Low-Speed Inducers

A study of optimum design parameters of the low-speed inducer indicated that for minimum overall horsepower requirements the inducer should be designed for maximum head and head coefficient. The turbine should require minimum weight flow and have a maximum number of stages. The design of the low-speed inducers for application to the J-2S engine was based on these optimum requirements and compromised with limitations of hardware fabrication, suction performance of the main pump, and overall efficiency.

Task II - Analysis of Low NPSP Unpressurized Hydrogen Feed System

Start transient and steady-state studies were made on a low-speed fuel inducer in the J-2S fuel feed system and the following conclusions were drawn from the results.

1. An engine with a low-speed inducer for LH_2 will start with a tank pressure set to give minimum inducer net positive suction pressure at steady state. The addition of the low-speed inducer results in a decrease of 2.5 psi in the minimum net positive suction pressure presently required.

2. During flight, where acceleration will increase the available net positive suction pressure, the engine with a low-speed LH_2 inducer will start from zero NPSP.

3. No special engine controls or major sequence changes are required.

4. Locating the inducer at the tank outlet takes maximum advantage of the pressure increase due to acceleration acting on the propellant height. About 70% of the available height is retained above the inducer while the line pressure drop is moved from the inducer inlet to the outlet.

Task III - Analysis of POGO Oscillation

An analysis was performed to determine if a low-speed inducer located in the J-2S LOX feed line could alter engine feed system frequency response characteristics. From the results, which express gain and phase of engine thrust relative to an input representing the vehicle structural acceleration, the following conclusions were drawn.

1. The gain and phase of engine thrust to structural acceleration can be significantly altered using a low-speed inducer located in the LOX feed line upstream of the main pump.

2. The low-speed inducer fluid inertance and the main pump inlet compliance cause a system resonance. If the frequency associated with this resonance is low, a beneficial gain reduction above this frequency is achieved. Therefore the inducer fluid inertance and the main pump inlet compliance are key parameters.

3. The resonance resulting in the maximum gain is caused by the low-speed inducer inlet line. Therefore, the low-speed inducer inlet compliance is a key parameter.

4. The maximum gain reduction occurs when the low-speed inducer inlet line frequency is low relative to possible structural frequencies.

5. Experimental work is desirable to verify or correct study findings with regards to:

   a. Determination of inducer inlet compliance obtainable with lower inlet pressure.

   b. Verification of resonant frequencies associated with combination of various compliances and inertances.

NOMENCLATURE

D = DIAMETER, IN.

H = HEAD RISE, FT

Q = FLOW, GPM

N = ROTATIONAL SPEED, RPM

NPSH = NET POSITIVE SUCTION HEAD, FT

ID = INSIDE DIAMETER, IN.

HP = HORSEPOWER

N_s = SPECIFIC SPEED, $N(Q)^{1/2}/(\Delta H)^{3/4}$

N_{ss} = SUCTION SPECIFIC SPEED, $N(Q)^{1/2}/(NPSH)^{3/4}$

ϕ = FLOW COEFFICIENT, $\left[4\ Q\ 229\ /448\ \pi\ D^3 N/(1-\xi^2)\right] 144$

ψ = HEAD COEFFICIENT, $32.2\ \Delta H\ 229^2\ /N^2 D^2$

P = PRESSURE RISE, PSI

$\dot{W}$ = WEIGHT FLOW, LB/SEC

η = EFFICIENCY

ρ = DENSITY, LB/FT^3

T = TORQUE, IN-LB

ξ = INDUCER DIAMETER HUB TO TIP RATIO

INTRODUCTION

Two major objectives in rocket engine feed system design are to minimize weight and provide sufficient net positive suction head to the turbopumps. Both objectives may be met by use of a low-speed hydraulic turbine driven inducer in the engine propellant feed system. The inducer is designed to operate at low tank pressures and to generate sufficient head to prevent cavitation of the main pump. The turbine which drives the inducer obtains its working fluid from the high pressure discharge of the main pump or inducer.

Recent technology advancements (Ref. 4) have demonstrated that a low-speed inducer can be designed that will provide the main pump with the required suction head at all times. It also has been established that a low-speed inducer has excellent starting and dynamic characteristics which can be accurately predicted by computer simulation. However, since the low-speed inducer absorbs power from the main turbopump, it is important to design an efficient and practical inducer-turbine combination which requires minimum horsepower from the hot gas turbine of the main turbopump.

The purpose of this study is to determine the parameters that affect the design of an optimum low-speed inducer for an engine feed system, and to design low-speed inducers for a typical LOX LH_2 feed system. Using performance curves developed for inducer designs, analog and digital computer system simulation were used to determine the inducers' steady state and transient performance. Of particular interest is the potential simplification of propellant tank pressurization and the elimination of feed system oscillations which lead to "POGO" type vehicle structural problems.

Engine start studies were performed using an analog computer model of the J-2S engine and a model of a low-speed inducer driven by a hydraulic turbine. The complete model has modifications to include fuel pump cavitation and propellant inlet line characteristics corresponding to those on the SIVB stage of the Saturn V vehicle. This model was used to study the start and steady state performance of the engine with and without the low-speed fuel inducer.

Low frequency longitudinal oscillations (POGO) have occurred on most rocket engine powered vehicle flights. These oscillations are caused by an instability in a closed loop system consisting of vehicle structure, propellant pump feed systems, and the engine. To eliminate these oscillations, the loop gain and/or phase shift must be changed in the critical oscillatory frequency ranges. Saturn flight data and analog model simulation indicate that the oscillations occur at a structural resonant frequency caused by a coupling of the engine and structure through the LOX pump feed line. Corrective devices have been used to change the natural frequency of the inlet line compliance. Addition of a low-speed inducer in the inlet line can also change these dynamic characteristics. The POGO study made was concerned with determining the feasibility of using a low-speed inducer to correct or control longitudinal oscillations and defining the significant variables associated with such a feed system.

HYDRODYNAMIC DESIGN OF LOW-SPEED INDUCERS

OPERATING REQUIREMENTS

The operating requirements for the LOX and LH_2 low-speed inducers were assumed to be the same as those experienced during a typical Apollo vehicle flight. Actual flight data from Apollo 8, 9, and 10 were analyzed for this purpose. (These data were obtained from Rocketdyne Flight Telemetry Data Files and published NASA Flight Evaluation Reports.) Based on this data analysis, parameters, such as speed, flow, inlet pressure, and tank ullage pressure for the LOX and LH_2 turbopumps from the S-II and S-IVB stages were established.

Without conventional tank pressurization being used on these stages, the net positive suction head (NPSH) then would be the difference between the total inlet head at the turbopump and the pressure above the fluid in the tank. This NPSH is plotted as a function of flight time in Figure 1. The data were presented in the form of data envelopes due to considerable scatter in the telemetry data. The following table presents available NPSH without tank pressurization and main pump required NPSH for the Saturn S-II and S-IVB stages:

Stage	Turbopump	Available NPSH-Ft	Minimum Main Pump Required NPSH
S-II	Fuel	26 - 65*	90
	LOX	6 - 15	35
S-IVB	Fuel	6 - 27*	90
	LOX	5 - 9	35

* Does not include thermodynamic suppression effects.

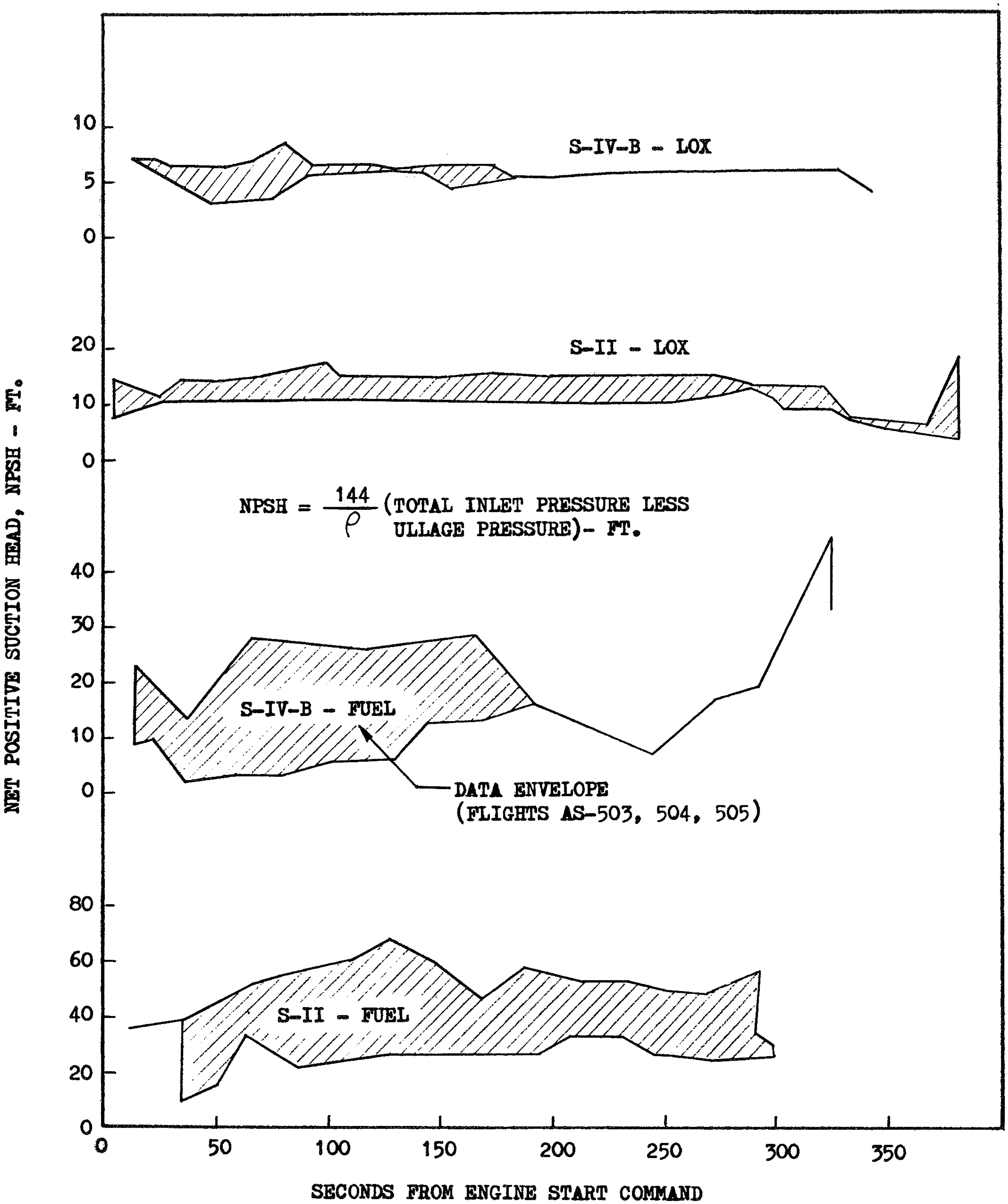

FIGURE 1. FLIGHT AVAILABLE NET POSITIVE SUCTION HEAD

The nominal operating requirements for low-speed inducers and main turbopumps for a J-2S 265,000 lb thrust engine were determined from the data to be:

	LH_2	LOX
Flowrate, gpm	9691	3291
Overall head rise, ft	58,009	3031
Minimum available NPSH, ft	23	6

OPTIMUM LOW-SPEED INDUCER DESIGN STUDY

The Apollo flight data provided the required flowrate, overall head rise, and minimum available NPSH for the low-speed inducer and turbopump combination. The low-speed inducer should be designed to operate with a very low NPSH and to generate sufficient head to prevent cavitation of the main pump at all times. The low-speed inducer absorbs power from the turbopump and it is important to design an efficient and compact inducer-turbine combination which requires minimum horsepower from the hot gas turbine.

Analysis of the system indicated that four primary interdependent variables will determine the low-speed inducer configuration. These are inducer head (ΔH), speed (n) and turbine weight flow ($\dot{w}$), and main turbopump speed (N). The manner in which the optimum low-speed inducer operating point was established for a given design requirement is described below.

By assuming a turbine weight flow and the low-speed inducer head, the main pump operating point for the required overall head rise and flow may be determined by trial and error. The inducer head coefficient is determined such that the power required by the inducer equals the power output of the turbine for the assumed weight flow. Calculations are repeated for several turbine weight flows and low-speed inducer heads, and parametric curves are generated from which the optimum design point is obtained. Figures 2 and 3 show the parametric design curves for a low-speed inducer operating with the J-2S turbopump.

The following design information must be used to generate the above parametric curves: The main pump performance characteristics, low-speed inducer and turbine tip diameters, and turbine efficiency and general design type. The low-speed inducer diameter is determined from duct size limitations and available suction pressure. Due to the particular design configuration, the turbine diameter is limited by the inducer size.

The following assumptions were also made in the optimum inducer design study:

1. Inducer tip diameter is constant.
2. Inducer efficiency is approximated by the square root of the product of π and the inducer head coefficient, for the range of 0.08 to 0.20 head coefficient.
3. The fluid is incompressible.
4. Turbine efficiency includes all bearing and seal losses, disc friction, etc.
5. All the high pressure available to the turbine (either from the main pump discharge or the main inducer discharge) is used in the turbine to generate power to drive the low-speed inducer (i.e., no throttling losses in the return line).

A study of the parametric curves in Figures 2 and 3 indicate that minimum overall horsepower is obtained for a low-speed inducer designed for maximum head and head coefficient, maximum number of turbine stages and blade height, and minimum turbine weight flow.

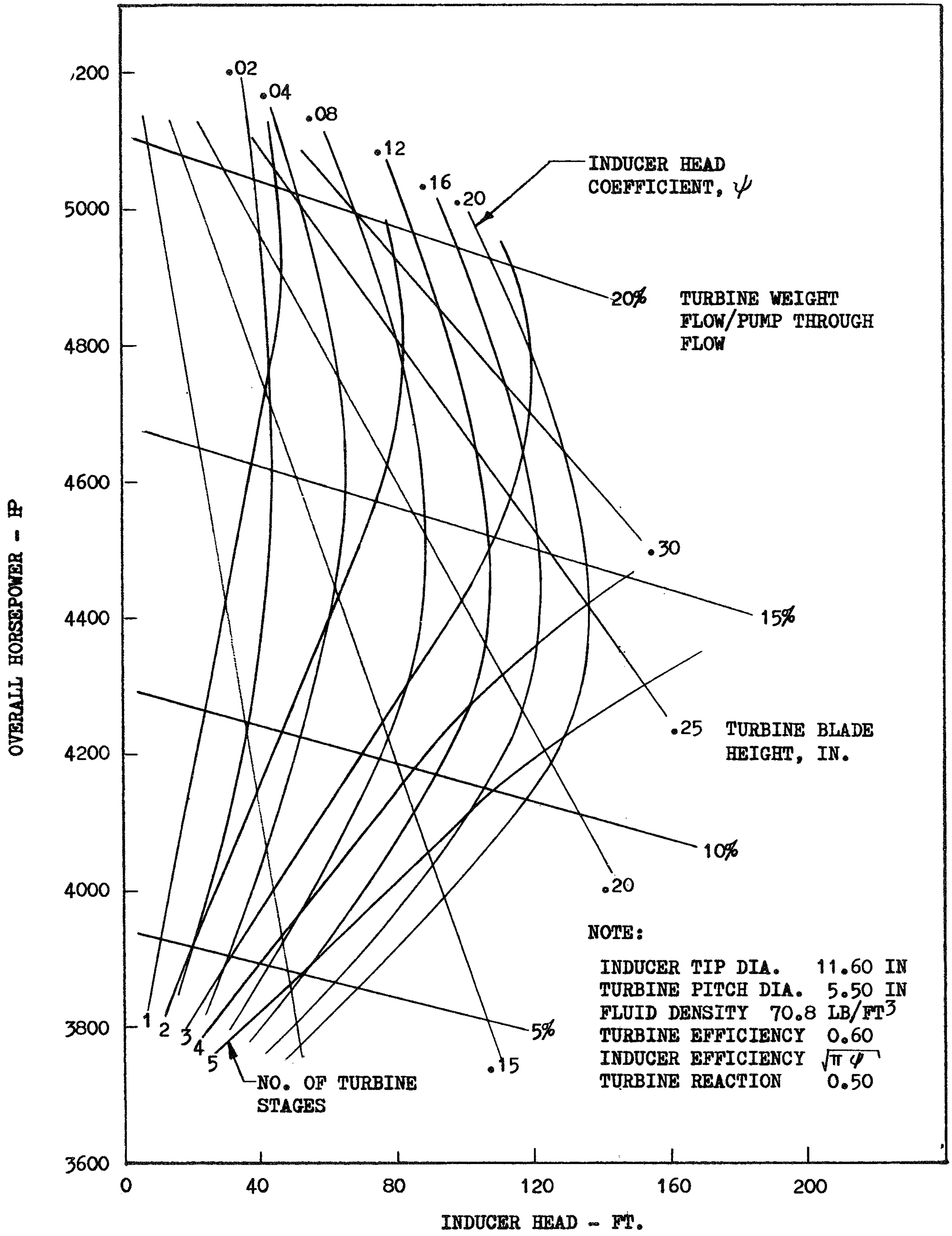

FIGURE 2. J-2S LOX LOW-SPEED INDUCER PARAMETRIC DESIGN CURVES

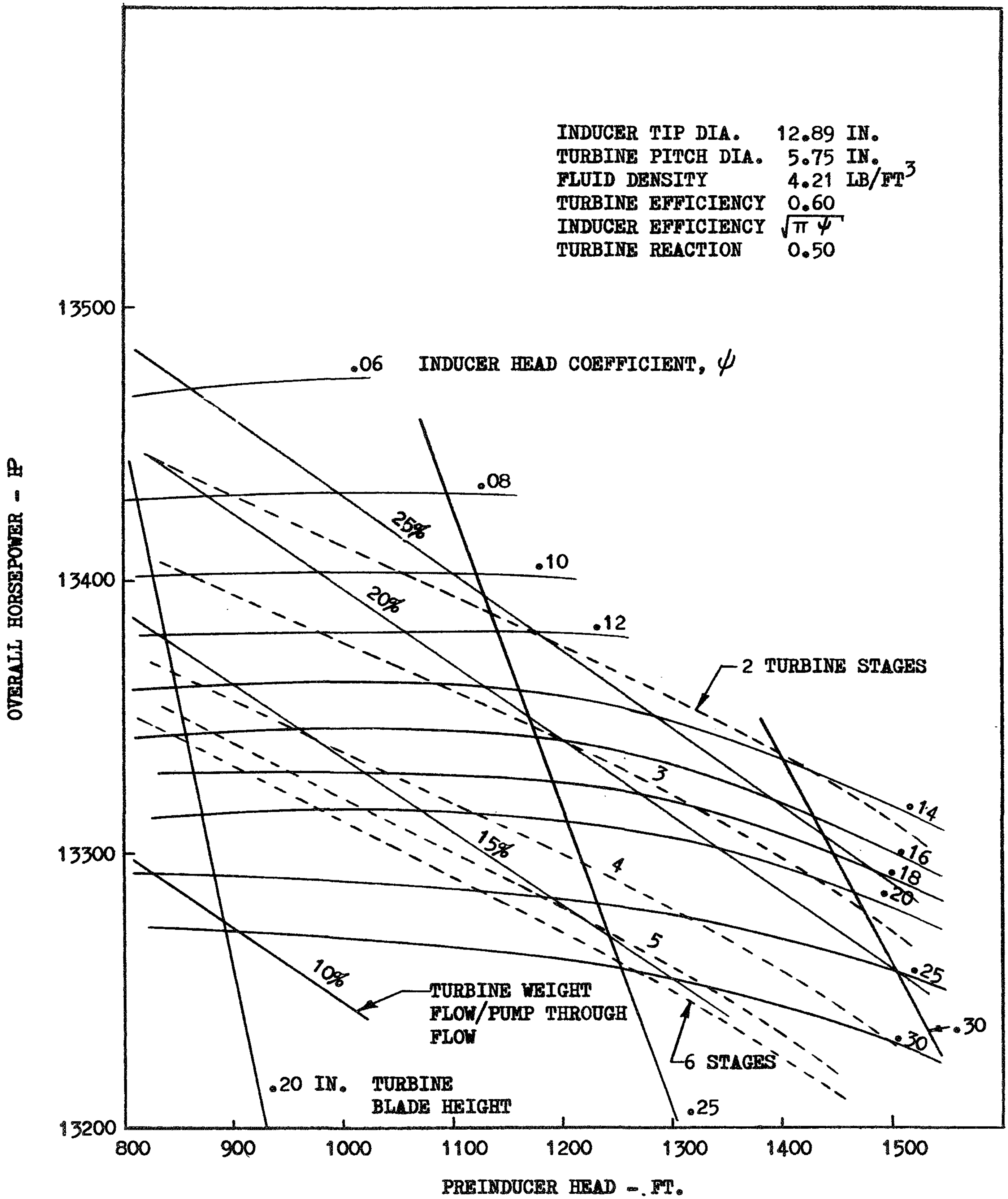

FIGURE 3. J-2S FUEL LOW SPEED INDUCER PARAMETRIC DESIGN CURVES

In the final design of the low-speed inducers, the optimum parameters must be modified to meet structural limitations, manufacturing capabilities, NPSH availability, main pump suction requirements, and the inevitability of throttling losses in the return line.

Figures 2 and 3 are for a particular low-speed inducer size and a fifty percent reaction turbine. A pure impulse stage absorbs twice the horsepower of a fifty percent reaction stage and would, therefore, require half the number of stages as shown in the figures (assuming comparable efficiencies).

THERMODYNAMIC CONSIDERATIONS

To investigate the thermodynamic properties of the cryogenic fluid, and insure that the fluid at all points was indeed a liquid, the energy balance and continuity equations for the low-speed inducer and main pump combination were used to calculate the fluid enthalpies. The various state points are plotted on an enthalpy-entropy diagram for oxygen and hydrogen shown in Figures 4 and 5. The critical state point for the fluid was found to be at the turbine discharge since it is nearest the saturation line. Assuming a reasonable operating point for the low-speed inducers, indications are that in LOX there are no limitations. This is due to the fact there are no high throttling losses in the turbine weight flow return line. A low-speed inducer operating with the main fuel pump, however, is limited by the amount of throttling that can be done in the return line before the liquid begins to boil. This limitation, in turn, determines the minimum pressure required at the turbine discharge. For 20 percent return flow this minimum pressure was 59 psi. As a result, the inducer head rise can be no less than 950 ft. or the possibility of the turbine discharge fluid flashing at the turbine exit exists.

HYDRODYNAMIC DESIGN

Based on the operating requirements obtained from flight data and information obtained from the optimization and thermodynamic analyses, preliminary designs of a LOX and fuel low-speed inducer were made.

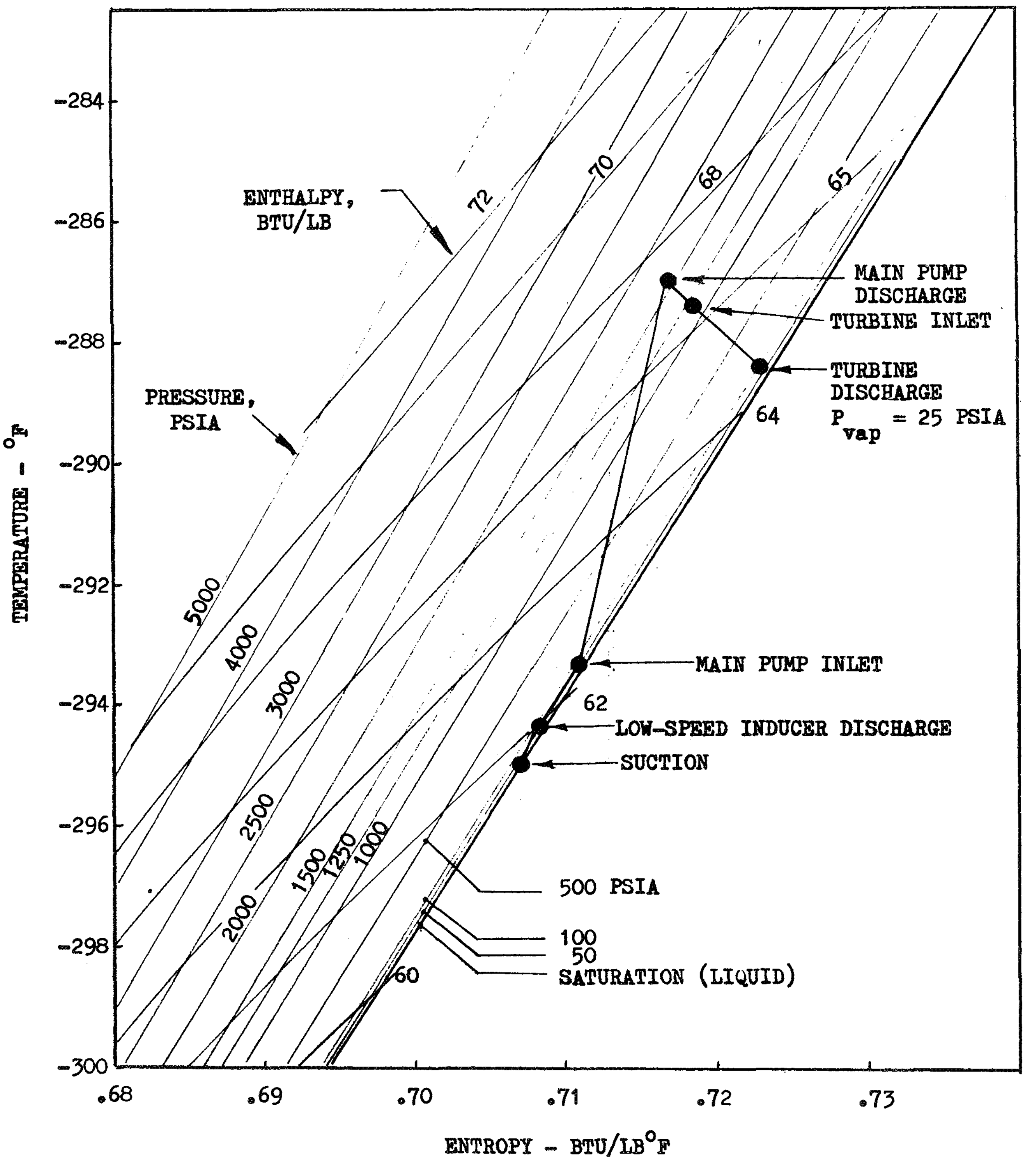

FIGURE 4. TEMPERATURE-ENTROPY DIAGRAM FOR OXYGEN

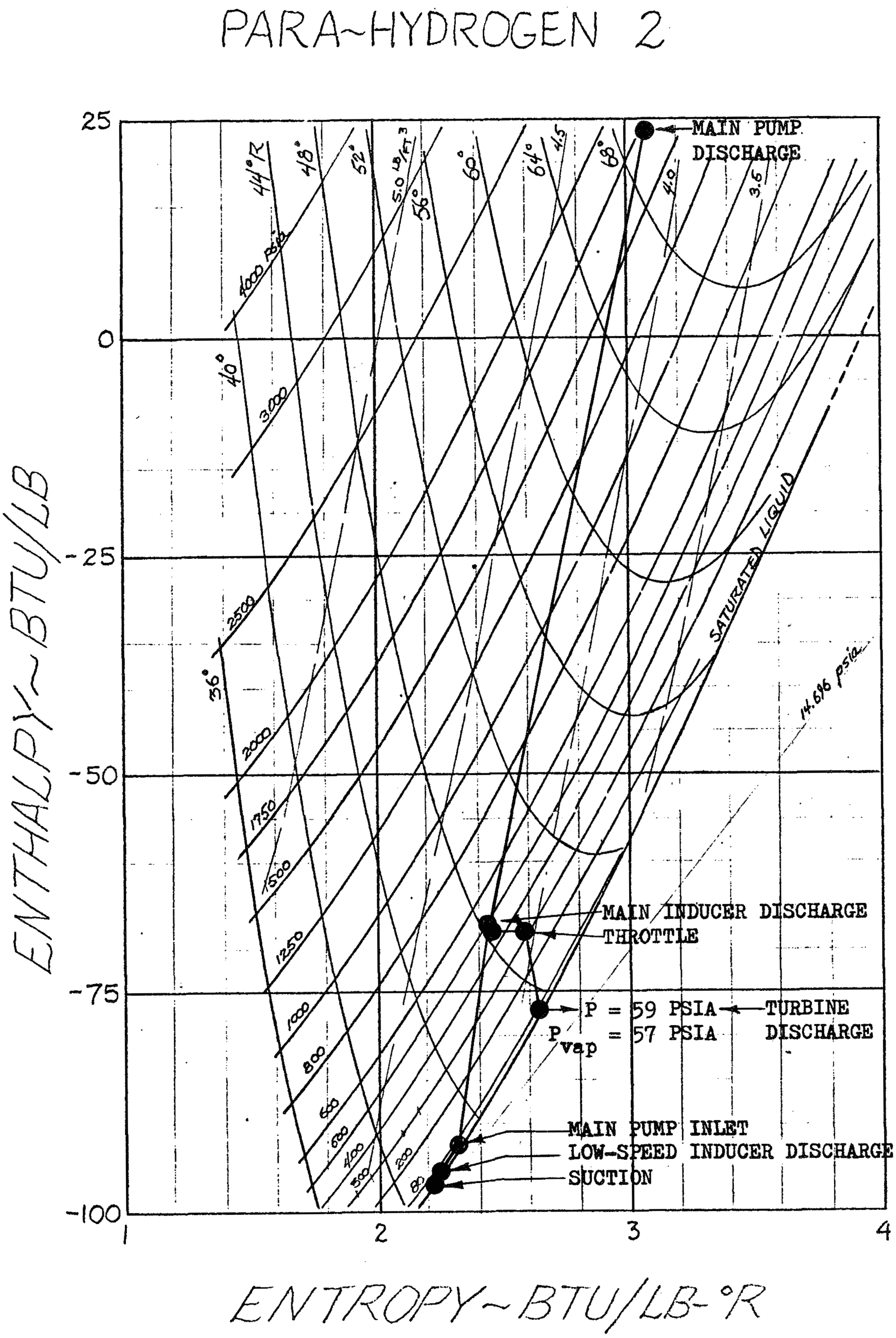

FIGURE 5. ENTHALPY-ENTROPY DIAGRAM FOR HYDROGEN

LOW-SPEED INDUCER FOR LH_2

The low-speed inducer for LH_2 was designed to be compatible with the characteristics of the J-2S fuel turbopump operating at a 265,000 lb. engine thrust level. This requires a through flow of 9691 gpm with an available NPSH of 23 feet. Due to the low NPSH level, the inlet duct size was chosen such that the velocity would be less than the $\sqrt{2gNPSH}$. Conservatively, this velocity would be 24 FPS which sets the inlet duct diameter at 12.814 inch. This pipe diameter will match the required inducer inlet dimensions.

For a high head rise and high head coefficient optimum inducer (a high head is also required to prevent any flashing at the inducer discharge), the inducer head was set at 984 ft. and the speed at 7100 rpm which resulted in the following design operating point for the low-speed inducer:

$Q = 9691$ gpm	$HP = 217$
$H = 984$ ft	$\phi = .07$
$N = 7100$ rpm	$\psi_t = .199$
$N_s = 3960$	$N_{ss} = 67{,}000$

The inducer design has a tapered hub and tapered tip with the following dimensions:

	Hub Diameter	Tip Diameter
Inlet	3.54	12.89
Discharge	8.23	11.80

The inducer was designed for free vortex flow at the discharge. Figures 6 and 7 are the estimated H-Q and suction performance curves for this inducer.

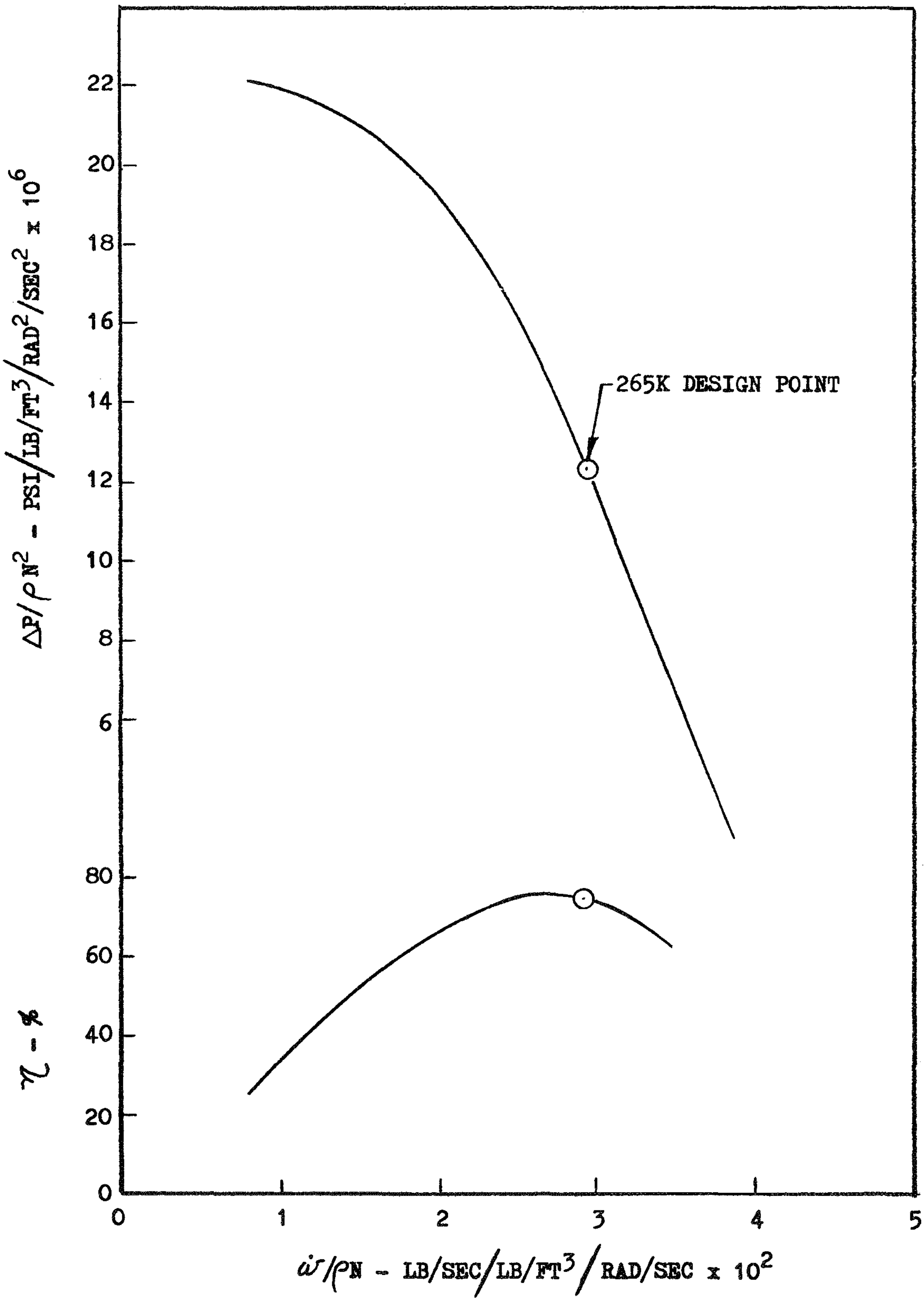

FIGURE 6. J-2S FUEL LOW-SPEED INDUCER ESTIMATED PERFORMANCE

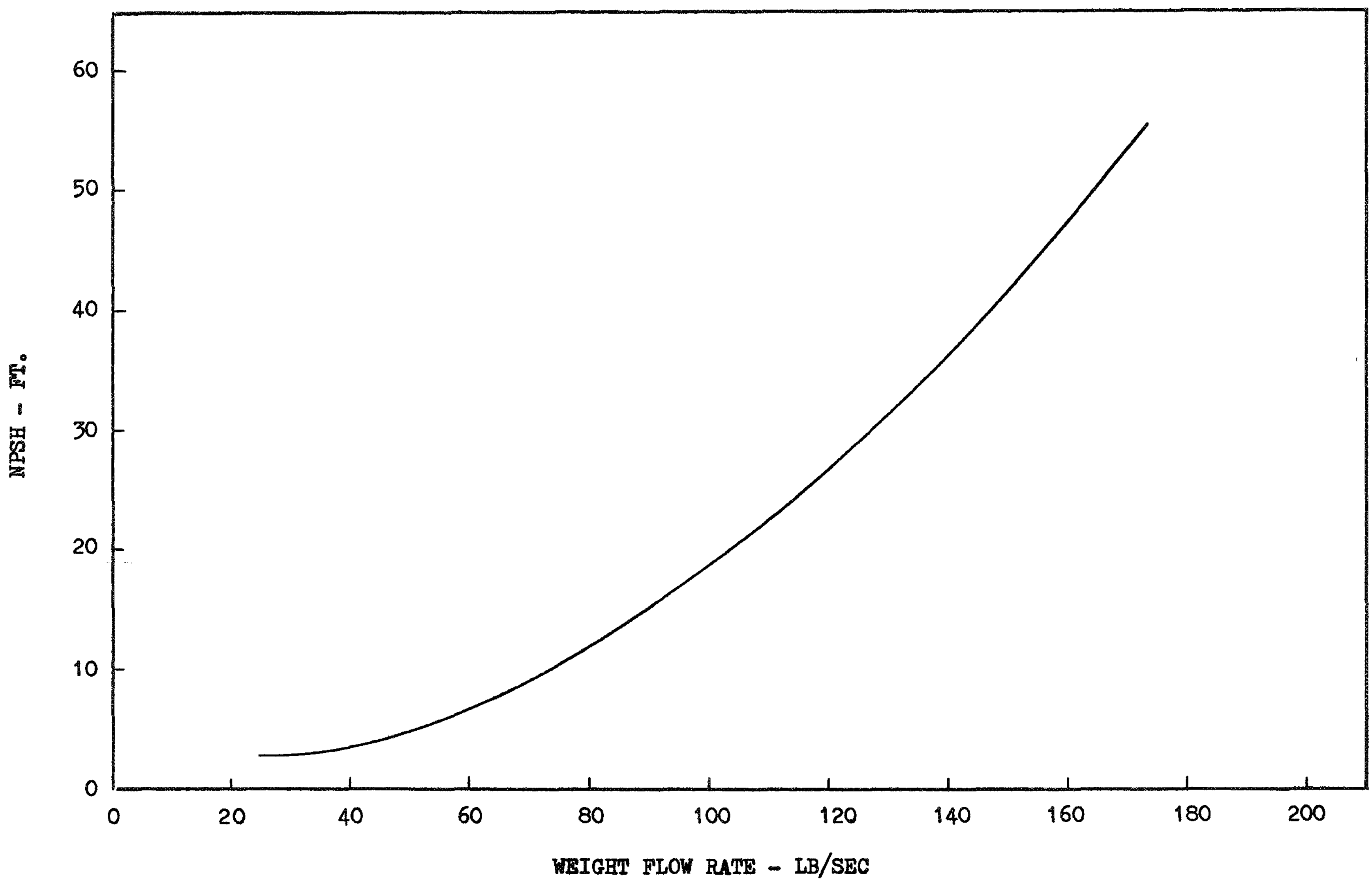

FIGURE 7. J-2S FUEL LOW-SPEED INDUCER ESTIMATED SUCTION PERFORMANCE

The inducer discharges to a set of 13 vanes which turn the flow 48° to axial, serve as structural support, and allow passage of the turbine weight flow through five 13/32 in. O.D. holes in each vane.

The turbine which drives the inducer has a diameter of 5.75 in. and four stages. The turbine obtains its working fluid from the main inducer discharge at an available head of 15,000 ft. Since the turbine requires a pressure of 262 psi for a weight flow of 16 lb/sec (17.6% main inducer through flow), the high pressure return flow must be throttled to about 10,000 ft. Figure 8 is an estimated performance map of the turbine. The turbine velocity ratio was .50 with an 18° nozzle spouting angle. All four stages are identical and the nozzle exit velocity is 356 FPS, the rotor inlet velocity is 194 FPS, and the rotor discharge velocity is 209 FPS.

A layout of the fuel low-speed inducer is shown in Figure 9 and from this layout the weight and moment of inertia were determined:

Rotor weight, lb = 27.4

Total weight, lb = 122.0

Moment of inertia, lb-in-sec^2 = 0.699

Since a part of the J-2S fuel pump discharge flow is used to drive the low-speed inducer turbine, the operating point of the fuel pump must be increased to a higher head and flowrate to maintain the 265,000 lb. thrust capability. The new operating point is as follows:

Q = 9691 gpm delivered
17.6% recirculated through the low-speed inducer turbine and the main inducer

H = 58,009 ft delivered overall head

H = 57,016 ft across the main pump

N = 30,100 rpm

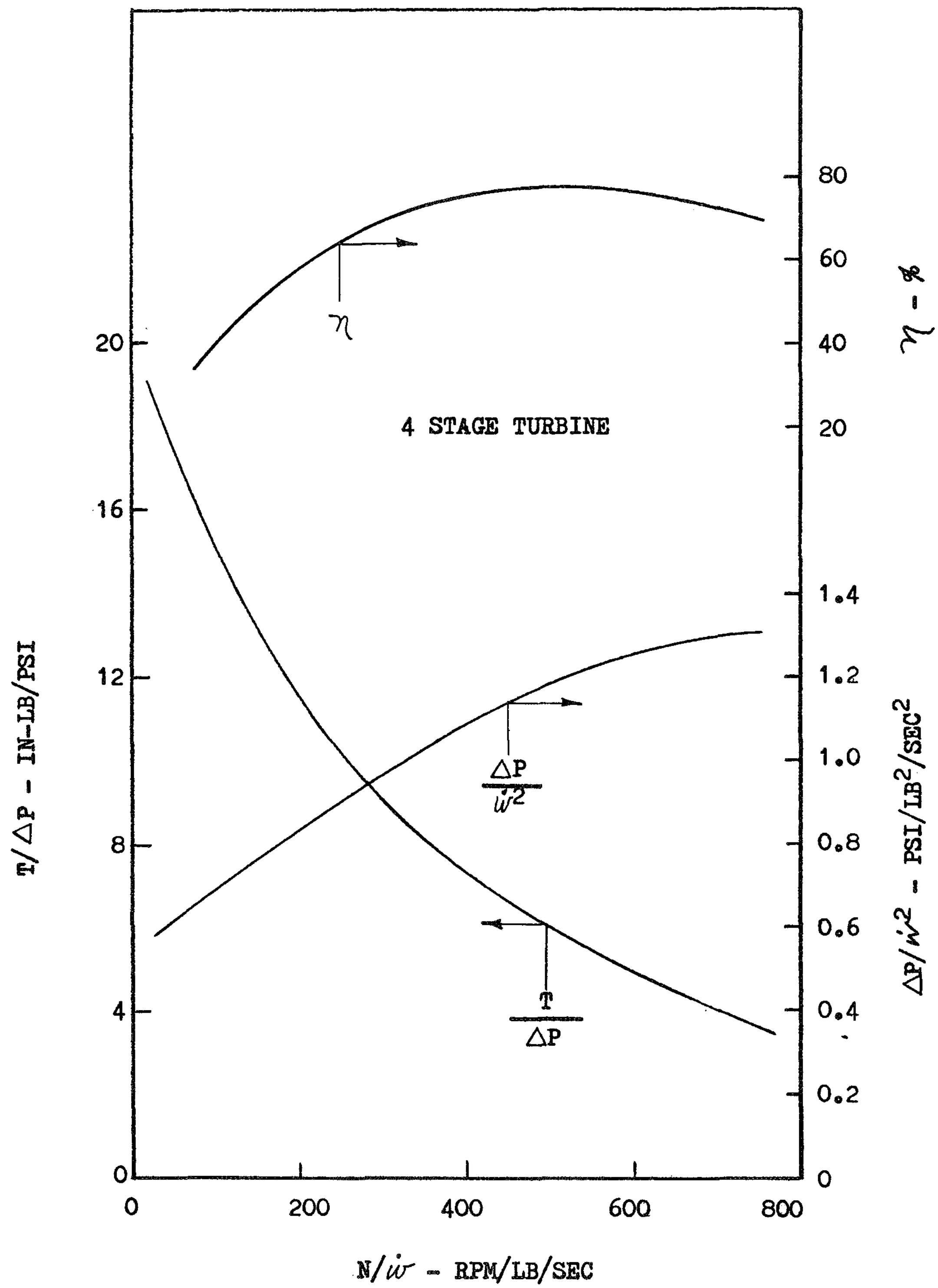

FIGURE 8. J-2S FUEL LOW-SPEED INDUCER TURBINE ESTIMATED PERFORMANCE

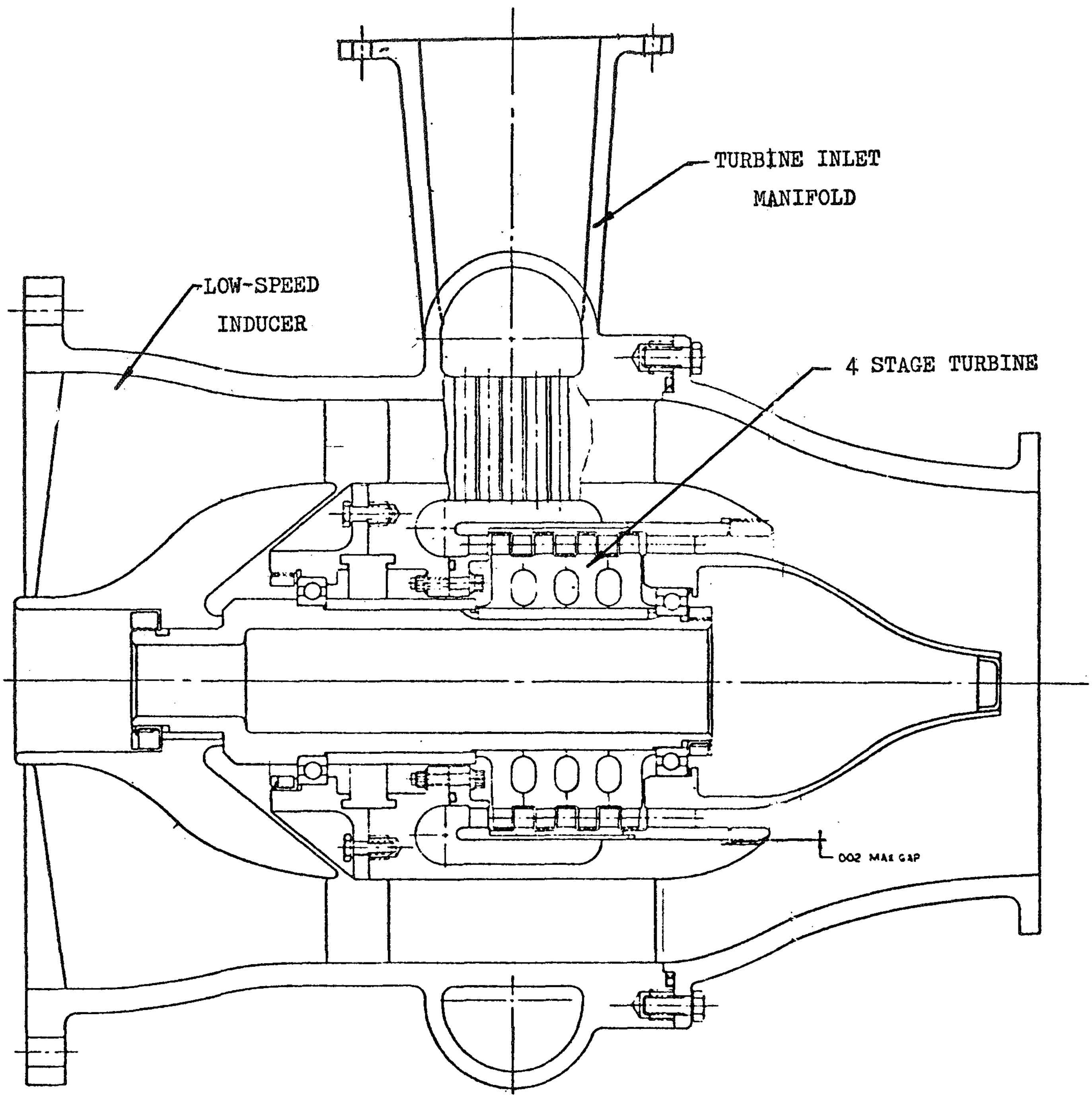

FIGURE 9. J-2S FUEL LOW-SPEED INDUCER

Figures 10 and 11 are actual performance maps of the J-2S fuel pump. The pressure at the turbine discharge is sufficient to preclude any vaporization as it exits at 2 psi above vapor pressure of the main stream.

LOW-SPEED INDUCER FOR LOX

The low-speed inducer for LOX was designed to be compatible with the characteristics of the J-2S LOX turbopump operating at the 265,000 lb. engine thrust level. This requires a through flow of 3291 gpm with an available NPSH of six feet. Due to the low NPSH level the inlet duct size was chosen such that the velocity would be much less than $\sqrt{2gNPSH}$. Thus, a velocity of 12.7 FPS was considered reasonable and was set at 11.75 in. diameter. This pipe diameter will match the required inducer inlet dimensions.

The J-2S inducer was scaled to a larger size to meet suction requirements. The scale factor used was 1.49 which gives an inlet tip diameter of 11.60 in. and a hub diameter of 4.30 in. The operating point for this inducer is as follows:

$Q = 3291$ gpm	$HP = 216$
$H = 175$ ft	$\phi = .07$
$N = 3400$ rpm	$\psi_t = 0.19$
$N_s = 4060$	$N_{ss} = 51{,}000$

The inducer was designed for a free vortex flow at the discharge. Figures 12 and 13 are estimated performance curves of the LOX low-speed inducer.

Two sets of turning vanes at the inducer discharge were used to turn the fluid to axial direction and to provide for structural support and passage of the turbine weight flow. The first row of 19 vanes

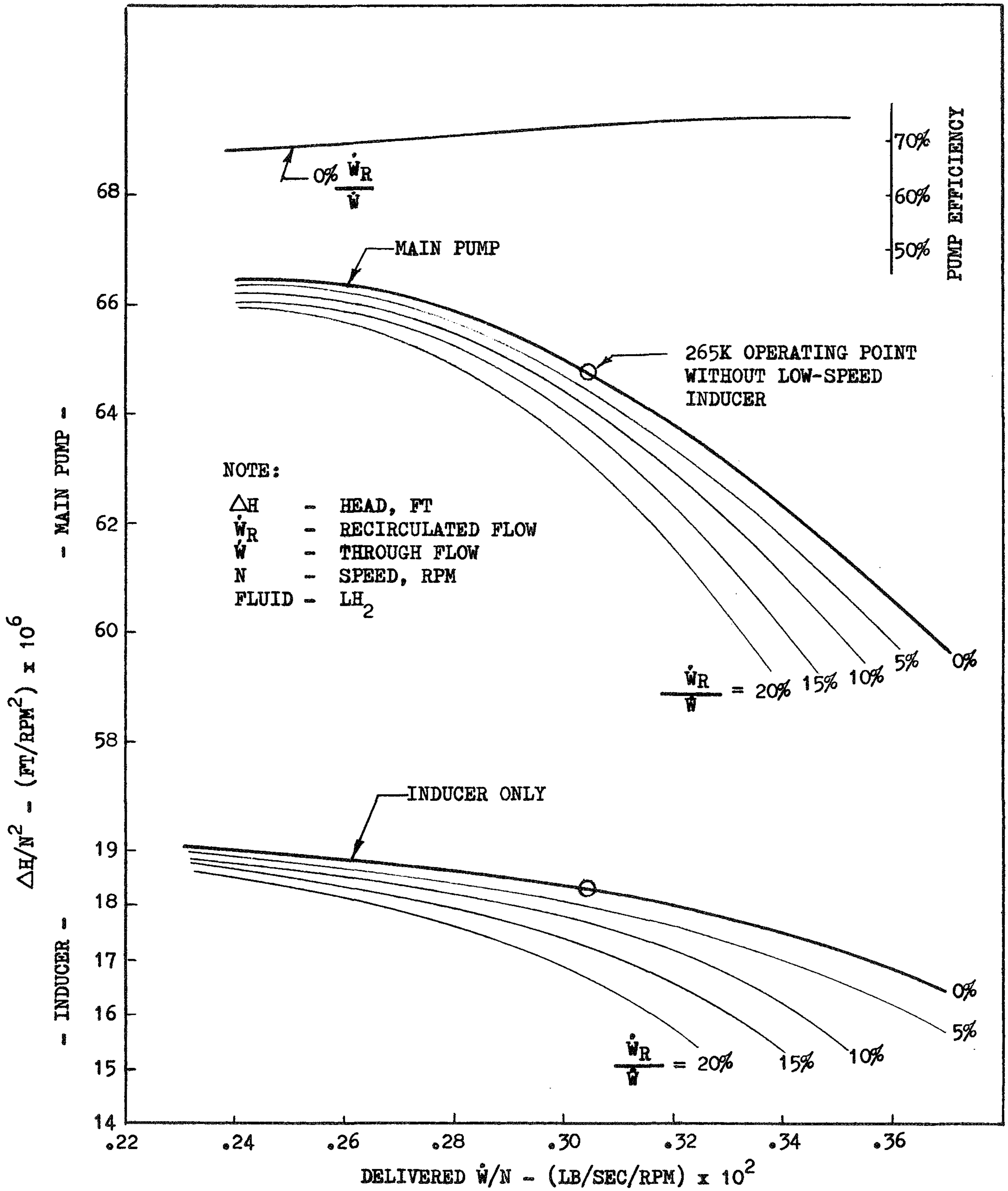

FIGURE 10. J-2S FUEL PUMP PERFORMANCE

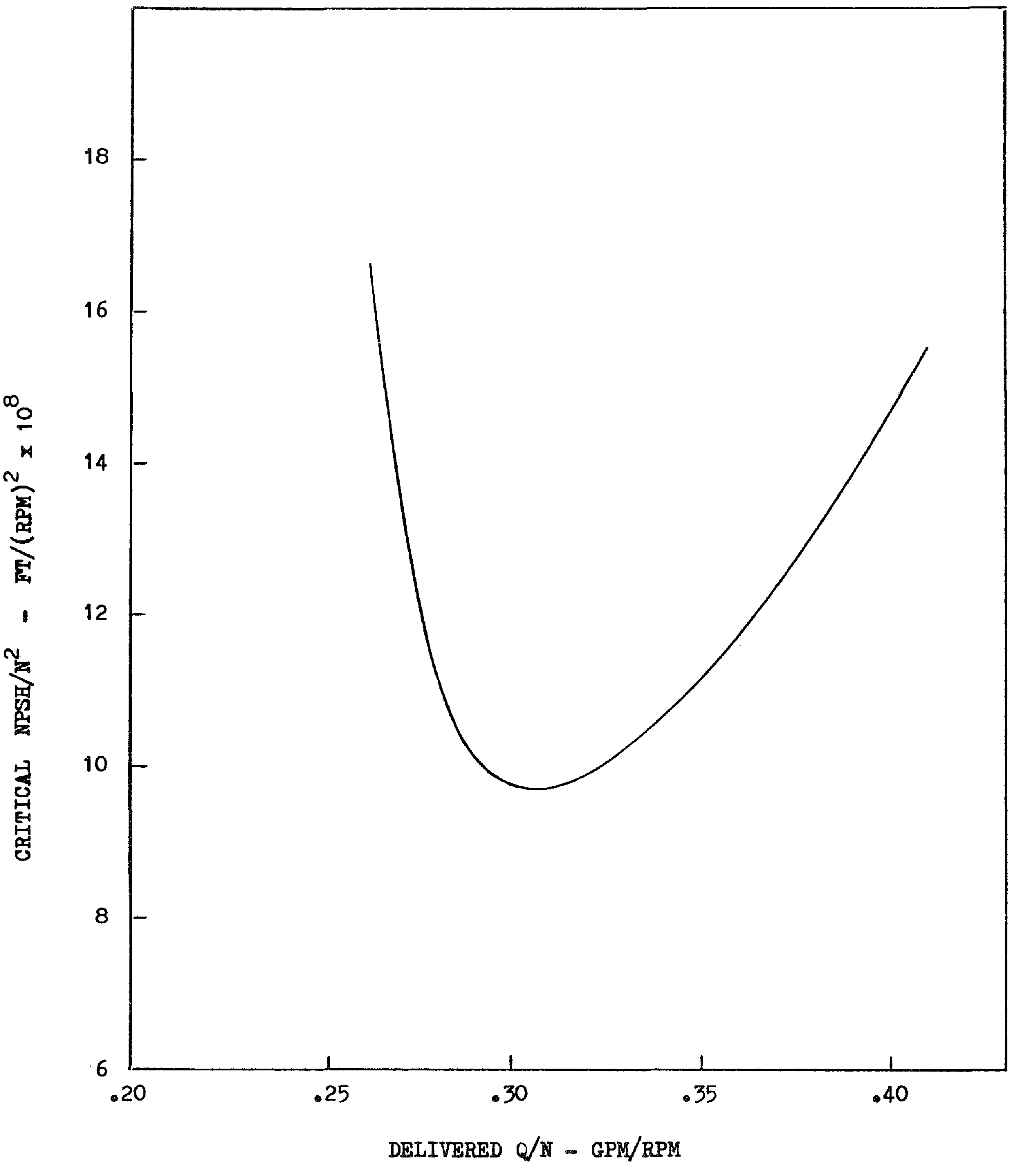

FIGURE 11. J-2S FUEL PUMP SUCTION PERFORMANCE

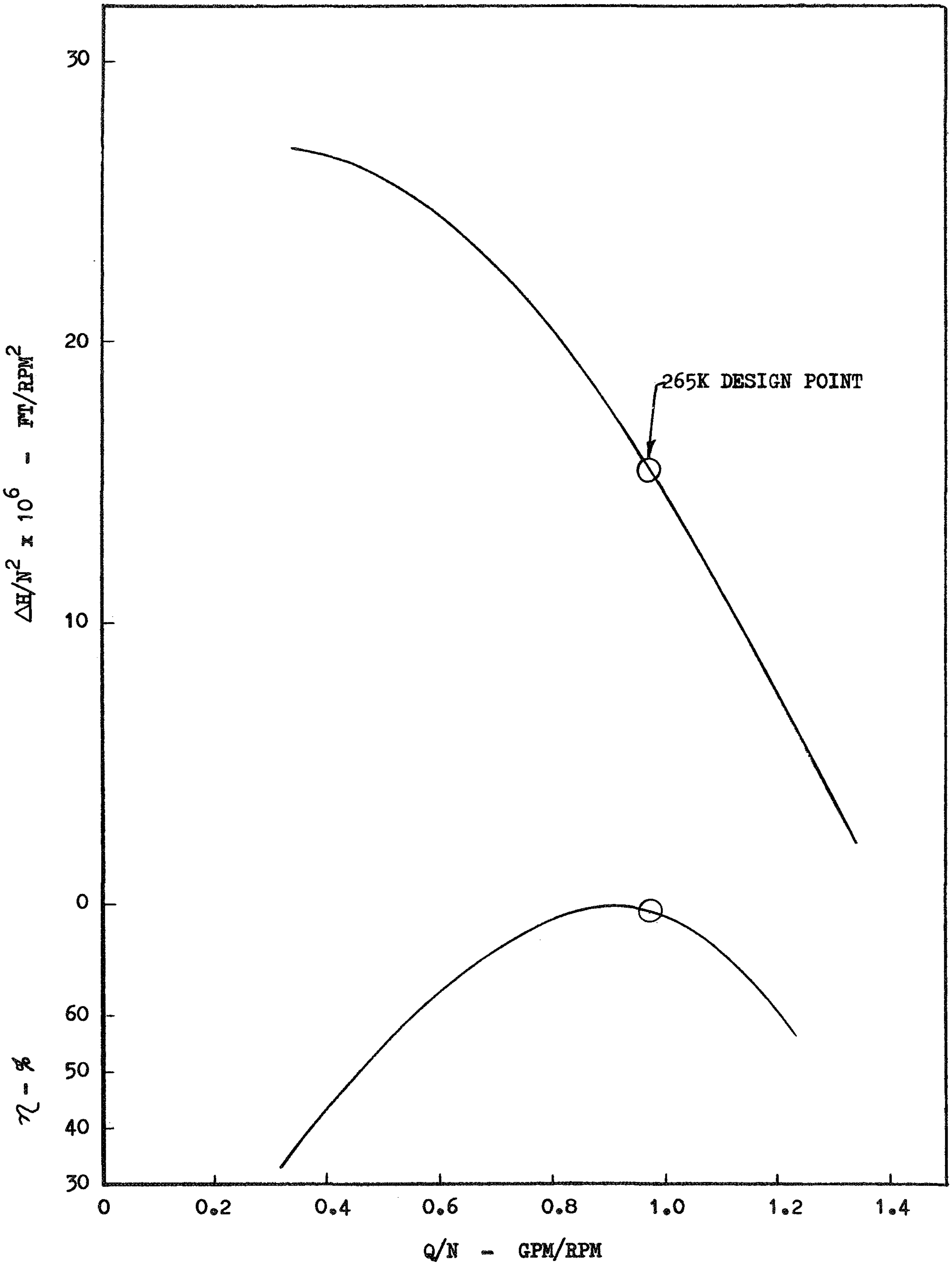

FIGURE 12. J-2S LOX LOW-SPEED INDUCER ESTIMATED PERFORMANCE

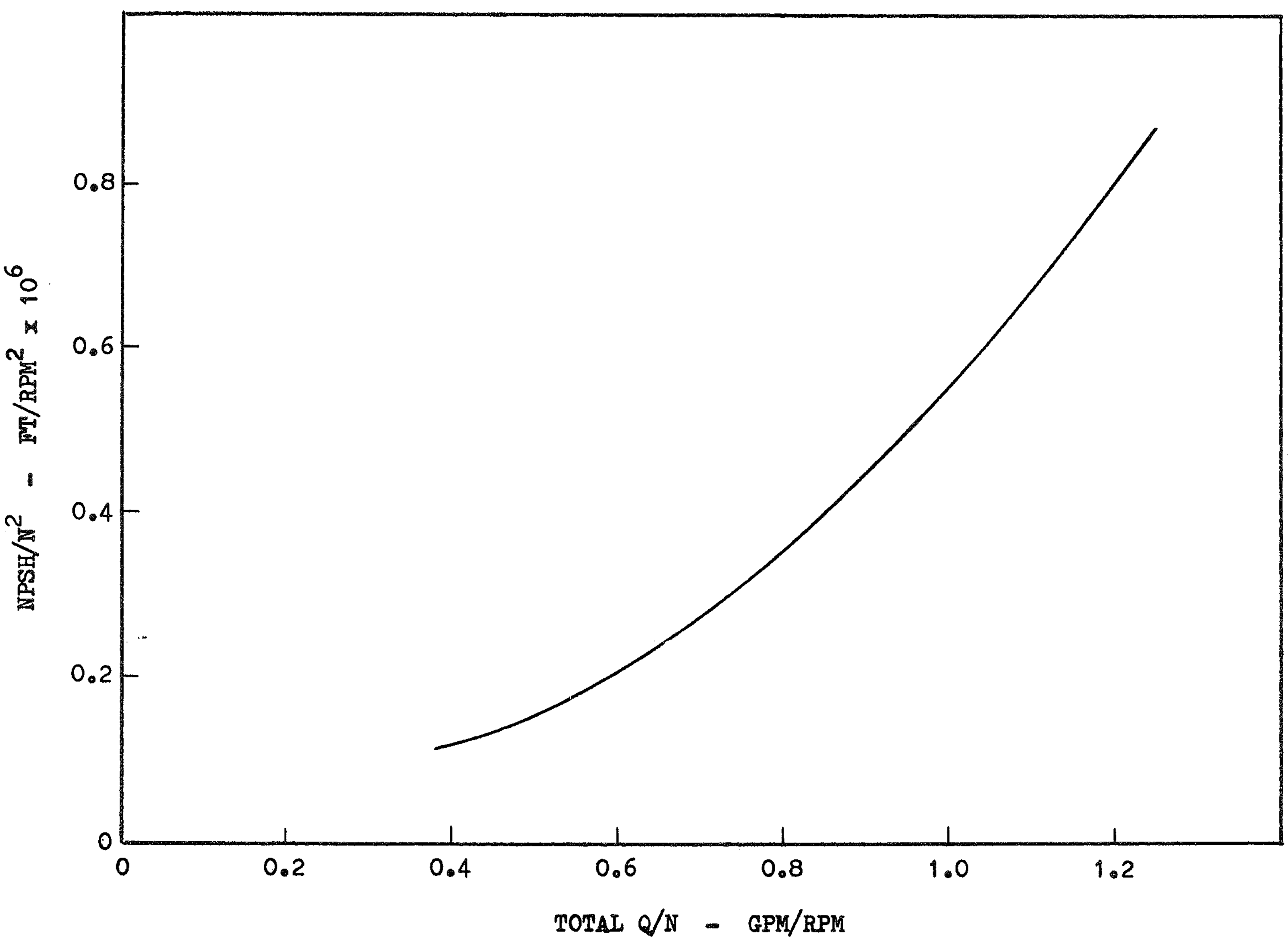

FIGURE 13. J-2S LOX LOW-SPEED INDUCER ESTIMATED SUCTION PERFORMANCE

takes the remaining whirl out of the flow and passes the turbine flow through three .302 in. diameter holes in each vane.

The turbine which drives the inducer was designed as a pure impulse, four stage turbine. The diameter was set at 5.50 in. The high pressure working fluid comes from the main pump discharge at an available head of 2500 ft. Allowing for return line losses the pressure drop across the turbine is 1045 psi for a weight flow of 71 lb/sec (13.60% of the main pump flow). Figure 14 is the estimated performance of the turbine with a velocity ratio of 0.50 and a nozzle spouting angle of 14 degrees. All stages are identical and the nozzle exit velocity is 170 FPS; the rotor inlet and discharge velocity is 92 FPS.

A layout of the LOX low-speed inducer is shown in Figure 15. From this layout the weight and moment of inertia were calculated to be:

Rotor weight, lb = 23.9
Total weight, lb = 125
Moment of inertia, lb-in-sec^2 = 0.495

Since a part of the J-2S LOX pump discharge flow is used to drive the low-speed inducer turbine, the operating point of the LOX pump must be increased to a higher head and flow to maintain 265,000 lbs. thrust capability. The new operating point is as follows:

Q = 3291 gpm delivered and
13.6% recirculated through the pump and
low-speed inducer turbine
H = 3031 ft delivered overall head
H = 2856 ft across the main pump
N = 10,410 rpm

Figure 16 is the actual performance map of the J-2S LOX pump.

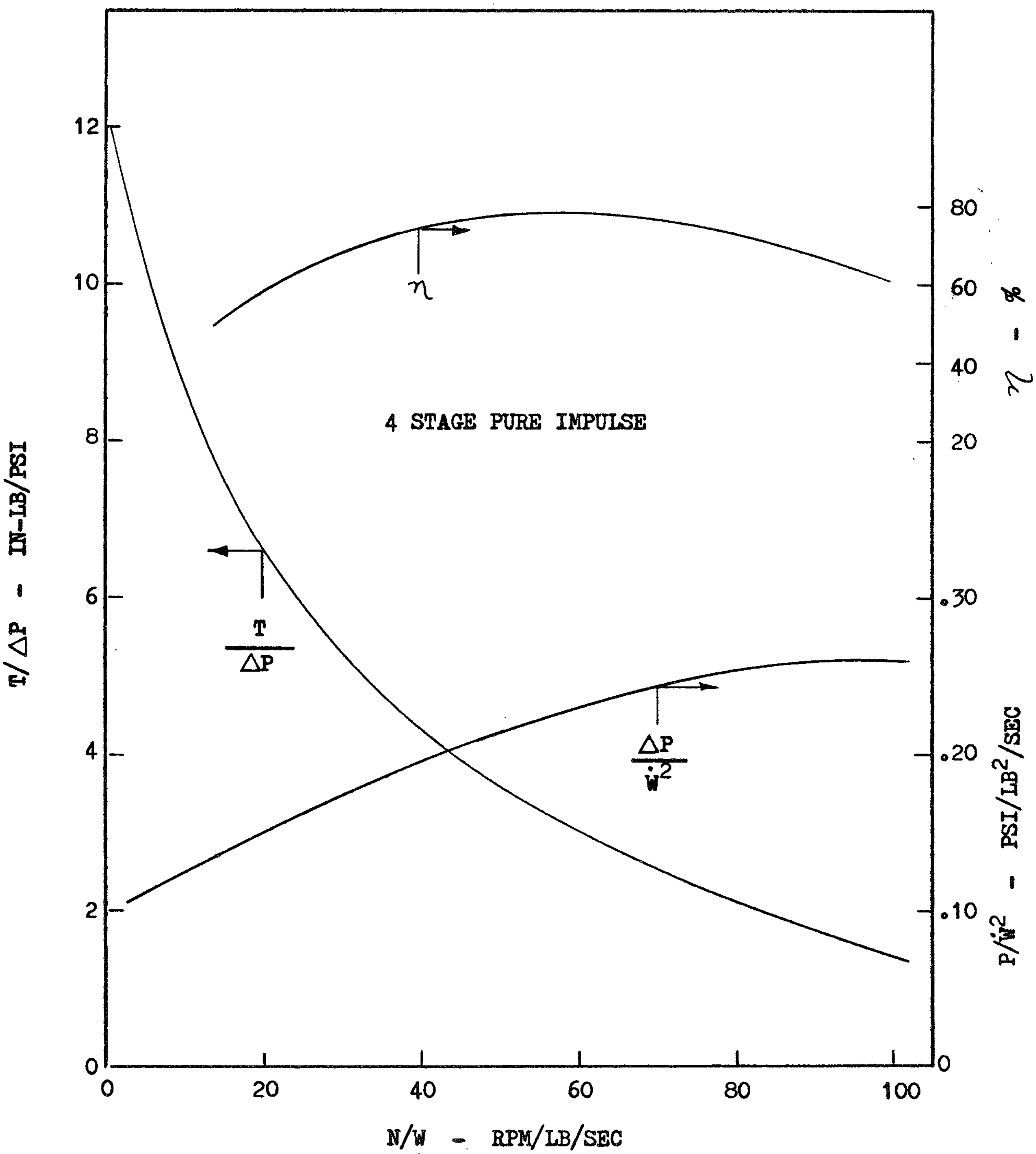

FIGURE 14. J-2S LOX LOW-SPEED INDUCER TURBINE ESTIMATED PERFORMANCE

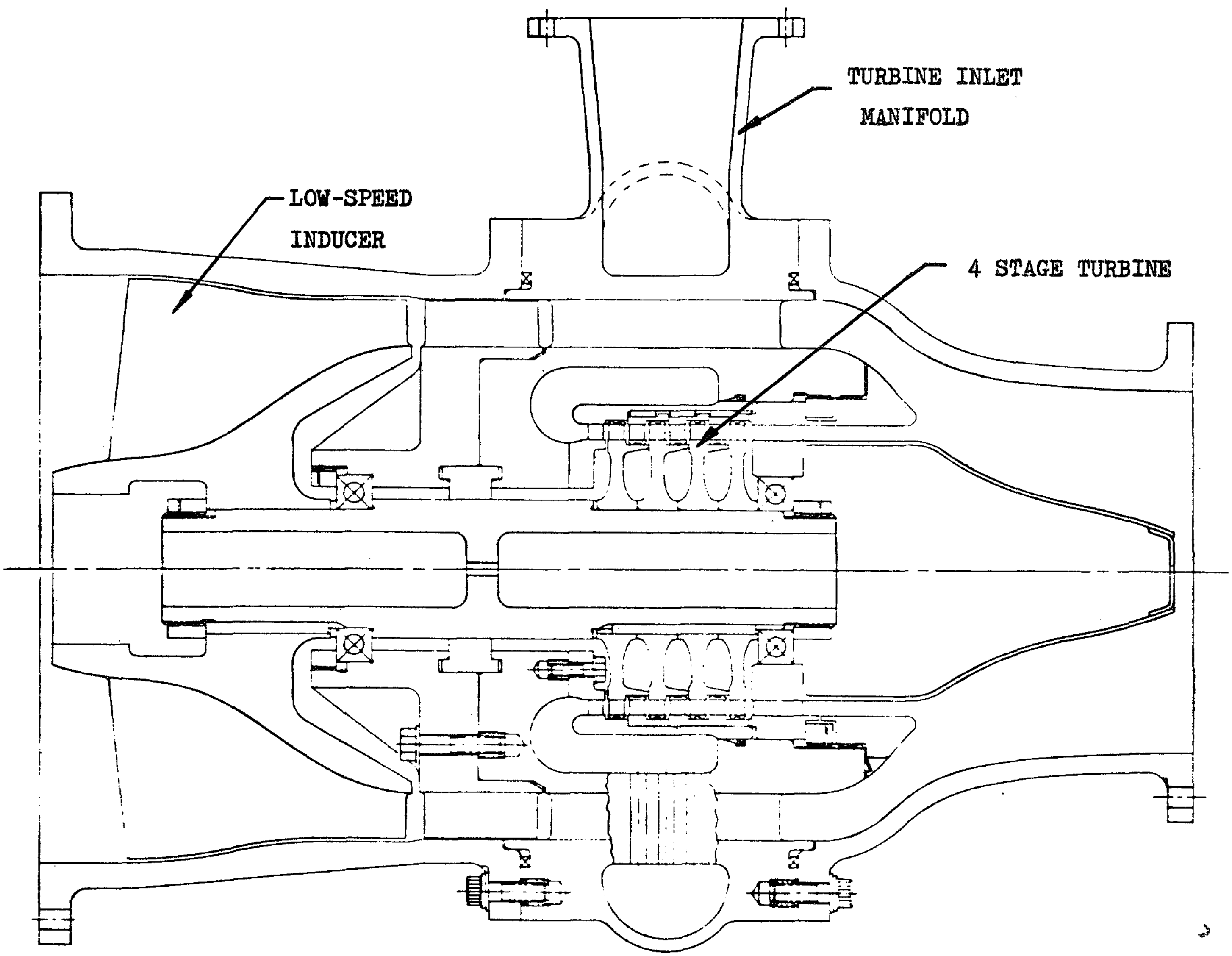

FIGURE 15. J-2S LOX LOW-SPEED INDUCER

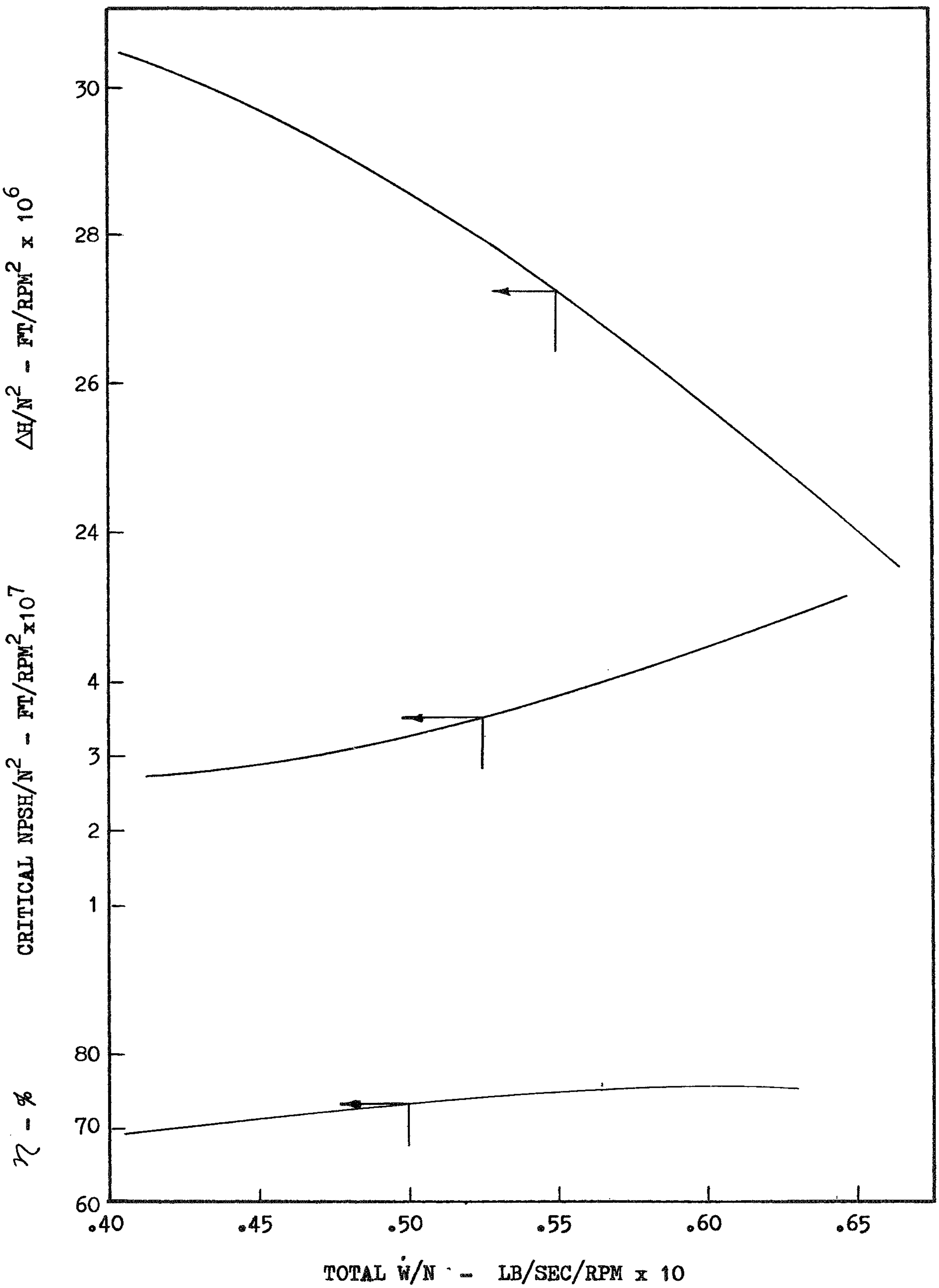

FIGURE 16. J-2S LOX PUMP PERFORMANCE

Application of an Existing Experimental Low-Speed LOX Inducer in LH_2

An analysis was made to determine the possibility of operating an experimental J-2 LOX partial flow low-speed inducer developed under Contract NAS3-10280, in liquid hydrogen. This low-speed inducer has been built and tested in water to verify computer system simulation techniques. The test results of this low-speed inducer may be found in Reference 1.

The following performance and design factors were reviewed for liquid hydrogen operation.

1. Operating point (head, flow, etc.) of the low-speed inducer coupled to the J-2S fuel pump.
2. Main pump operating point for a 265K engine thrust level application.
3. Low-speed inducer suction performance.
4. Thermodynamic process.
5. Hydraulic turbine design.
6. Existing structural limitations.

At the optimum flow coefficient the low-speed inducer operating point in LH_2 would be:

$Q = 9691$ gpm	Fluid: SAT. LH_2 at 41°R
$N = 16{,}000$ rpm	$\Delta H = 2695$ ft
$\phi = 0.07$	$\Delta P = 79$ psi
$N_{ss} = 107{,}000$ (63,600 in water)	$HP = 593$
$NPSH = 36$ ft	$\eta = 0.75$

Under the above conditions the J-2S fuel pump must develop a head of 55,153 ft. at a flow of 9691 gpm and at speed of 29,600 rpm. The head of the low-speed inducer is sufficient to keep the main pump from cavitating at all times and to preclude any vaporization at the turbine discharge. The turbine flow discharges to a back pressure of 110 psi and at a temperature which corresponds to a vapor pressure of 60 psi.

A high efficiency three stage hydraulic turbine would be necessary to produce the required horsepower if the same diameter as the J-2 LOX low-speed inducer turbine is used. For the available pressure of about 450 psi at the main inducer discharge, 19 percent of the main inducer through flow would be used to drive the turbine. Structurally, the existing design will be adequate to meet the operating pressures and rotor axial thrust. The bearings are also capable of high speed operation in liquid hydrogen, however, the shaft speed may be near a critical speed and will be a limiting design consideration.

This brief analysis has indicated that with a minimum of hardware modification, the J-2 LOX low-speed inducer could be tested in LH_2 at the 265K J-2S engine operating point.

ANALYSIS OF LOW NPSP UNPRESSURIZED HYDROGEN FEED SYSTEM

An analytical study was made to estimate the required NPSH for starting an engine with a low-speed hydraulic turbine driven inducer in the LH_2 feed line.

To perform the engine start studies, an analog computer start model of the J-2S liquid hydrogen, liquid oxygen engine was used. The model was modified to include fuel pump cavitation and oxidizer and fuel pump inlet lines corresponding to the lines used on the S-IVB stage of the Saturn vehicle. In addition, an analog computer model of a low speed, hydraulic turbine driven inducer (including inlet and outlet lines) was set up and used to replace the fuel pump inlet line. With these two models, the start and steady state performance of the engine with and without the low-speed fuel inducer was studied.

The complete system is shown in Figure 17. It consists of the propellant feed tanks, pump inlet lines (fuel inlet line with or without a low-speed inducer) and the J-2S engine. The analog computer diagrams representing the complete system model are included in Appendix A.

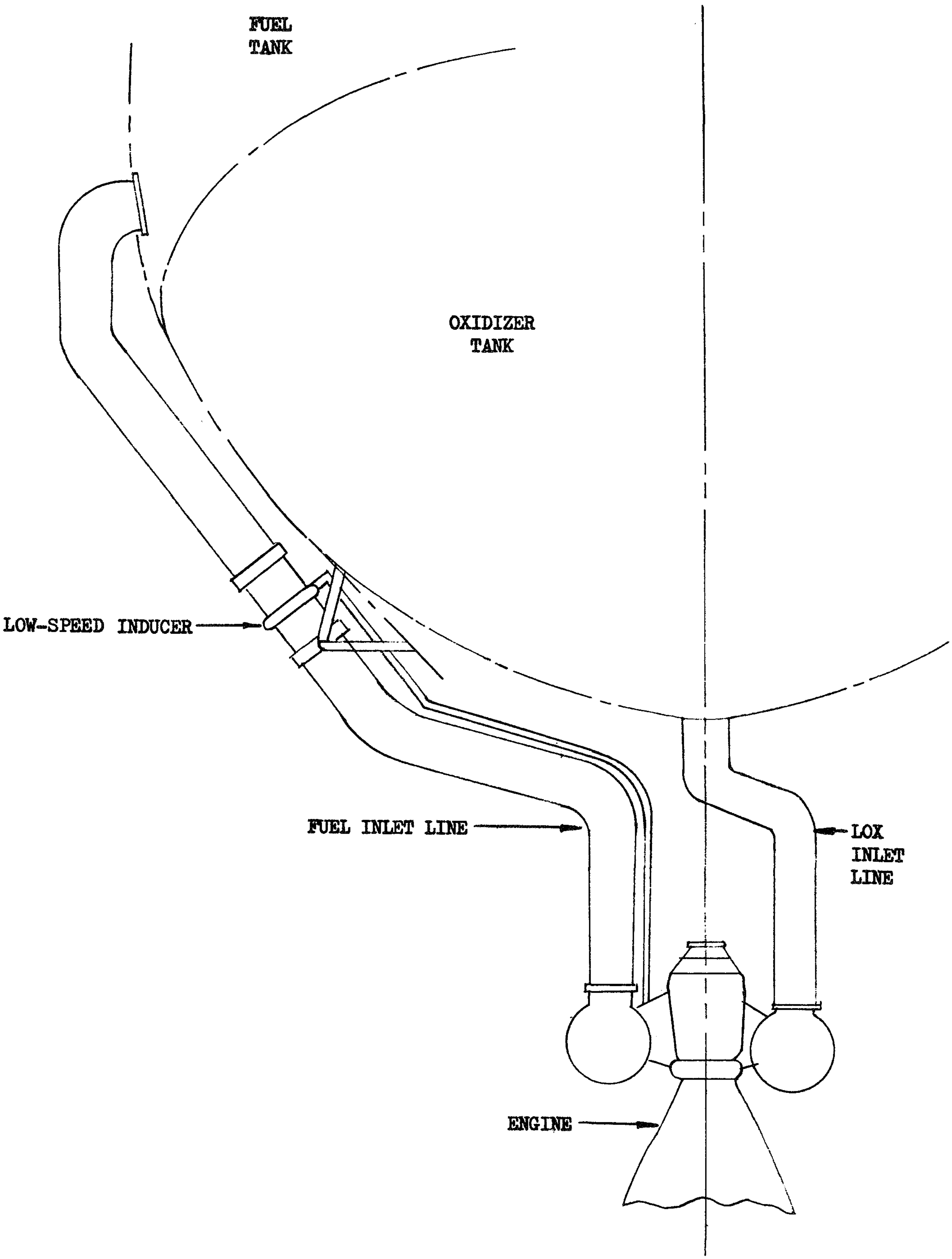

FIGURE 17. S-IVB ENGINE AND FEED SYSTEM

ENGINE DESCRIPTION

The basic engine is defined in the study to include everything downstream of the main pump inlets. It consists of: a fuel and an oxidizer turbopump driven by a series arrangement of hot gas turbines; a regeneratively fuel cooled thrust chamber; a thrust chamber hot gas tapoff for supplying the turbine drive gases; and required valves and ducting.

The pump inlet line characteristics represent those used for the Saturn S-IVB stage. Other ducting consists of: a high pressure oxidizer line which routes oxidizer from the oxidizer pump discharge through the main oxidizer valve to the injector; a high pressure fuel line which routes fuel from the fuel pump discharge through the main fuel valve to the cooling tube inlet manifold; and a cooling tube bypass which routes fuel from the fuel pump discharge through a bypass valve directly to the fuel injector.

Valves required for starting are the main oxidizer and fuel valves and the fuel cooling tube bypass valve. To start the engine the main fuel and cooling tube bypass valves are opened. This allows fuel to flow through the engine. After some period of fuel lead (one second for this study) the main oxidizer valve is opened to a nominal 12 degree step position. This step position is held for approximately 4 seconds allowing the engine to reach an intermediate operating level. At the completion of the 4-second step, the main oxidizer valve is ramped open in 0.8 seconds and the cooling tube bypass valve is closed in 0.8 seconds. A nominal engine start with pump inlet pressure of 30 psia, fuel and 40 psia oxidizer is shown in Figures 18 and 19.

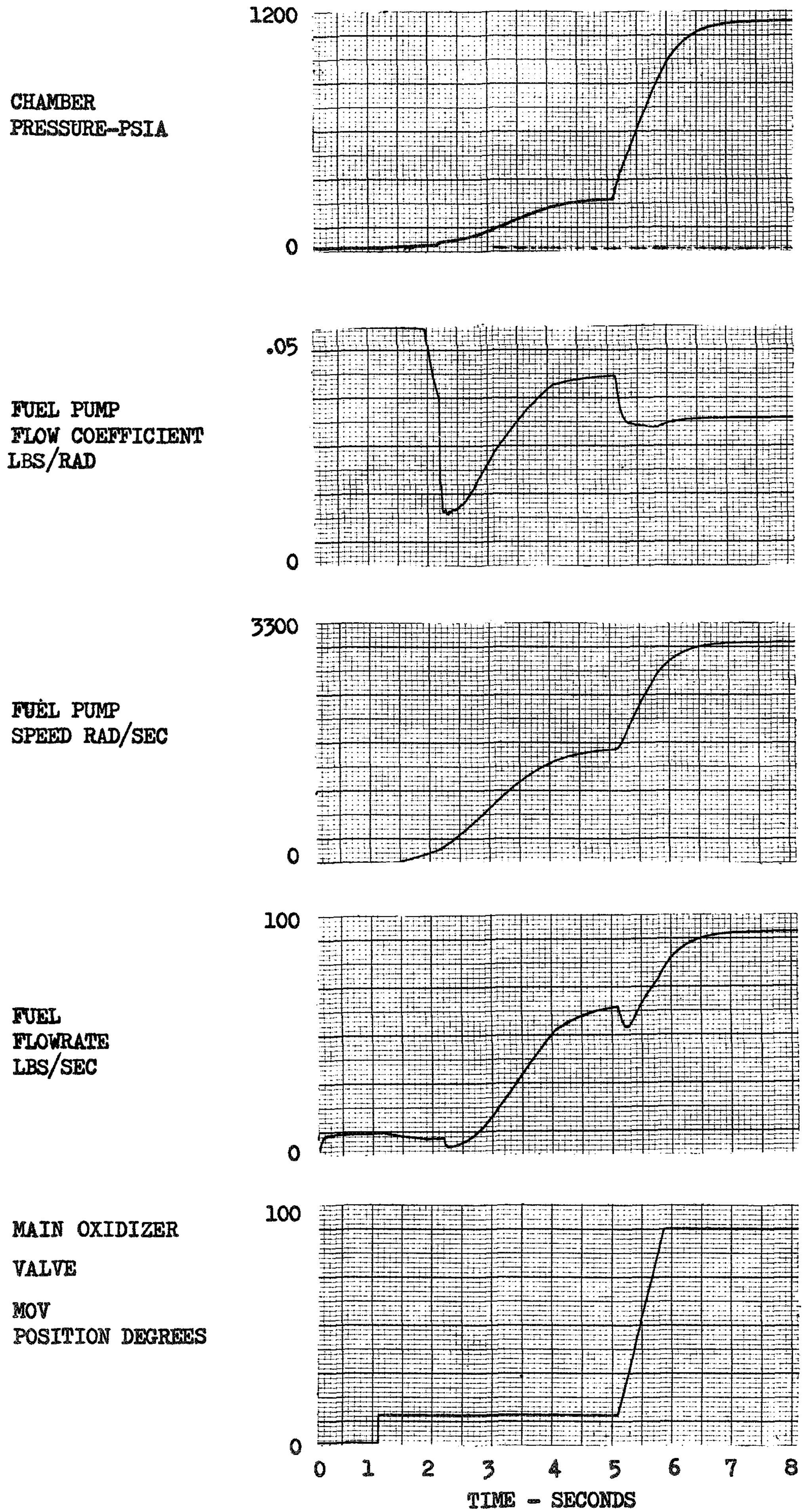

FIGURE 18. ENGINE START - $NPSP_f$ = 10 psi

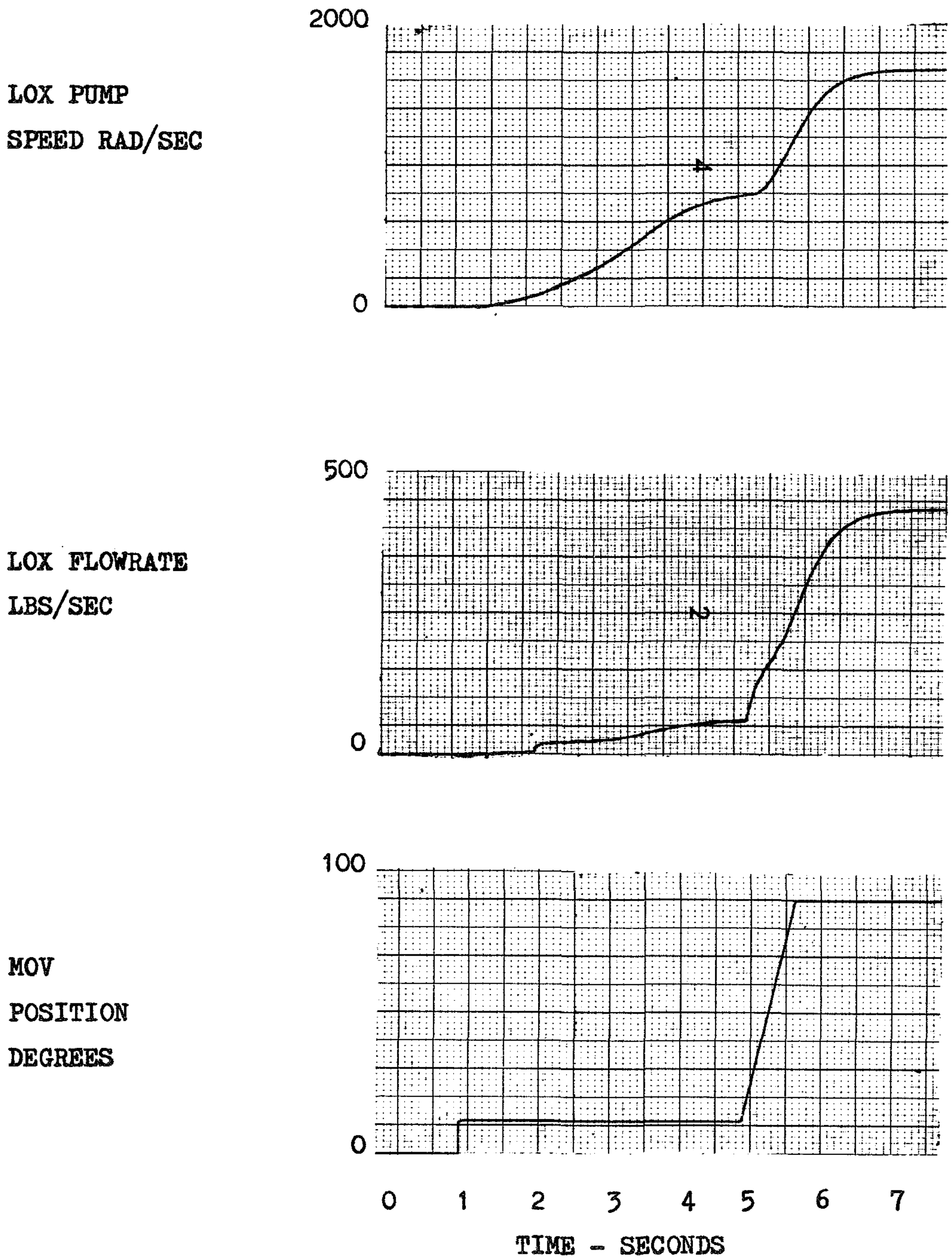

FIGURE 19. ENGINE START - $NPSP_f$ = 10 psi

Fuel Pump NPSP

NPSP is defined as the pressure difference between the total pump inlet pressure and the fluid vapor pressure. An LH_2 vapor pressure of 20 psia was used for this study. Where NPSH in feet is referred to, it is the net positive suction pressure (NPSP) converted to feet using a density of 4.0 pounds per cubic foot.

SYSTEM WITHOUT LOW-SPEED INDUCER

Model results for low NPSP performance of the engine without the low-speed inducer were obtained to establish a reference for evaluating the results of the system with a low-speed inducer. To establish the steady state and start reference performance two types of runs were made. These were: (1) Reduction of NPSP with the engine running at nominal performance and (2) starts at low NPSP. The limit for low NPSP operation is determined by the fuel pump cavitation performance. Referring to figure 20, the ratio of actual to non-cavitating head is dependent on the ratio of net positive suction head to speed squared. As a result, the lower the speed, the lower the required NPSP to maintain pump performance.

For steady state performance, the computer model engine was started with a fuel pump NPSP of 10 psi (approximately 345 feet of hydrogen). From this point, the NPSP was reduced until oscillations due to deep cavitation occurred. As the NPSP was reduced, the fuel pump discharge pressure, fuel flowrate and chamber pressure decreased due to increasing cavitation while the fuel pump speed increased due to the fuel pump requiring less power. Severe oscillations occurred when the NPSP was reduced below 3.5 psi (approximately 120 feet). The results are shown in Figure 21.

The results for starting from low (3.5 psi) NPSP, shown in Figures 22 and 23, indicate that the engine will start at a tank pressure that results in minimum running NPSP. The only apparent difference between 10 and 3.5 psi NPSP is a lower minimum fuel pump flow coefficient for the low NPSP condition.

The minimum flow coefficient is about 0.8 of the nominal NPSP minimum value due to a lower initial fuel flowrate under the low tank pressure condition.

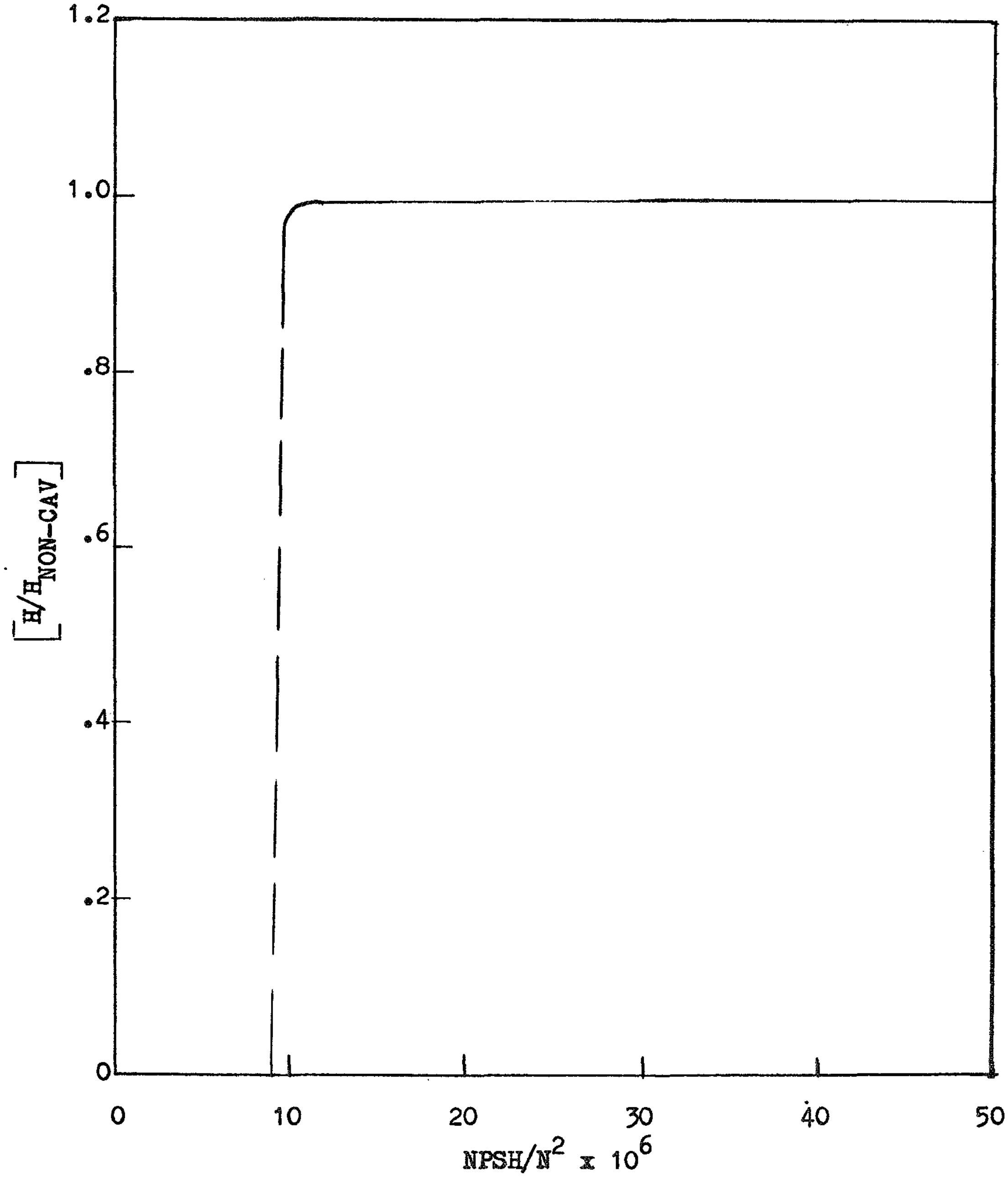

FIGURE 20. MARK 29-F CAVITATION PERFORMANCE (BASED ON LH2 TEST DATA)

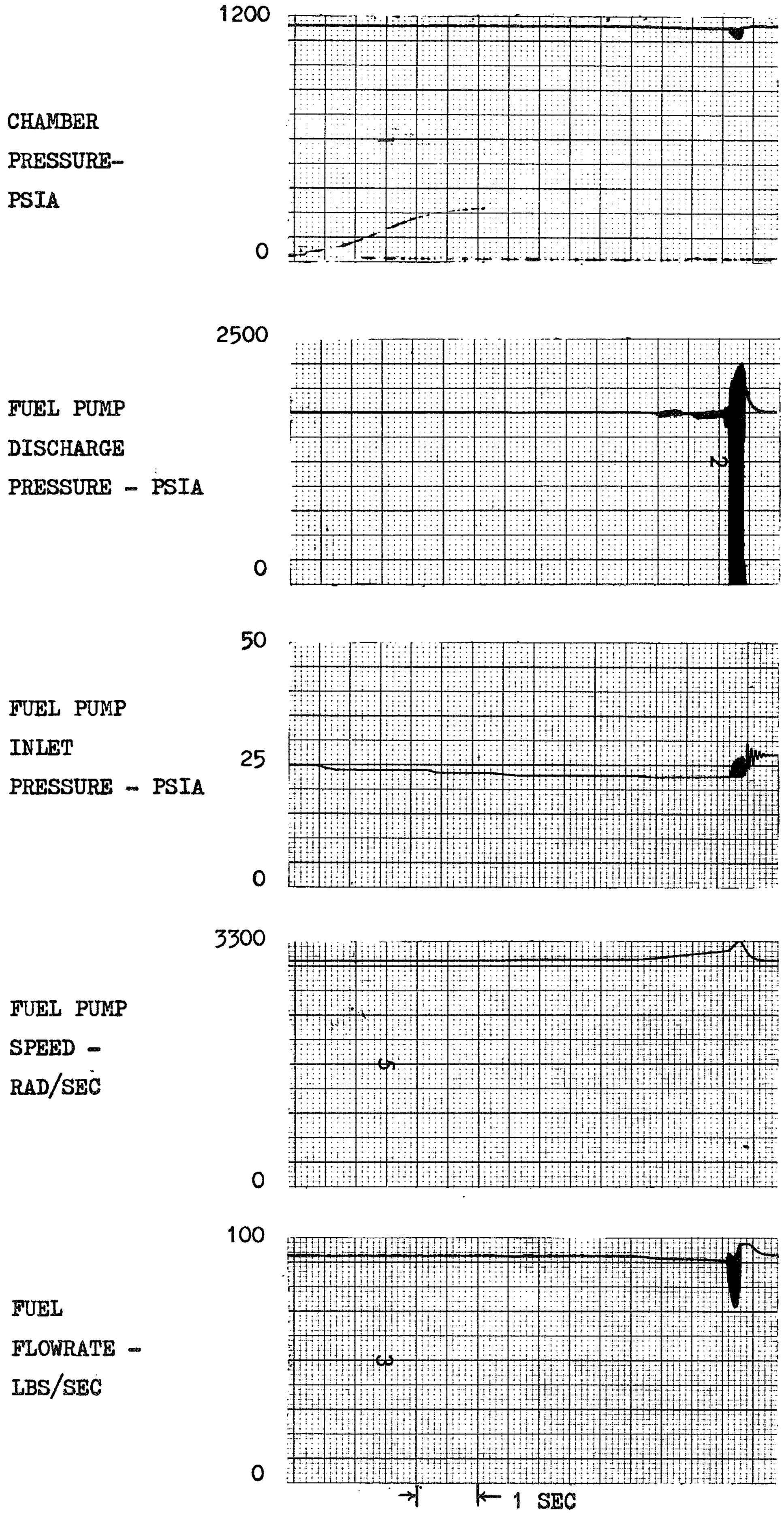

FIGURE 21. ENGINE MODEL PERFORMANCE WITH FUEL PUMP CAVITATION

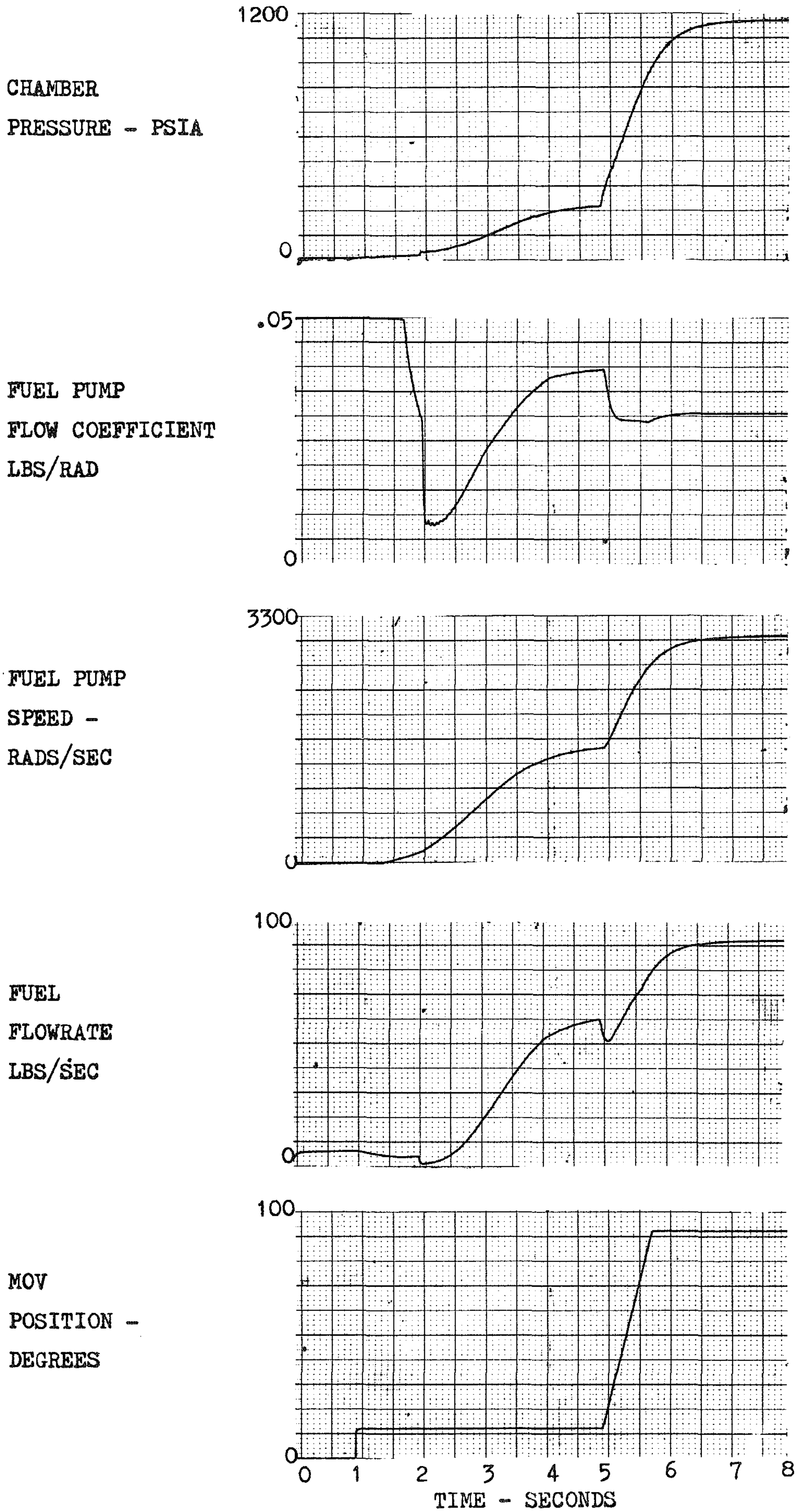

FIGURE 22. ENGINE START - $NPSP_f$ = 3.5 psi

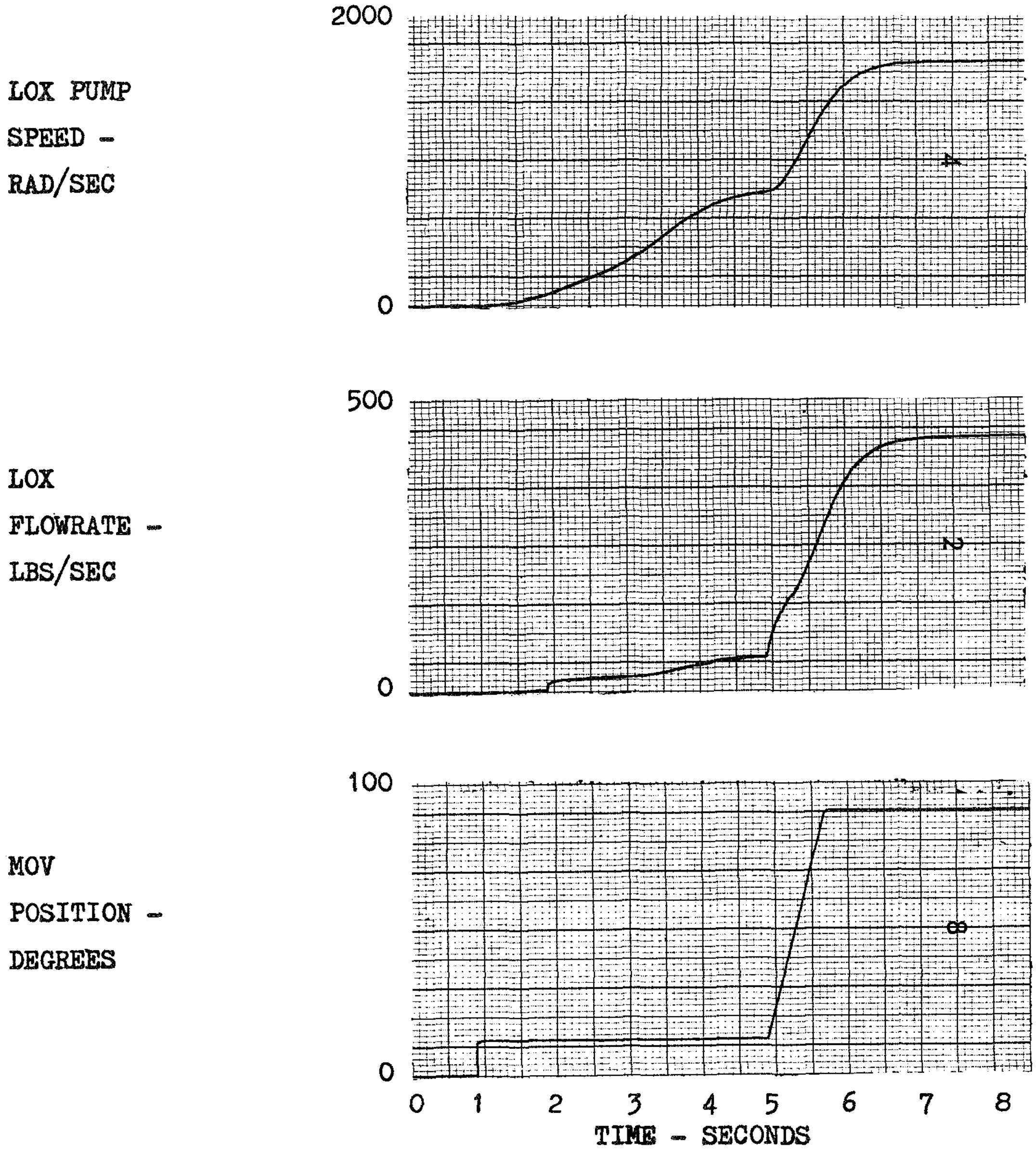

FIGURE 23. ENGINE START - $NPSP_f$ = 3.5 psi

SYSTEM WITH LOW-SPEED INDUCER

When a low-speed inducer is incorporated into the fuel feed system, no change is required in the basic configuration of the engine or the oxidizer inlet line. The inducer is mounted in the fuel inlet line at a position chosen to be midway between the fuel tank outlet and the main pump inlet. The fluid used to drive the inducer hydraulic turbine is taken from the discharge of the main pump inducer section and routed to the turbine inlet manifold. Characteristics representative of low head and high head inducers were considered in the study.

Low-Head Inducer

To investigate the characteristics of low-head inducers, four operating points of inducer head rise and head coefficient were selected for study. These points were:

H ft	ψ
300	.12
300	.02
700	.20
700	.065

The reason for selecting these four points was to determine if there were any start effects due to inducer head and head coefficient.

Using the main pump and turbine performance curves for each of the selected low-speed inducer operating points, a series of starts was run for various fuel tank pressures. The results showed that there was no significant difference in starting performance for this range of head rise and head coefficient. A low NPSP (approximately 1 psi) start for an inducer designed for 300 feet of head at a head coefficient of 0.12 is shown in Figures 24 through 26 . Comparing these results

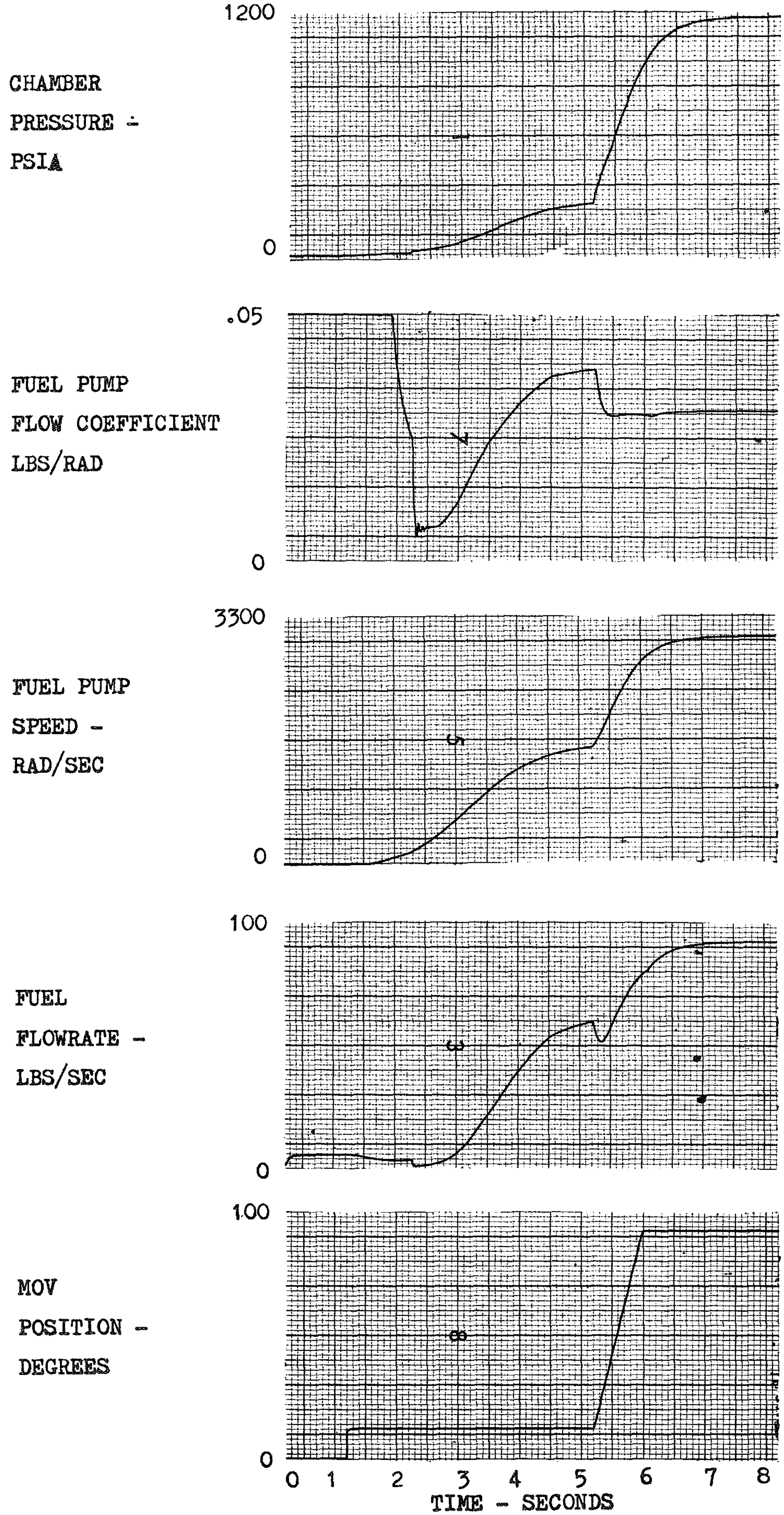

FIGURE 24. ENGINE START - LOWHEAD INDUCER - $NPSP_f$ = 1 psi

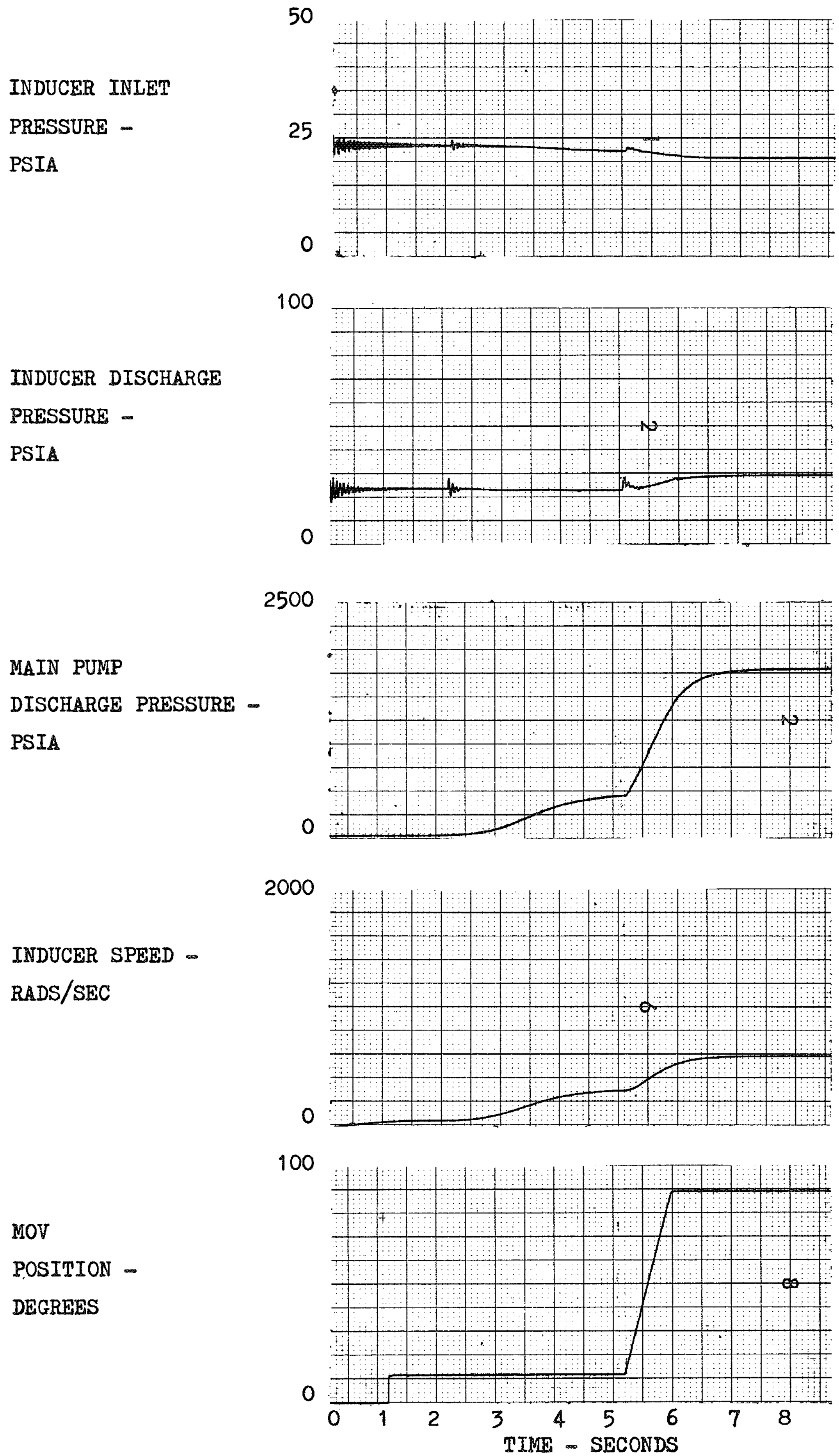

FIGURE 25. ENGINE START - LOW HEAD INDUCER - $NPSP_f$ = 1 psi

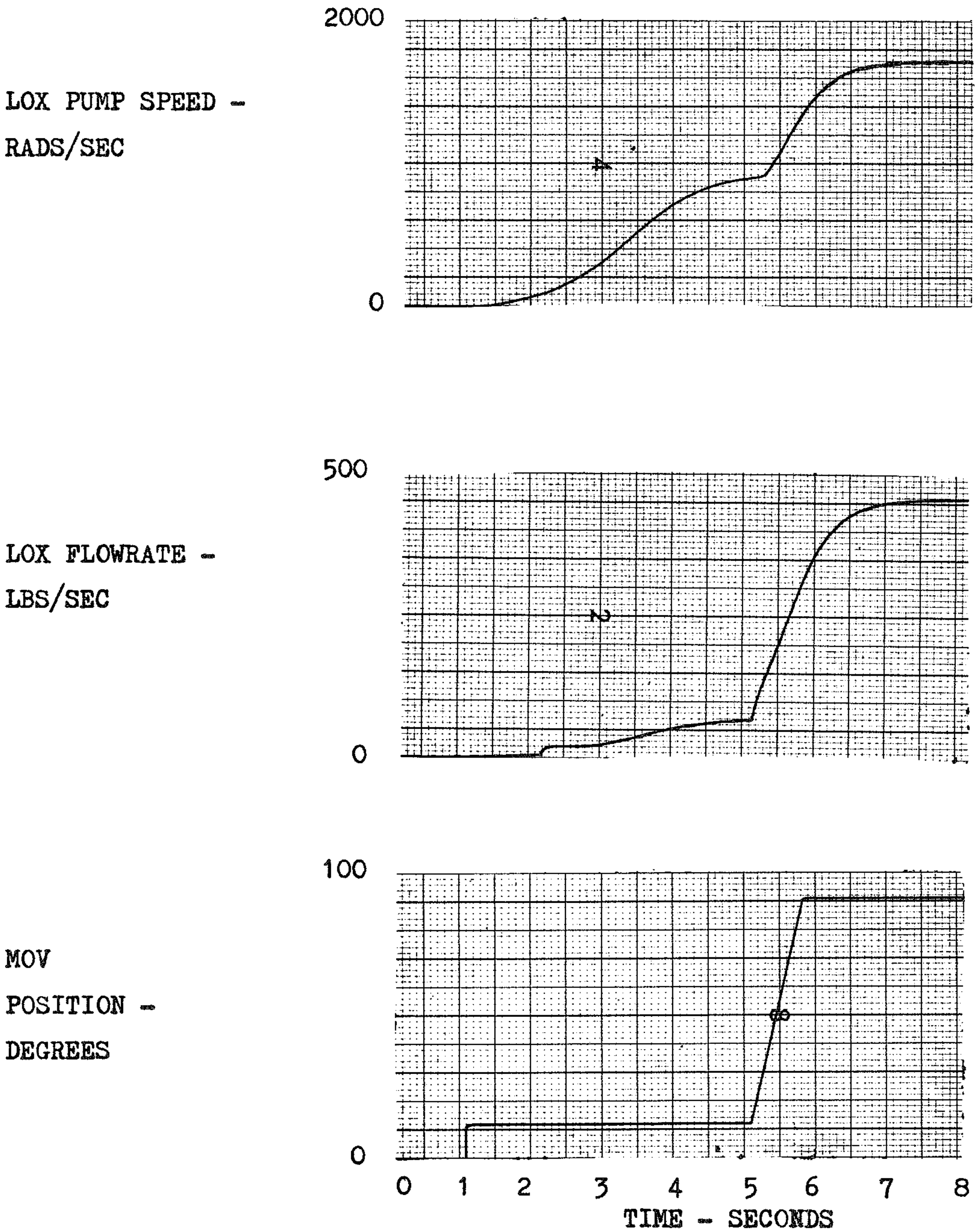

FIGURE 26. ENGINE START - LOW HEAD INDUCER - $NPSP_f$ = 1 psi

to those of Figures 22 and 23 for the low NPSP start for an engine without an inducer, the only noticeable difference is a further reduction in the minimum fuel pump flow coefficient. The inducer does generate sufficient head so that the main pump does not cavitate. No consideration was given to changes in valve sequencing or inducer location because a check of the hydrogen conditions at rated performance showed the fluid to be two-phase at the exit of the hydraulic turbine. Thus, a low-head inducer would not be suitable for use as a low-speed inducer. Referring to Figure 25 , oscillations are evident in the inducer pressures starting at zero time. These are due to establishing fuel flow when the fuel valve is opened.

High-Head Inducer

The high head inducer characteristics used in the study are shown in Figures 6, 7, and 8. With these characteristics in the model, the minimum steady state NPSP was determined by decreasing the fuel tank pressure until severe inducer cavitation oscillations appeared. Figure 27 shows some of the resultant system variables with the cavitation oscillations beginning at about 35 feet NPSH (1.1 psi NPSP). The results for the main engine performance, shown by chamber pressure, fuel pump discharge pressure and fuel pump speed, show that the performance does not significantly shift with reduced tank pressure. This occurs because the inducer pressure rise is always sufficient to prevent main pump cavitation and the pressure rise through the main pump represents about 94% of the total pressure rise. Therefore, the inducer pressure rise can decrease with only a slight effect on the total head rise.

The start transient with the tank pressure set to give a running NPSP of about 1.2 psi is shown in Figures 28 through 30 . The valve sequence used is the same as for the engine without a low-speed inducer which is:

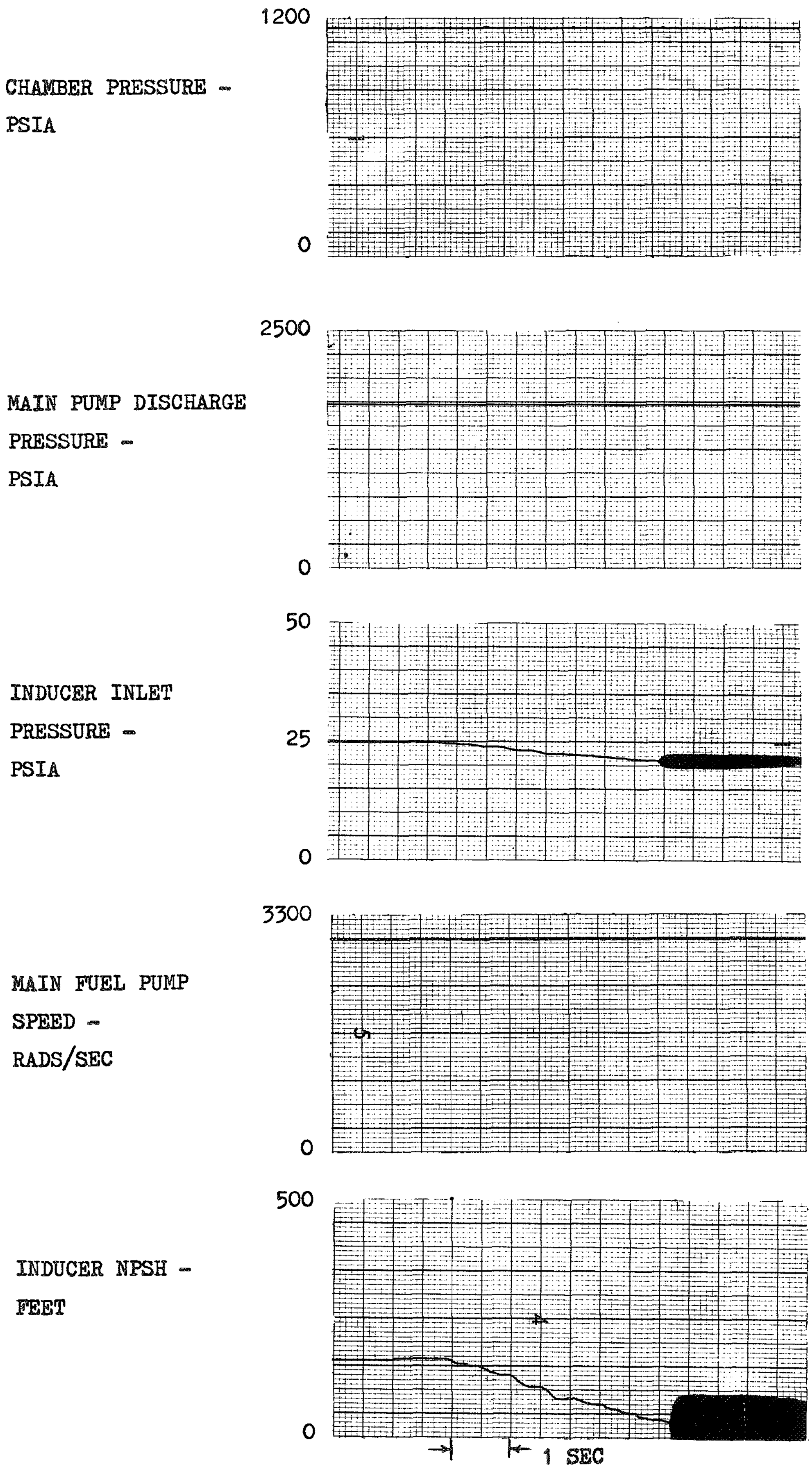

FIGURE 27. ENGINE MODEL PERFORMANCE WITH FUEL INDUCER CAVITATION

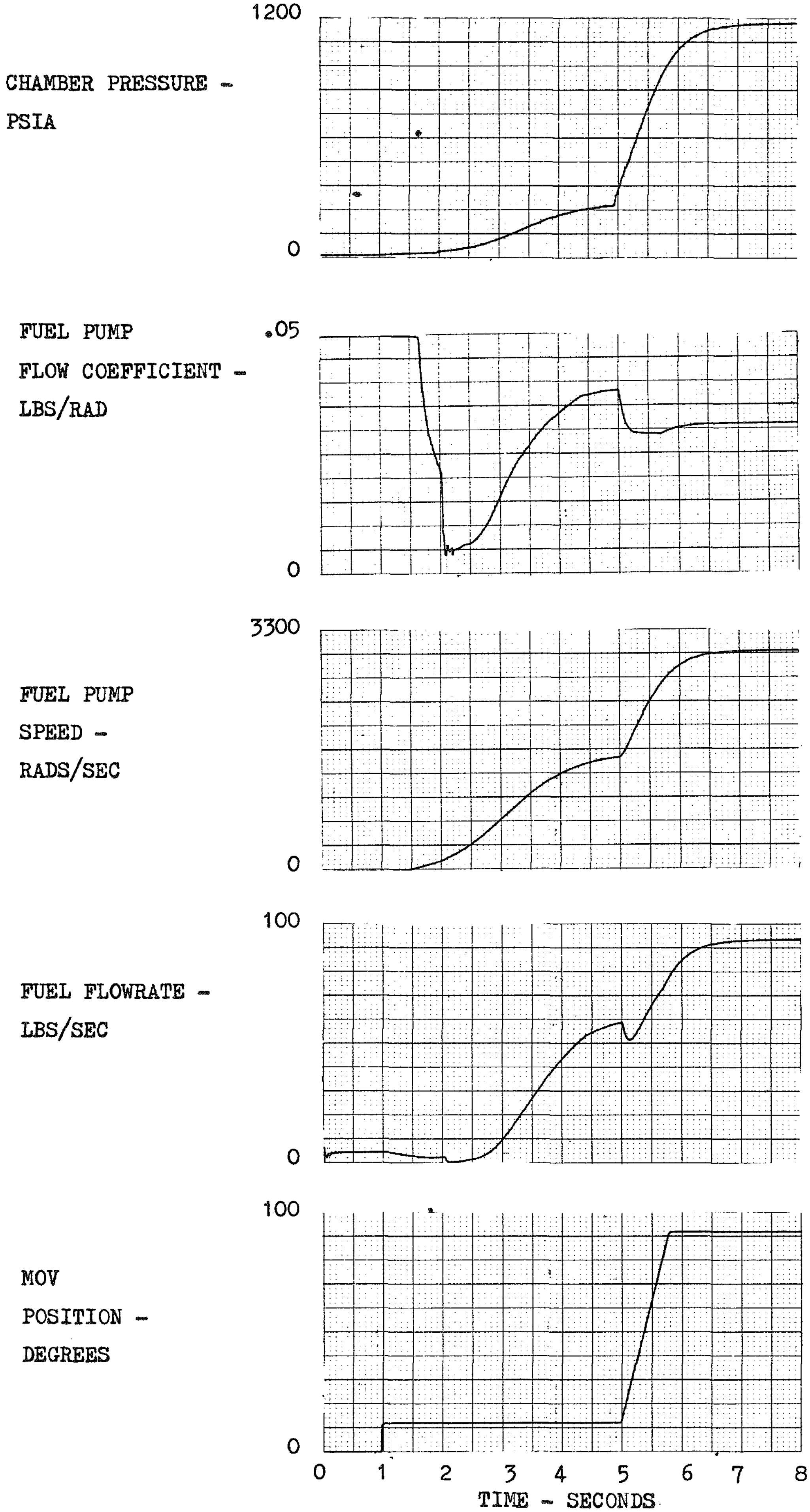

FIGURE 28. ENGINE START - HIGH HEAD INDUCER - $NPSP_I$ = 1.1 psi

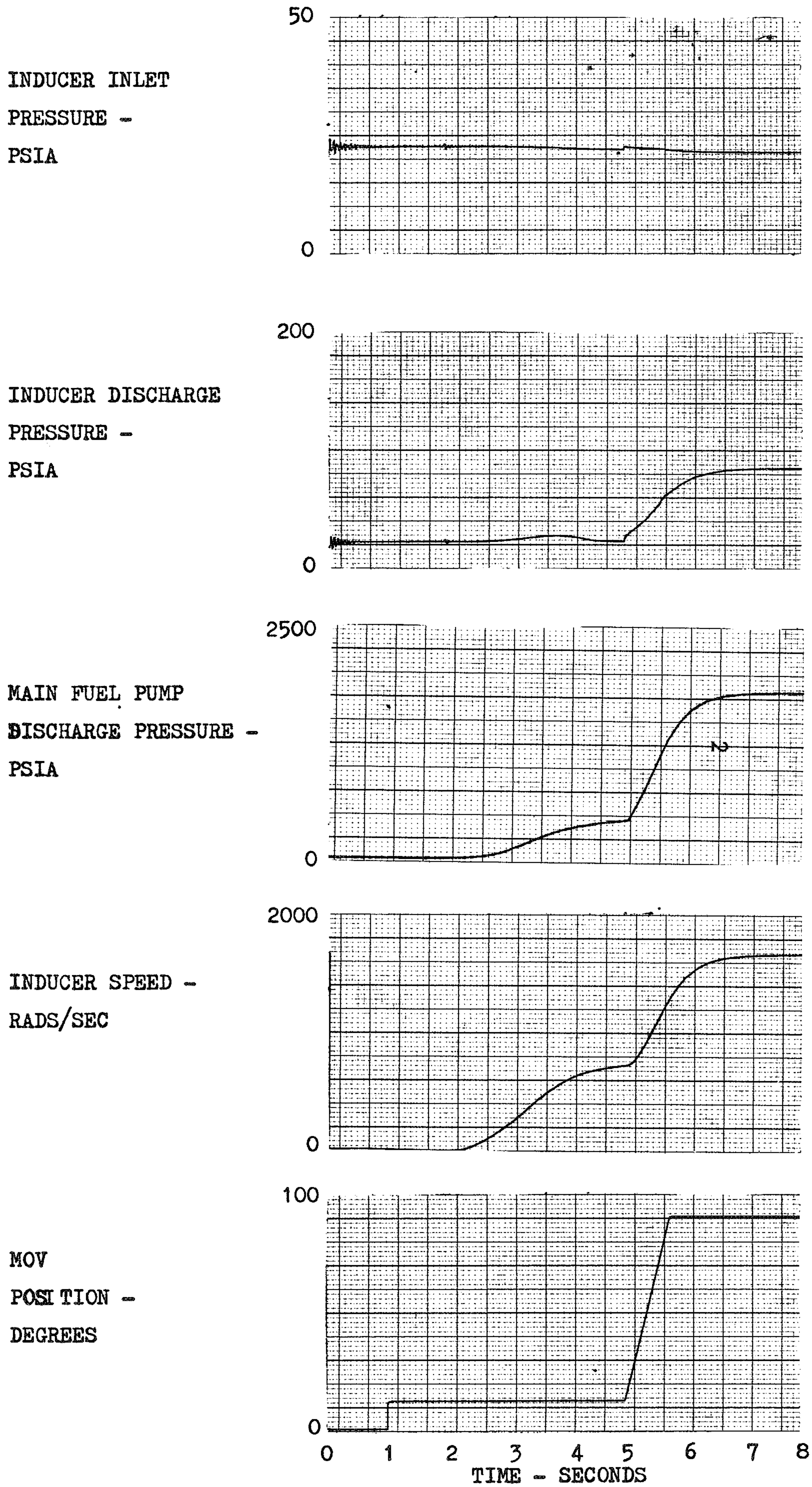

FIGURE 29. ENGINE START - HIGH HEAD INDUCER - $NPSP_i$ - 1.1 psi

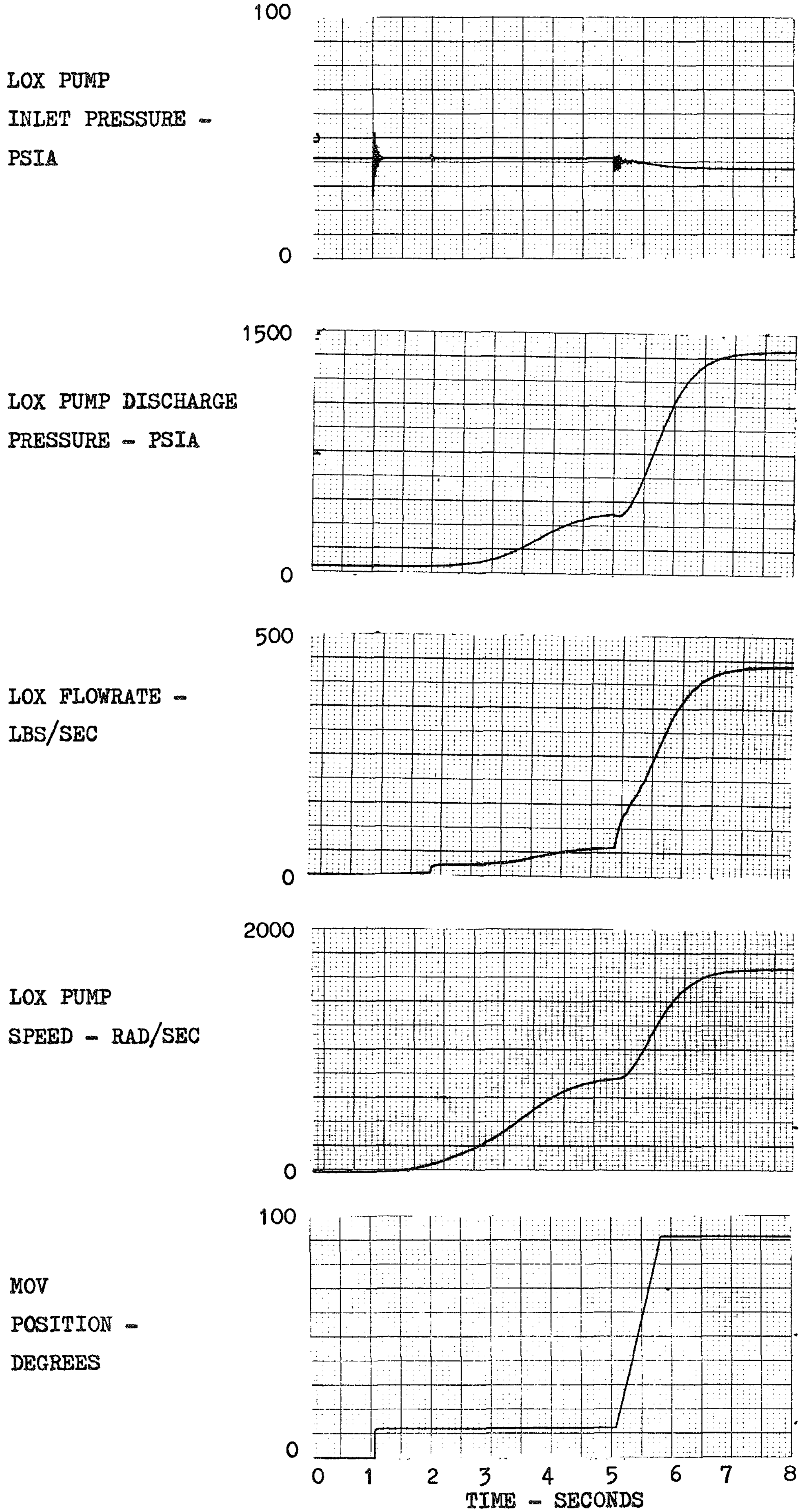

FIGURE 30. ENGINE START - HIGH HEAD INDUCER - $NPSP_f$ = 1.1 psi

1. Main fuel and fuel chamber bypass valves open at time zero.
2. Main oxidizer valve open to a 12 degree step position at one second.
3. Main oxidizer valve ramped from 12 degrees to full open in 0.8 second starting at 5 seconds.
4. Chamber bypass valve ramped closed in 0.8 second starting at 5.0 seconds.

The results indicate that the engine will start with a tank pressure setting which will result in the minimum required running NPSP. The start is very similar to the low-head inducer start with the exception of the inducer outlet pressure. With the high-head inducer, the outlet pressure is much higher during the buildup from the step MOV position to full operation. From a practical standpoint, this adds assurance that the main pump will not cavitate. When the tank pressure was reduced further, severe cavitation of the inducer resulted as steady state operation was reached.

The limiting factor on the minimum required fuel tank pressure has been the cavitation performance of the main pump or low-speed inducer. To determine the possibility of starting the engine if the inducer could operate at zero NPSP, starts were run with: zero inducer cavitation head loss; the fuel tank ullage pressure set to the vapor pressure; and the effect of inlet line acceleration head included. The acceleration was assumed proportional to chamber pressure and the increase in inducer inlet pressure at rated chamber pressure was 2 psi.

The zero NPSP start with no change in valve sequencing is shown in Figure 31. Main pump cavitation results about 0.5 seconds prior to ramping the MOV open. The cavitation occurs when the main pump speed reaches a value which requires an NPSH higher than the inducer can supply.

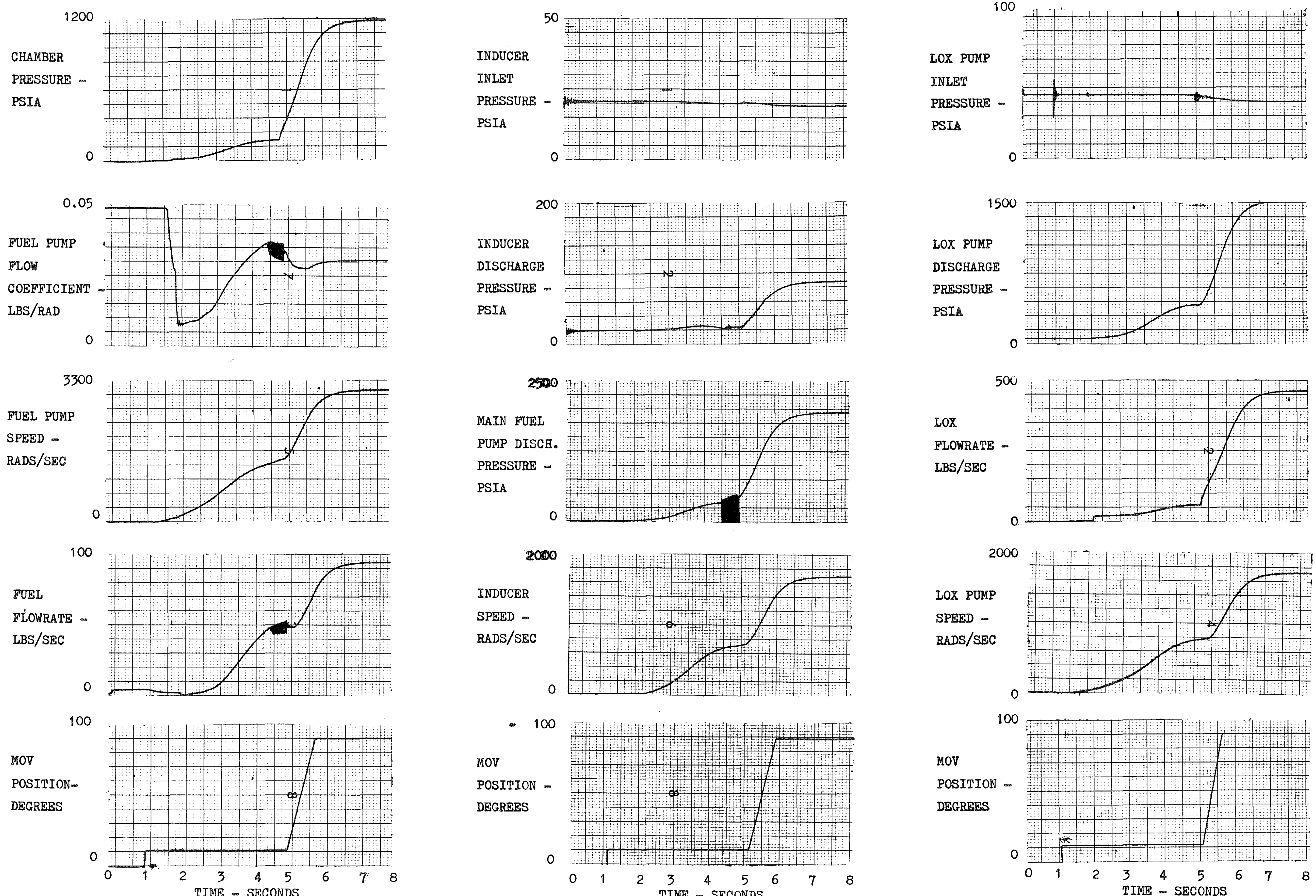

FIGURE 31. ZERO FUEL INDUCER NPSP - 12° MOV STEP

Reducing the MOV step position to 10 degrees eliminated the oscillation as shown in Figure 32 . For an engine using a chamber tapoff for supplying turbine power, decreasing the MOV step position decreases the supplied turbine power. The reduced turbine power results in a lower main pump speed and hence lower required NPSH. The reduced main pump operation also results in a lower inducer speed, an effect which, by itself, would result in reduced inducer pressure rise. However, the fuel flowrate is also reduced which lowers the inducer flow coefficient and increases the head coefficient. The net effect is that the inducer discharge pressure remains fairly constant for the 2 degree change in MOV step position. The NPSH supplied to the main pump is therefore constant while the required NPSH is reduced.

To determine the effect of sequencing changes on the tendency of the main pump to cavitate, the MOV step duration was increased and the time of bypass valve closure relative to the MOV opening ramp was varied. Increasing the MOV step duration to 6 seconds while closing the bypass valve after 4 seconds of the step position resulted in a good start. The longer step duration resulted in increased pump speeds and required main pump NPSH but closure of the bypass valve resulted in increased inducer pressure rise due to the increased head coefficient. This was further shown on a case where the bypass closure was delayed until the MOV ramp was initiated. Main pump cavitation resulted approximately 1 second prior to the MOV opening ramp when the inducer could not supply the required main pump NPSH. The inducer pressure rise was too low because of the higher flow rate with the bypass open.

To relax the requirement that the inducer must be able to operate at zero NPSP regardless of the inducer flow and speed conditions, the inducer could be located at the tank exit. This location eliminates the pressure drop in the line between the tank and inducer

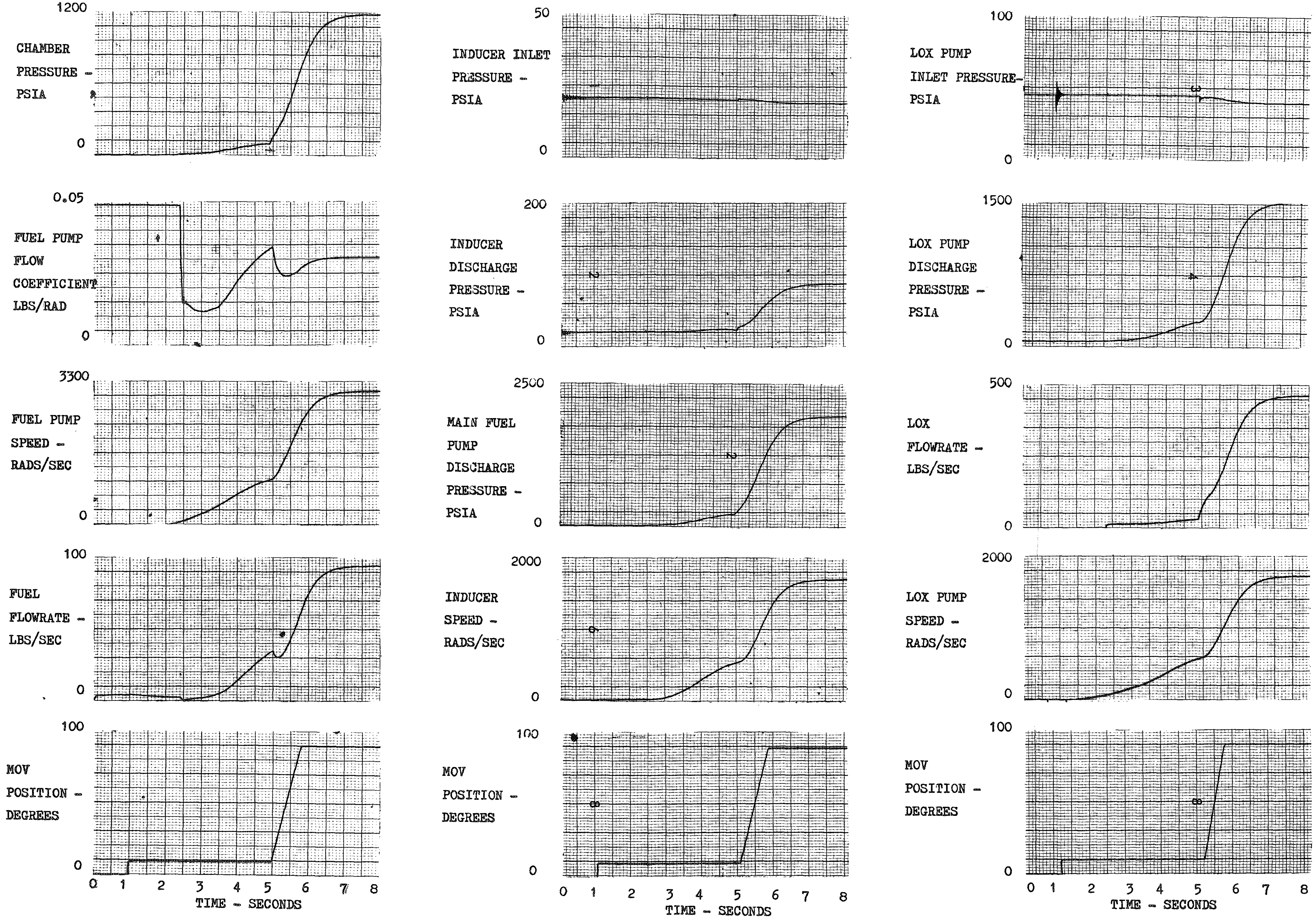

FIGURE 32. ZERO FUEL INDUCER NPSP START - 10° MOV STEP

inlet and retains about 70% of the propellant head above the inducer. This will tend to result in some positive inducer NPSP as soon as the thrust chamber ignites. It should be noted that the inducer inlet line pressure drop which is eliminated is added to the line connecting the inducer and main pump. However, the total frictional pressure drop is not increased, hence, the main pump inlet pressure will be no lower than with the inducer located some distance from the tank.

The significance of the above results is that an engine with a low-speed fuel inducer designed for high head can be successfully started at very low or zero inducer NPSP. In a vehicle installation, the acceleration will generate some inlet pressure so that the inducer will see zero NPSP only at low speed and flow. The results also indicate that no special engine controls or major changes in sequencing are required.

SUMMARY AND CONCLUSIONS

Based on the results of the studies, the following conclusions are drawn:

1. An engine with a low-speed fuel inducer can be successfully started with a tank pressure that provides the minimum required steady state NPSP.
2. With a low-speed inducer, engine starts can be achieved with no propellant tank pressurization and steady state operation can be obtained with the increased NPSP supplied by vehicle acceleration for an engine system utilizing a hydraulic turbine driven low-speed inducer.
3. There are no special controls or major sequence changes required.
4. Locating the low-speed inducer at the tank exit improves the inducer inlet conditions by retaining about 70% of the propellant head above the inducer while moving the inlet line pressure drop from the inducer inlet to the inducer discharge.

ANALYSIS OF POGO OSCILLATION

Low frequency longitudinal oscillations have occurred on most rocket engine powered vehicle flights. These oscillations commonly called POGO are caused by an instability in a closed loop system consisting of the vehicle structure, the propellant pump feed systems, and the engine. The loop is most easily visualized by tracing the response of the system components to a perturbation of the structural acceleration. The acceleration oscillations cause pump inlet flow oscillations which result in pump inlet pressure oscillations, which in turn depend on the feed line and pump inlet dynamics. The pump inlet pressure oscillations are transmitted through the engine and produce thrust oscillations. The thrust oscillations then feed back through the structure, producing acceleration oscillations. This system will be unstable if the closed loop gain becomes greater than one, and the net loop phase shift approaches zero.

To eliminate these oscillations, the loop gain and/or phase shift must be changed in the critical oscillatory frequency ranges. Saturn flight data and analog model simulation analysis indicate that the oscillations occur at a structural resonant frequency, and are caused by coupling of the engine and structure through the LOX pump feed line. The critical LOX feed line frequency is the lumped parameter resonant frequency defined by $(1/CL)^{1/2}$, where C is the effective line termination compliance and L is the fluid inertance of the feed line.

Corrective devices have been added to the LOX feed line on the Saturn vehicle to change the natural frequency of the pump inlet line. These devices change the effective inlet line compliance by using an accumulator partially filled with a gas. Another potential method of altering the inlet line dynamic characteristics is the addition of a low speed, inducer upstream of the main pump.

Results were obtained in terms of the gain and phase of the output variable to the input variable as a function of the simulated structural acceleration frequency. The gain is expressed in decibels defined as 20 $\log_{10}$ (AR) where AR is the amplitude ratio of the output to input variables. Referring to Figure 34 , AR is the ratio of chamber pressure variation to oxidizer pump inlet pressure variation at a given input frequency. The pressure variations are changes about the steady state values. If the gain is one, the log is zero and hence the db is zero. If the gain is less than one, the log is negative, resulting in a negative db; the more negative the db value the lower the gain. As a reference, a change of -6 db means the gain is halved.

STRUCTURAL ACCELERATION INPUT

The forcing input to the model is representative of a structural acceleration. Several combinations of points of application of the acceleration were considered. In all cases the tank ullage pressure was considered constant and an input representing tank bottom motion was used. This resulted in a line inlet pressure variation defined by:

$$P_{\text{LOX TANK DISCHARGE}} = \frac{h_T \rho \ddot{x}}{g} + P_{\text{ULLAGE}}$$

where:

P_{ULLAGE} = CONSTANT

h_T = height of propellant in tank - IN

ρ = propellant density - LB/IN^3

$\ddot{x}$ = tank bottom acceleration - IN/SEC^2

g = gravitational constant - IN/SEC^2

This single acceleration input was used for the reference conditions and the inducer parameter variation cases. To consider the effect of flight conditions with additional acceleration inputs occurring, cases were run where pressure variations at the low speed inducer and/or at the main pump inlet due to inlet line fluid column heights, were included.

FEED SYSTEM INLET LINES

The feed system inlet lines, and low speed inducer turbine feed line, were described by the linearized lumped parameter equation:

$$P_1 - P_2 = \bar{R}_L \dot{w} + L_L \, (d\dot{w}/dt)$$

where:

P_1 = line inlet pressure - LB/IN^2

P_2 = line discharge pressure - LB/IN^2

$\bar{R}_L$ = linearized resistance - SEC/IN^2

L_L = fluid inertia - SEC^2/IN^2

$\dot{w}$ = mass flowrate - LB/SEC

The fluid inertia L, is a function of the line geometry and equals ℓ/gA,

where:

ℓ = line length - IN

g = gravitational constant - IN/SEC^2

A = cross sectional area - IN^2

MATHEMATICAL MODEL

An analysis was performed to determine if a low speed, hydraulic turbine driven inducer, located in the LOX feed line upstream of the main pump, can alter the engine feed system frequency response characteristics, and correct or control longitudinal oscillations. A mathematical model of the J-2 engine and the Saturn S-II stage center engine LOX feed system was formulated and solved for the frequency response characteristics. The results express the gain and phase of engine thrust relative to an input representing the vehicle structural acceleration at the LOX tank bottom.

Longitudinal oscillations experienced on vehicle flights have been shown to be a closed loop instability problem. Elimination or control of this instability requires a change in the loop gain and/or phase lag in the range of oscillatory frequencies. It is desired to determine if the addition of a low speed inducer in the LOX feed line can alter the frequency response characteristics of the engine and LOX pump inlet system portion of the closed loop.

To evaluate the effects of adding a low speed inducer to a LOX feed system, on the POGO phenomenon frequency response characteristics were determined for an engine feed system both with and without an inducer. The systems considered are shown schematically in Figure 33 . They consist of an inlet line, a main pump, a line coupling a low speed inducer and main pump where applicable, and an engine. Equations describing the low frequency perturbation dynamics of these systems were formulated, and programmed into a digital computer program to obtain their frequency response to a simulated structural acceleration input.

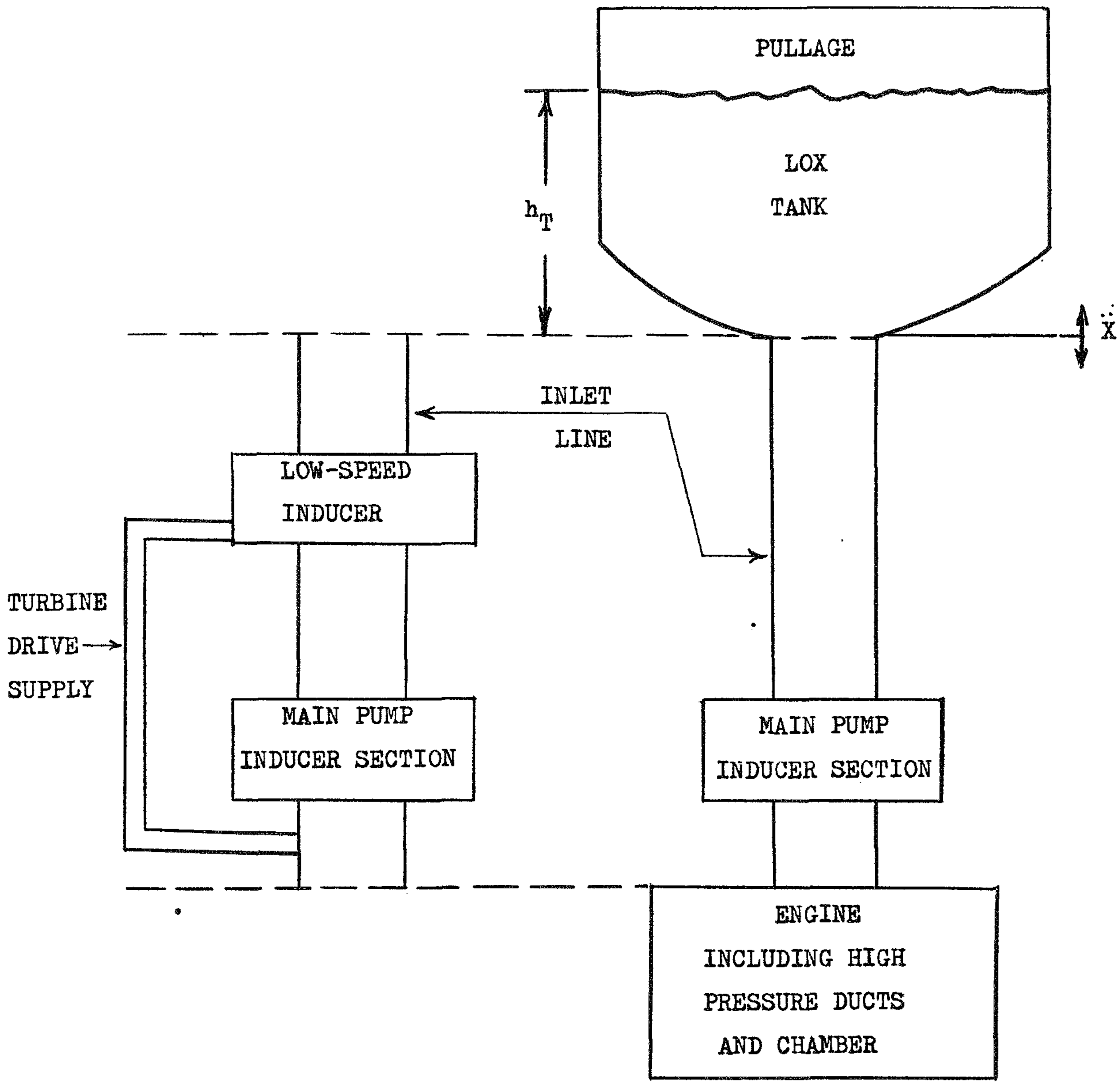

FIGURE 33. SYSTEM SCHEMATIC

ENGINE DYNAMICS

Engine performance was described using a transfer function relating chamber pressure to LOX pump inlet pressure and relating engine LOX flow rate to main pump inducer discharge pressure. Transfer functions for three engines - H-1, F-1 and J-2 were available which can be used in the study. The H-1 and F-1 transfer functions were determined from engine mathematical models and the J-2 transfer function was determined from engine test data. Figures 34 and 35 show the open loop P_c/P_{os} gain and phase lag respectively for these three engines. The general shapes of the curves is similar for all three engines, with the H-1 and F-1 being almost identical. The characteristics of the J-2 and F-1 have been used in vehicle - engine simulations and resulted in reasonable correlation of the oscillations experienced in flight. Since the low speed LOX inducer was designed for the J-2 engine feed system and extensive work has been done to determine J-2 pump and engine dynamics, the J-2 engine and S-II stage center engine inlet duct were used for this study. Also, since the engine transfer functions for the three engines are similar, only the J-2 engine system was considered. The engine transfer functions used were:

$$P_c/P_{os}(S) = \frac{.651\left[1 + S/4.03\right]\left[1 + S/55.7\right]}{\left[1 + S/2.92\right]\left[1 + S/5.79\right]\left[1 + .9245\, S/124.6 + (S/124.6)^2\right]}$$

$$F/P_c = 305$$

$$\dot{W}_{op}/P^1_{os}(S) = \frac{.446\left[1 + S/7.74\right]\left[1 + S/42.9\right]}{\left[1 + S/4.5\right]\left[1 + S/73.6\right]\left[1 + S/280\right]}$$

where:

- F = engine thrust - lbs
- P_c = chamber pressure - lbs/in^2
- P_{os} = main LOX pump inducer inlet pressure - lb/in^2
- S = Laplace transfer variable
- $\dot{W}_{op}$ = main pump (engine) LOX flow rate - lb/sec

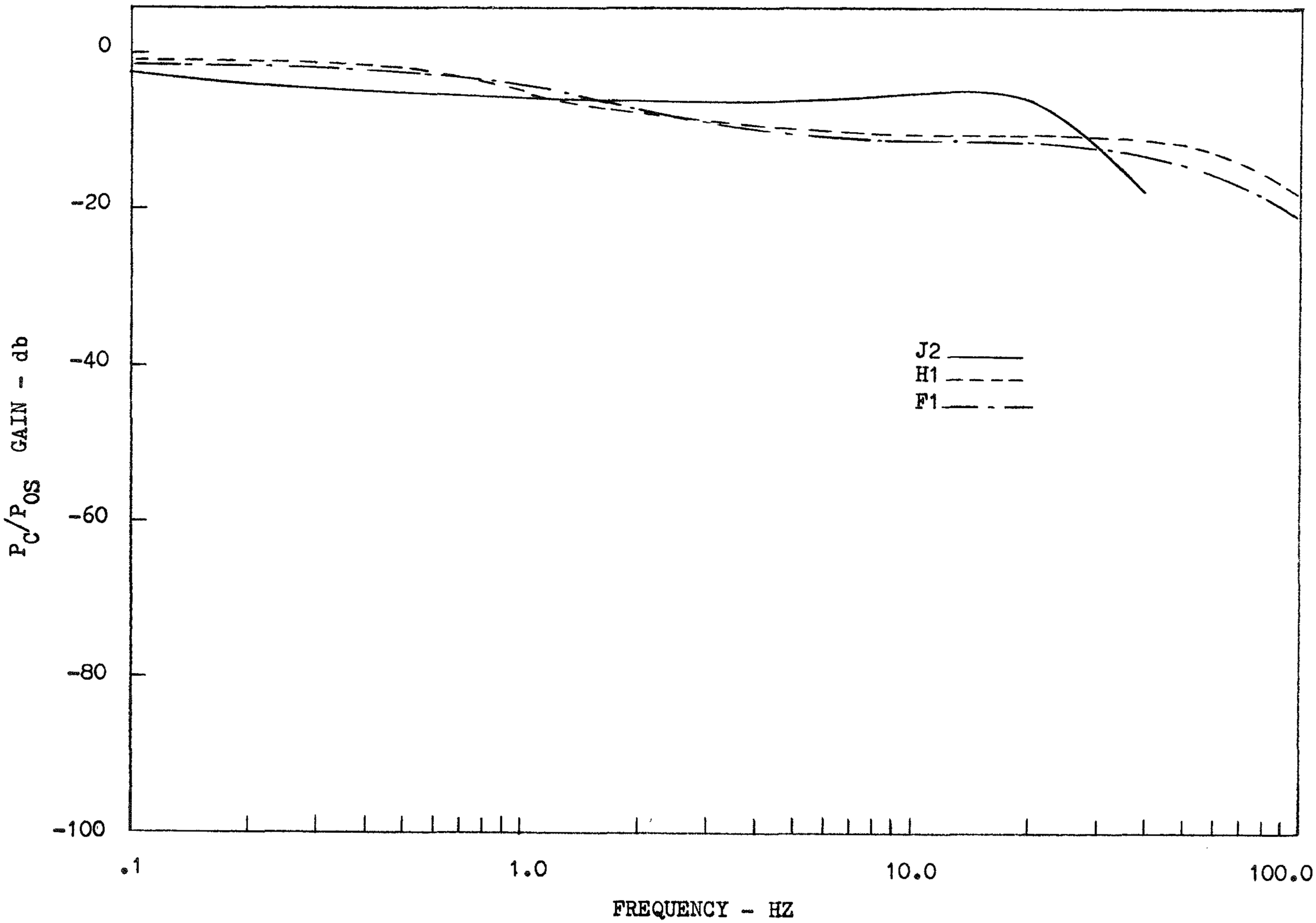

FIGURE 34. COMPARISON OF ENGINE TRANSFER FUNCTION GAIN

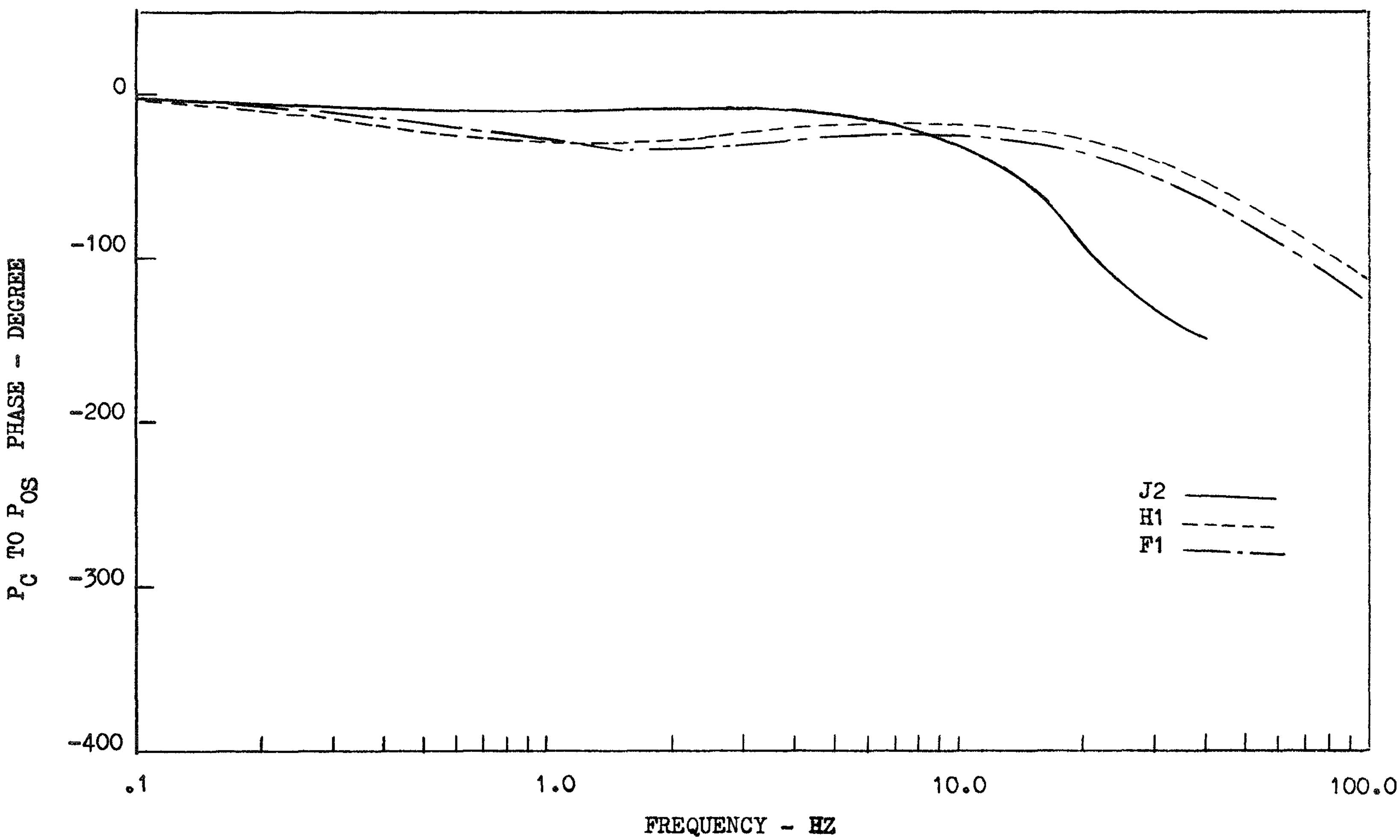

FIGURE 35. COMPARISON OF ENGINE TRANSFER FUNCTION PHASE

PUMP DYNAMICS

The engine flow rate equation requires the main pump inducer discharge pressure to be known. Extensive testing of the J-2 LOX pump has established that the best dynamic representation of the pump consists of an inducer inlet and discharge compliance separated by a resistance and an inertance, and a side branch resistance, inertance and compliance coupled to the discharge compliance. The following are the necessary pump dynamic equations:

$$P_{os} = 1/C_{PI} \int_o^t (\dot{W}_{os} - \dot{W}_p)dt$$

$$P_{os} = \bar{R}_p \dot{W}_p - P_{os}^1 = L_p (d\dot{W}p/dt)$$

$$P_{os}^1 = 1/C_{PD} \int_o^t (\dot{W}_p - \dot{W}_{SB} - \dot{W}_{op})dt$$

$$P_{os}^1 = P_{SB} + \bar{R}_{SB} \dot{W}_{SB} + L_{SB} (d\dot{W}_{SB}/dt)$$

$$P_{SB} = 1/C_{SB} \int_o^t \dot{W}_{SB}\, dt$$

where:

C_{PI}, C_{PD}, & C_{SB} = compliances of the main pump inducer inlet, discharge and side branch - in^2

L_p, L_{SB} = inertances of the main pump inducer and side branch - sec^2/in^2

P_{os}, P_{os}^1, P_{SB} = pressures at the main pump inducer inlet, discharge and side branch - lb/in^2

$\bar{R}_{PI}$ $\bar{R}_{SB}$ = linearized resistances of the main pump inducer and side branch - sec/in^2

$\dot{W}_{os}$, $\dot{W}_p$, $\dot{W}_{op}$, $\dot{W}_{SB}$ = LOX flowrates in the inlet line, main pump inducer ,engine, and side branch. - lb/sec

LOW-SPEED INDUCER DYNAMICS

The low-speed inducer dynamics were represented by an inlet and discharge compliance separated by a resistance and an inertance. The dynamic equations representing the low-speed inducer are:

$$P_{II} = 1/C_{II} \int_o^t (\dot{W}_{II} - \dot{W}_I)\, dt$$

$$P_{II} - \bar{R}_I \dot{W}_I - P_{ID} = L_I \,(dW_I/dt)$$

$$P_{ID} = I/C_{ID} \int_o^t (\dot{W}_I - \dot{W}_{ID})\, dt$$

where:

P_{II}, P_{ID} = pressures at the low-speed inducer inlet and discharge-lb/in^2

C_{II}, C_{ID} = compliances at the low-speed inducer inlet and discharge-in^2

L_I = low speed inducer fluid inertance - sec^2/in^2

$\bar{R}_I$ = liniarized restance of the low-speed inducer - sec/in^2

$\dot{W}_{II}$, $\dot{W}_I$, $\dot{W}_{ID}$ = mass flowrates in the low-speed inducer inlet line, main inducer, and main pump inlet line - lb/sec

A block diagram showing the relationship between the equations is presented in Figure 36. In order to solve the equations, values had to be assigned to the compliances and inertances. The values assigned to establish a reference condition are given in Table I . To determine the effect of individual parameters some of these parameters were varied about their reference value.

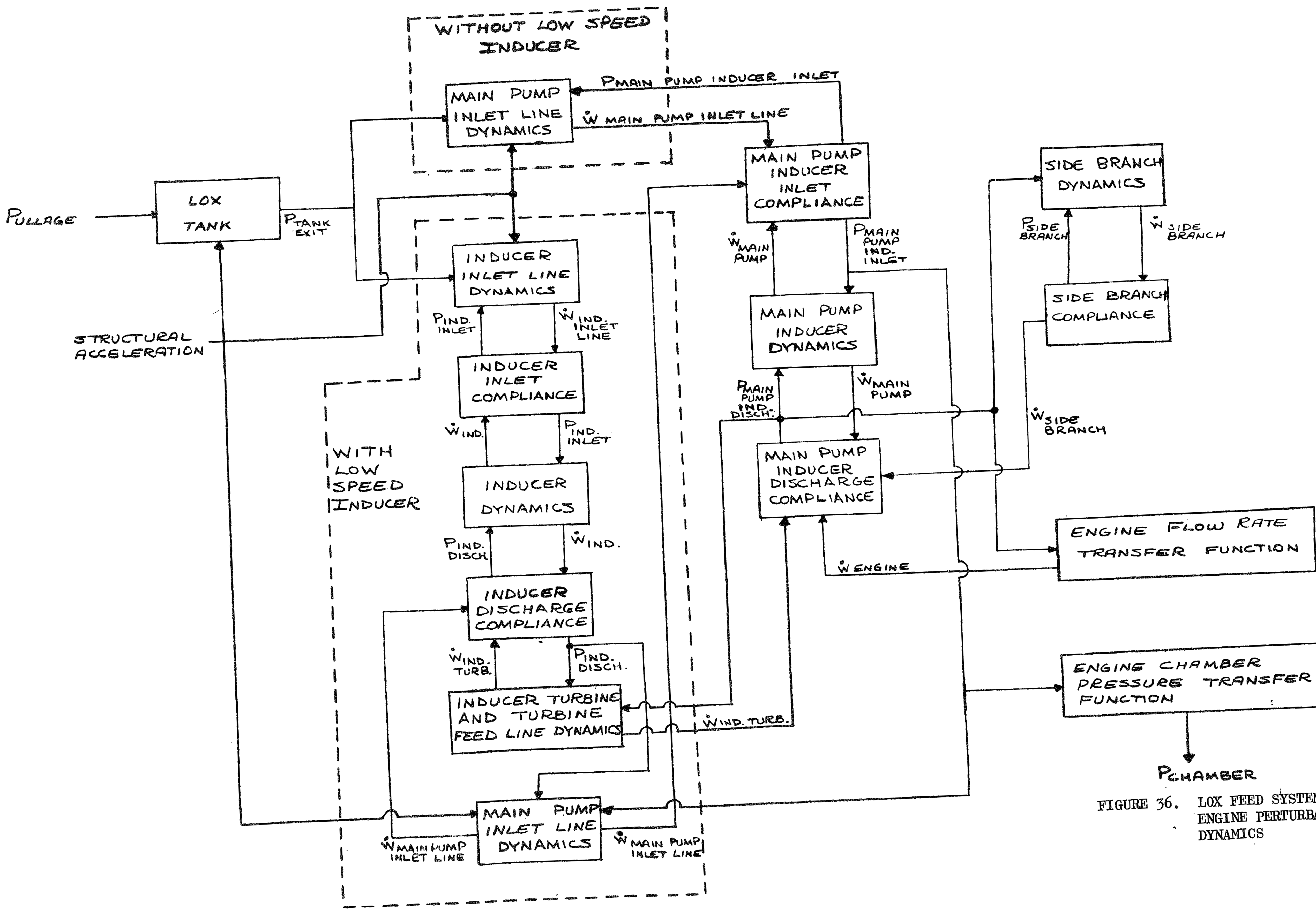

FIGURE 36. LOX FEED SYSTEM AND ENGINE PERTURBATION DYNAMICS

TABLE I

SYSTEM REFERENCE VALUES

PARAMETER	UNITS	WITHOUT LOW-SPEED INDUCER	WITH LOW-SPEED INDUCER
TANK PROPELLANT HEIGHT	inches	50	50
INLET LINE			
RESISTANCE	sec/in^2	.01335	.00667
INERTIA	sec^2/in^2	.00298	.00149
INDUCER			
INLET COMPLIANCE	in^2	-	.025
FLUID INERTIA	sec^2/in^2	-	.04
OUTLET COMPLIANCE	in^2	-	.001
RESISTANCE	sec/in^2	-	.393
COUPLING LINE			
RESISTANCE	sec/in^2	-	.00667
INERTIA	sec^2/in^2	-	.00149
MAIN PUMP			
INLET COMPLIANCE	in^2	.00667	.00667
FLUID INERTIA	sec^2/in^2	.0025	.0025
OUTLET COMPLIANCE	in^2	.001	.001
RESISTANCE	sec/in^2	.363	.363
SIDE BRANCH RESISTANCE	sec/in^2	.5	.5
INERTIA	sec^2/in^2	.02	.02
COMPLIANCE	in^2	.00667	.00667
FLUID DENSITY	lbs/in^3	.0413	.0413
TURBINE FEED LINE			
RESISTANCE	sec/in^2	-	29.2
INERTIA	sec^2/in^2	-	.0395

FREQUENCY RESPONSE ANALYSIS

To evaluate the effects of the low-speed inducer on engine feed system responses it must be recalled that if the closed loop is unstable it will be at a structural frequency where the loop gain is greater than one and the loop phase shift is zero. If the gain of the engine-LOX feed system portion of the loop can be reduced, the effect is stabilizing. At a structural resonance, engine thrust leads the structural acceleration by 90 degrees. To provide the zero degree phase condition for instabilities, the thrust must lag the acceleration by 90^o through the engine and LOX feed system. Therefore, changing the phase lag of thrust to acceleration in the range of critical structural frequencies is stabilizing. The critical frequency range encountered on rocket-powered vehicles is about 5 to 20 Hz.

It should be noted that the gain expresses the ratio of chamber pressure variation in lbs/in^2 to structural acceleration in inches/second squared. If the structural acceleration were expressed in terms of g's rather than $inches/sec^2$, the gain curves would be shifted by + 52 db, the -55 db shown in Figure 37 at .1 Hz becoming -3db. A change in units does not affect the phase shift.

SYSTEM WITHOUT LOW-SPEED INDUCER

The gain and phase lag data determined for the system without a low-speed LOX inducer are shown in Figures 37 and 38. The gain plot is fairly flat from 0.1 Hz to 40 Hz, with the resonance due to the inlet system at about 36 Hz. Other noticeable effects are the engine resonance near 20 Hz and the side branch anti-resonance at about 15 Hz.

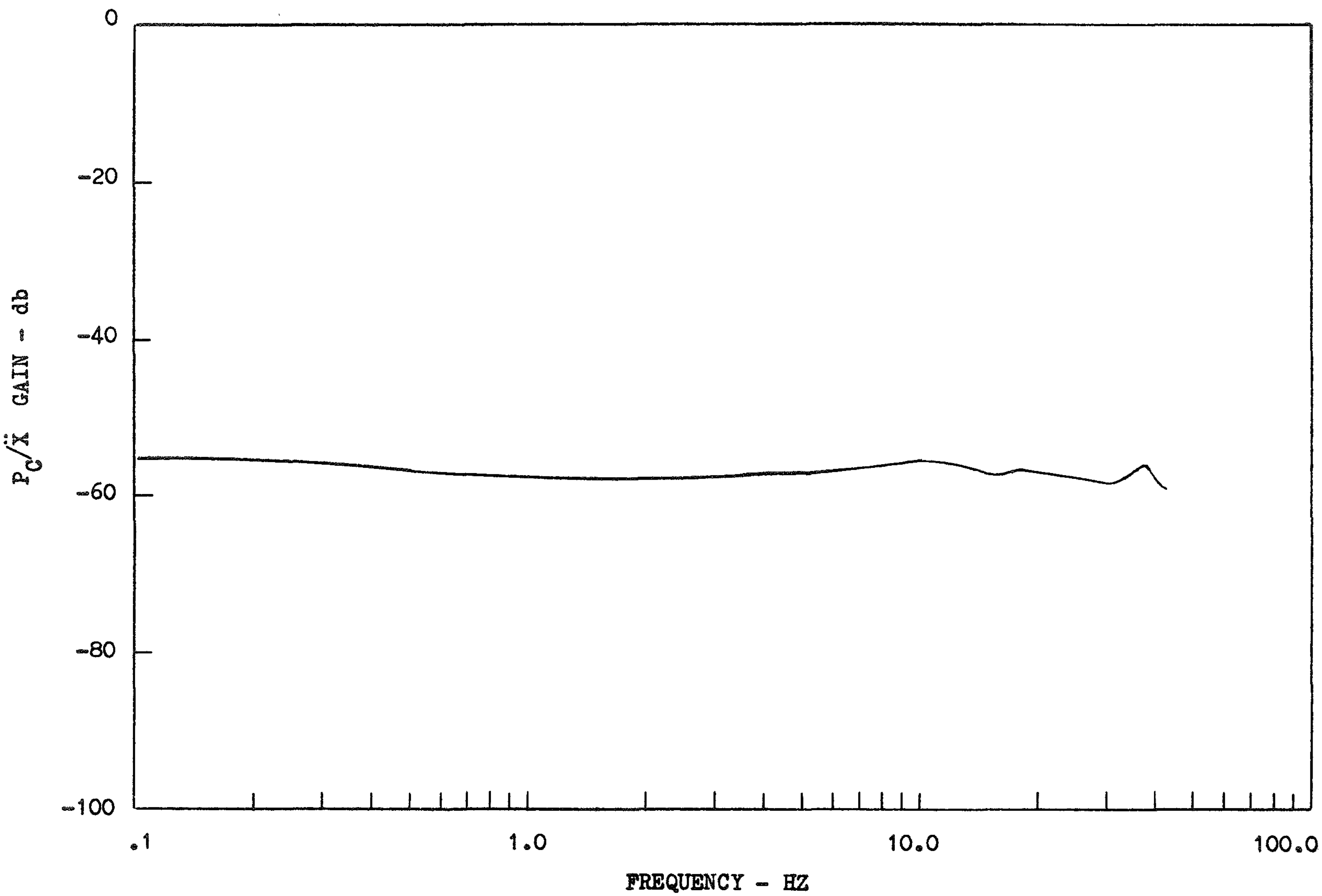

FIGURE 37. S II CENTER ENGINE GAIN

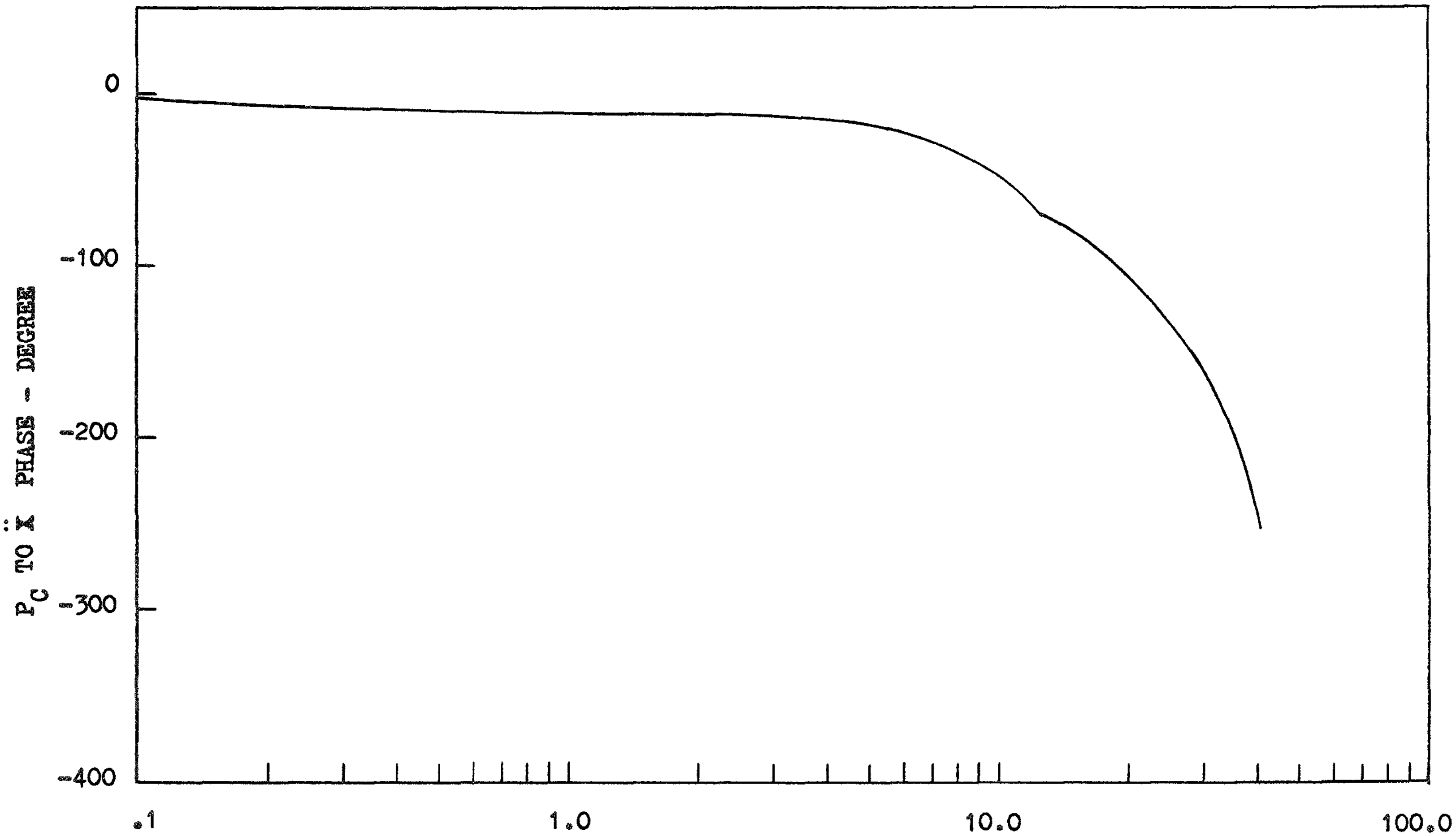

FIGURE 38. S II CENTER ENGINE PHASE

SYSTEM WITH LOW-SPEED INDUCER

A low-speed hydraulic turbine driven inducer was located in the LOX feed line halfway between the tank exit and the main pump. The following nominal values for the low-speed inducer were used:

$$1/C_{II} = 40.0 \text{ in}^{-2}$$

$$L_I = 25.0 \text{ sec}^2/\text{in}^2$$

$$I/C_{ID} = 1000.0 \text{ in}^{-2}$$

Gain and phase lag results for the reference run are shown in Figures 39 and 40. For comparison, the system response without a low-speed inducer is shown in the same figures. The low-speed inducer reduces the gain between approximately 5 and 25 Hz and increases the phase lag for essentially all frequencies in the range covered.

Analysis of the frequency response data, for the low-speed inducer system, shows a resonance occurring at approximately 5 Hz due to the combination of the main pump inlet compliance and the fluid inertance of the inducer and coupling line. For the feed system considered the inducer fluid inertance is much larger than the coupling line fluid inertance so that changing the coupling line dimensions has very little effort on the system resonances. Also evident are the anti-resonance of the main pump side branch occurring at about 13 Hz and the resonance at 26 Hz due to the inducer inlet compliance and inlet line inertance.

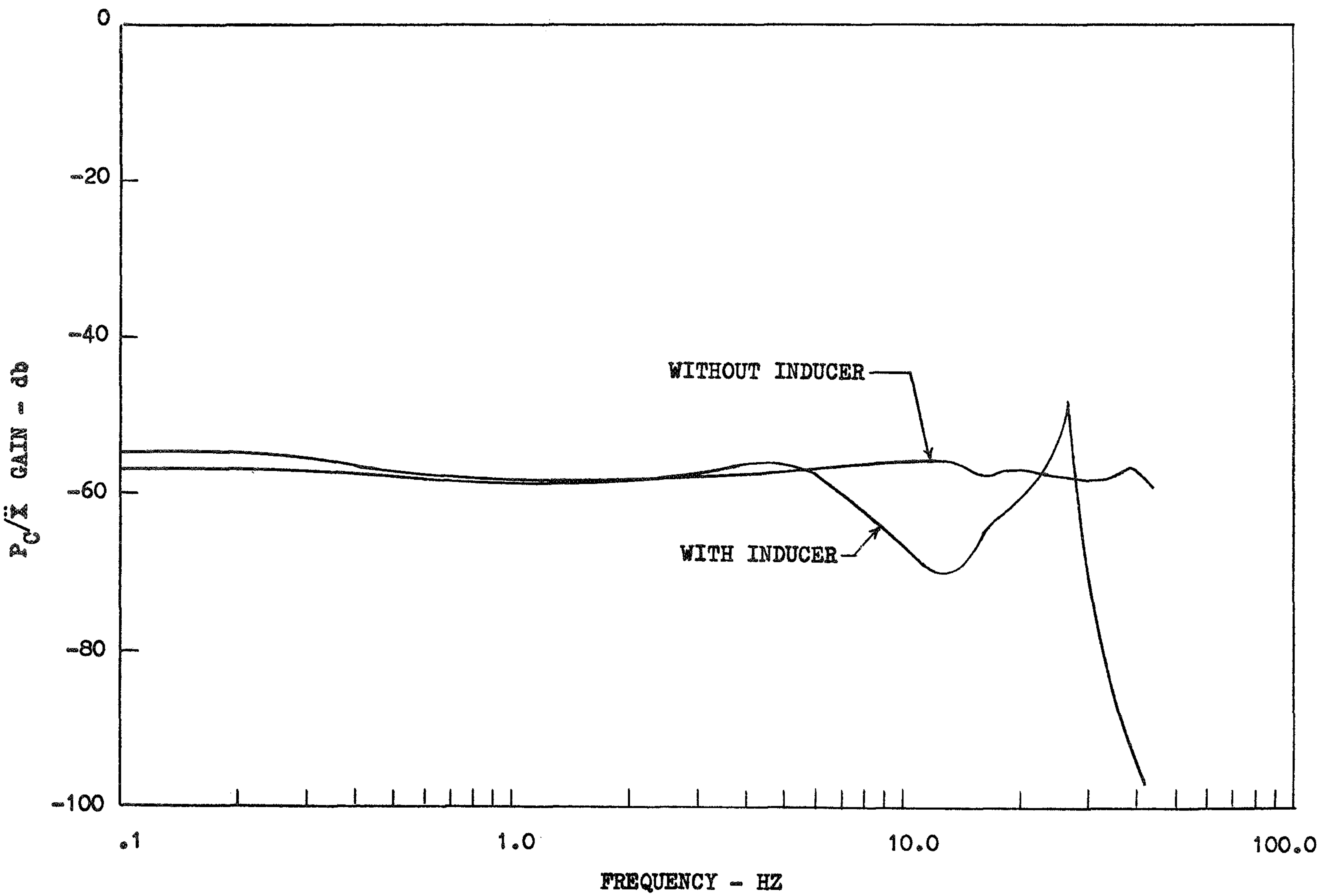

FIGURE 39. COMPARISON OF S II CENTER ENGINE GAIN WITH AND WITHOUT A LOW-SPEED LOX INDUCER

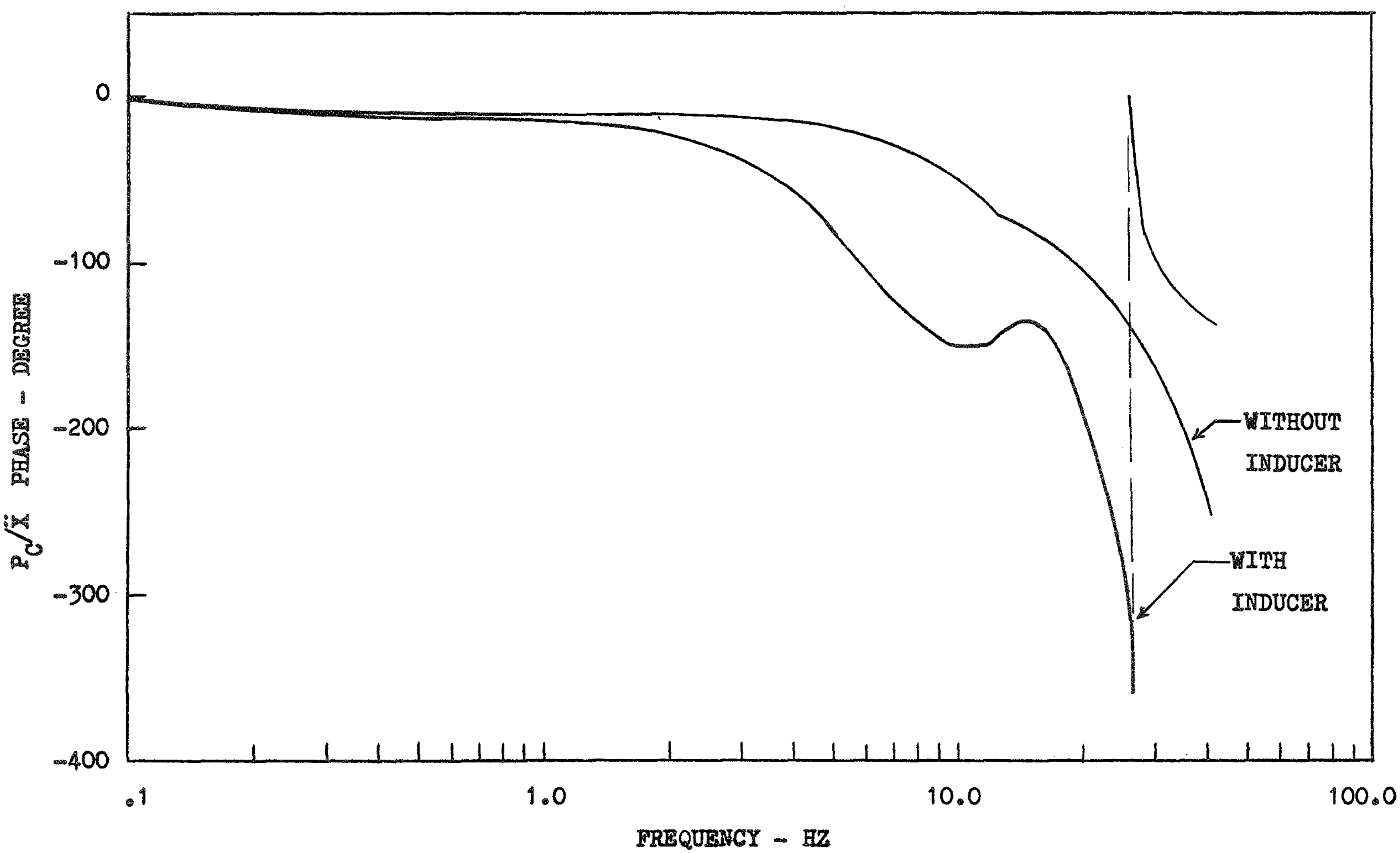

FIGURE 40. COMPARISON OF S II CENTER ENGINE PHASE WITH AND WITHOUT A LOW-SPEED LOX INDUCER

EFFECT OF VARYING LOW-SPEED INDUCER DYNAMIC PARAMETERS

Inducer Inlet Compliance

The effect of increasing the inducer inlet compliance on system frequency response characteristics is shown in Figures 41 and 42 ; the dashed curves represent a compliance value of 2 in^2 and the solid curves represent the reference compliance of 0.025 in^2. The inlet line resonance is lowered to approximately 3 Hz; the gain is significantly decreased above approximately 4 Hz, and more phase shift is evident for nearly all frequencies in the range considered.

Dynamic testing of pumps and a low-speed inducer has shown that the inlet compliance varies with NPSH (net positive suction head); the compliance increasing with decreasing NPSH. Therefore, feed line frequencies can be controlled somewhat by control of NPSH. It must be remembered that the frequency is also dependent on the inlet line fluid inertia and, in some cases, the inlet duct mechanical compliance, in addition to the fluid compliance. To date, no correlation has been found between compliance-NPSH functions for different turbopumps. To determine this relationship, a carefully controlled series of tests including the pump and low-speed inducer would be required.

Inducer Fluid Inertance

Figures 43 and 44 show the effects on gain and phase shift due to increasing the inertance of the fluid in the inducer. The dashed curves represent an inertance value of 0.25 sec^2/in^2 and the solid curves represent the reference inertance of 0.04 sec^2/in^2. The increased inertance reduces the gain for frequencies above approximately 1 Hz, and increases the phase shift up to about 20 Hz. The fluid inertance is generally difficult to determine and values used for the J-2 turbopump were derived from test data.

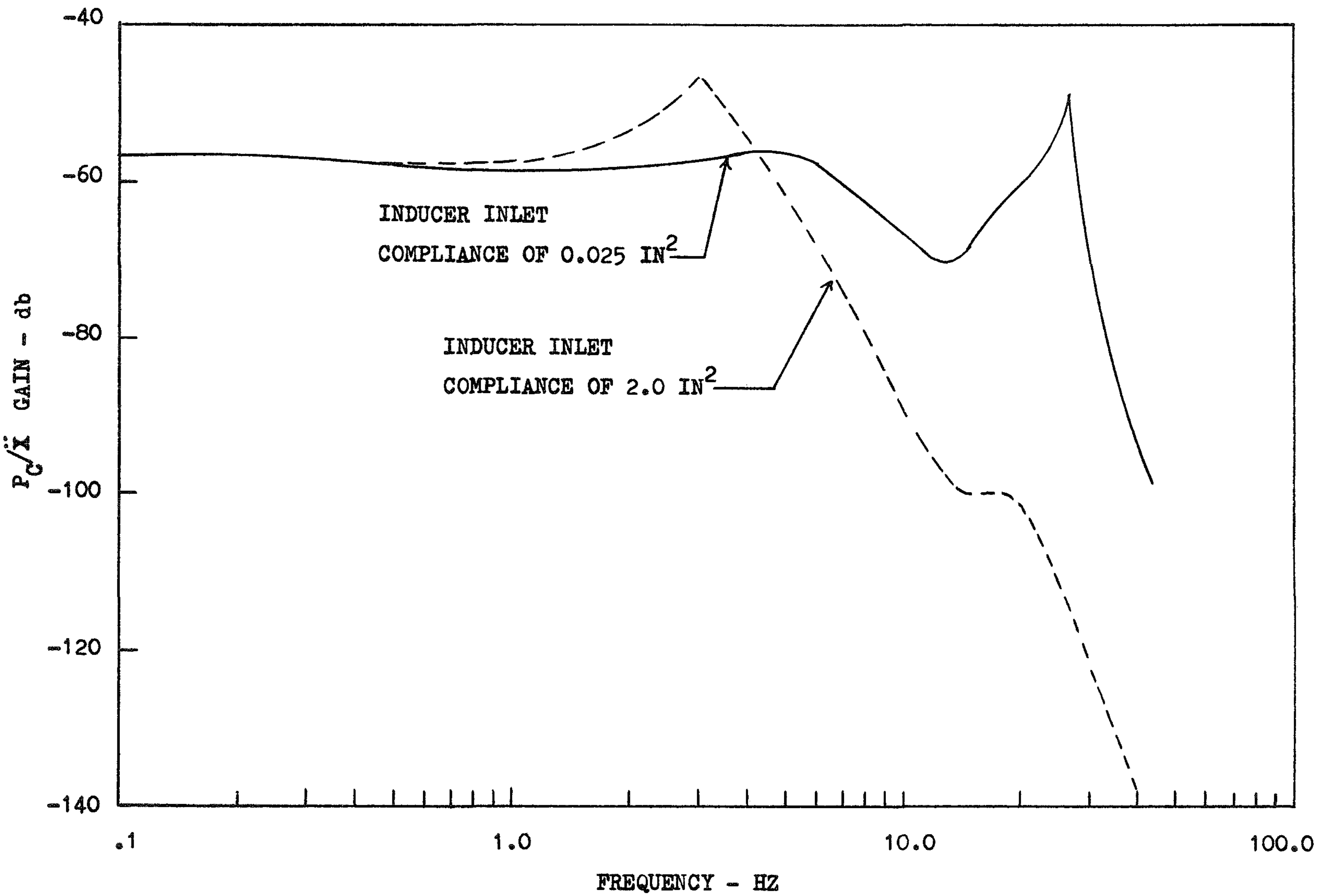

FIGURE 41. EFFECT OF INDUCER INLET COMPLIANCE ON GAIN

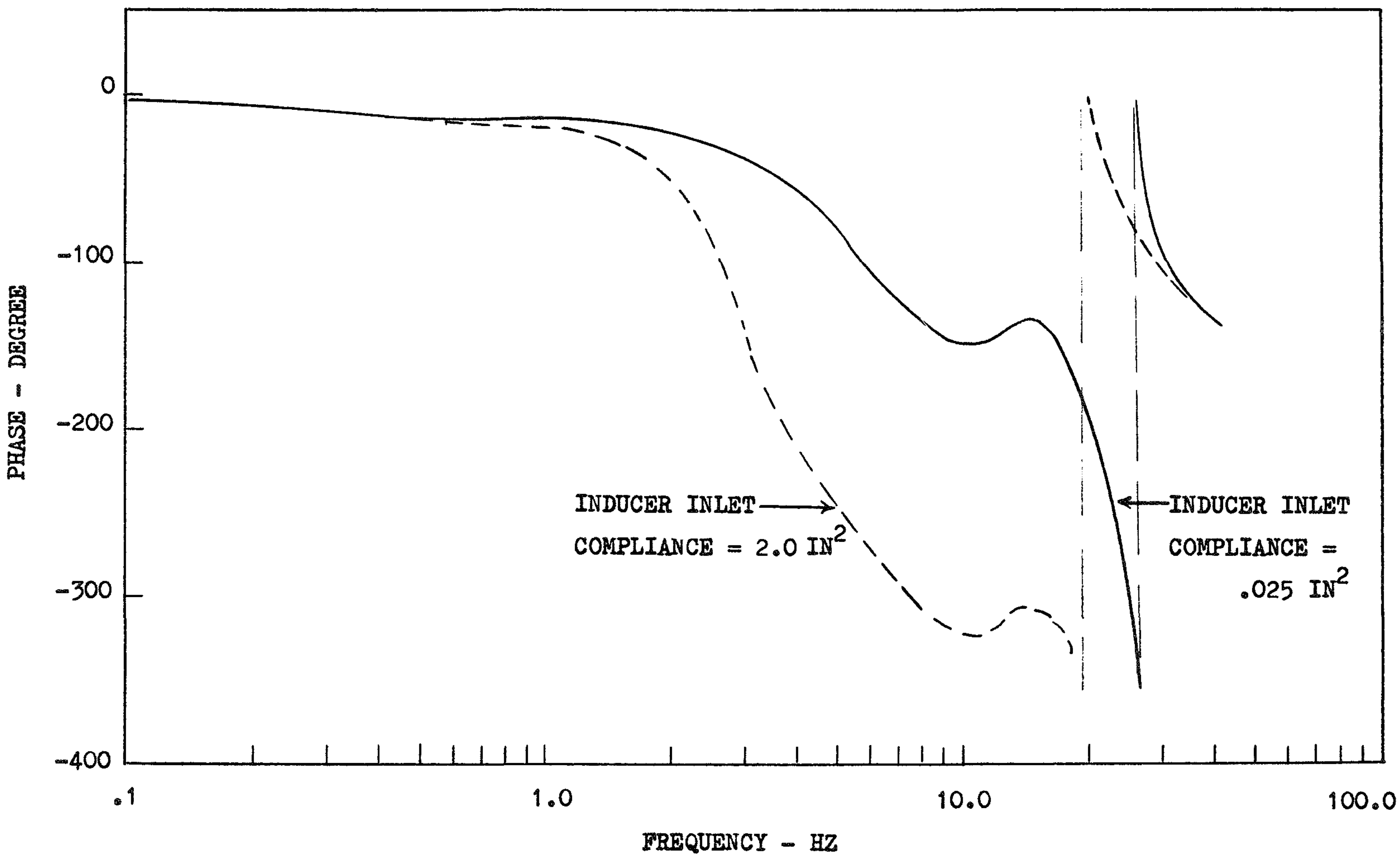

FIGURE 42. EFFECT OF INDUCER INLET COMPLIANCE ON PHASE

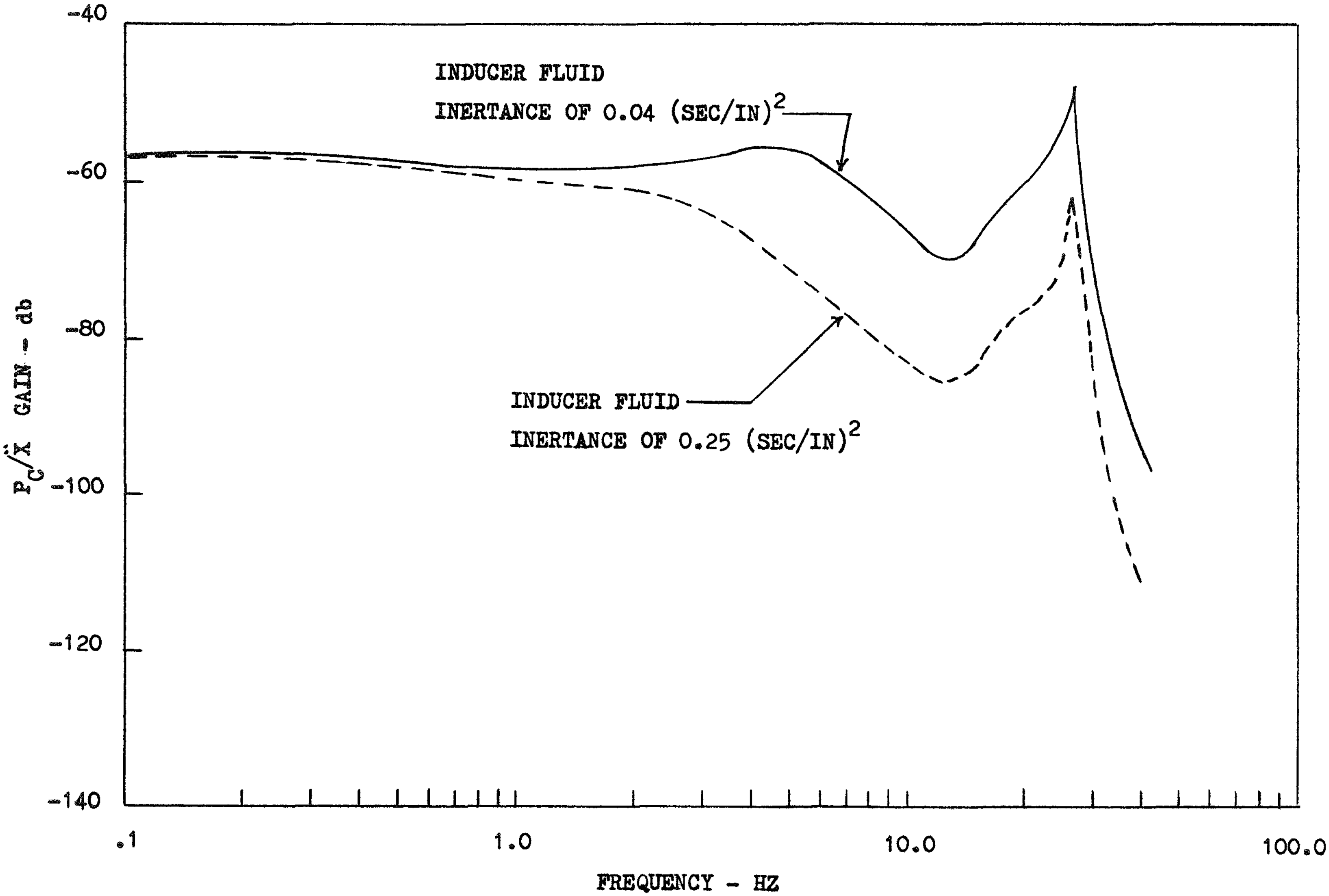

FIGURE 43. EFFECT OF INDUCER INERTANCE ON GAIN

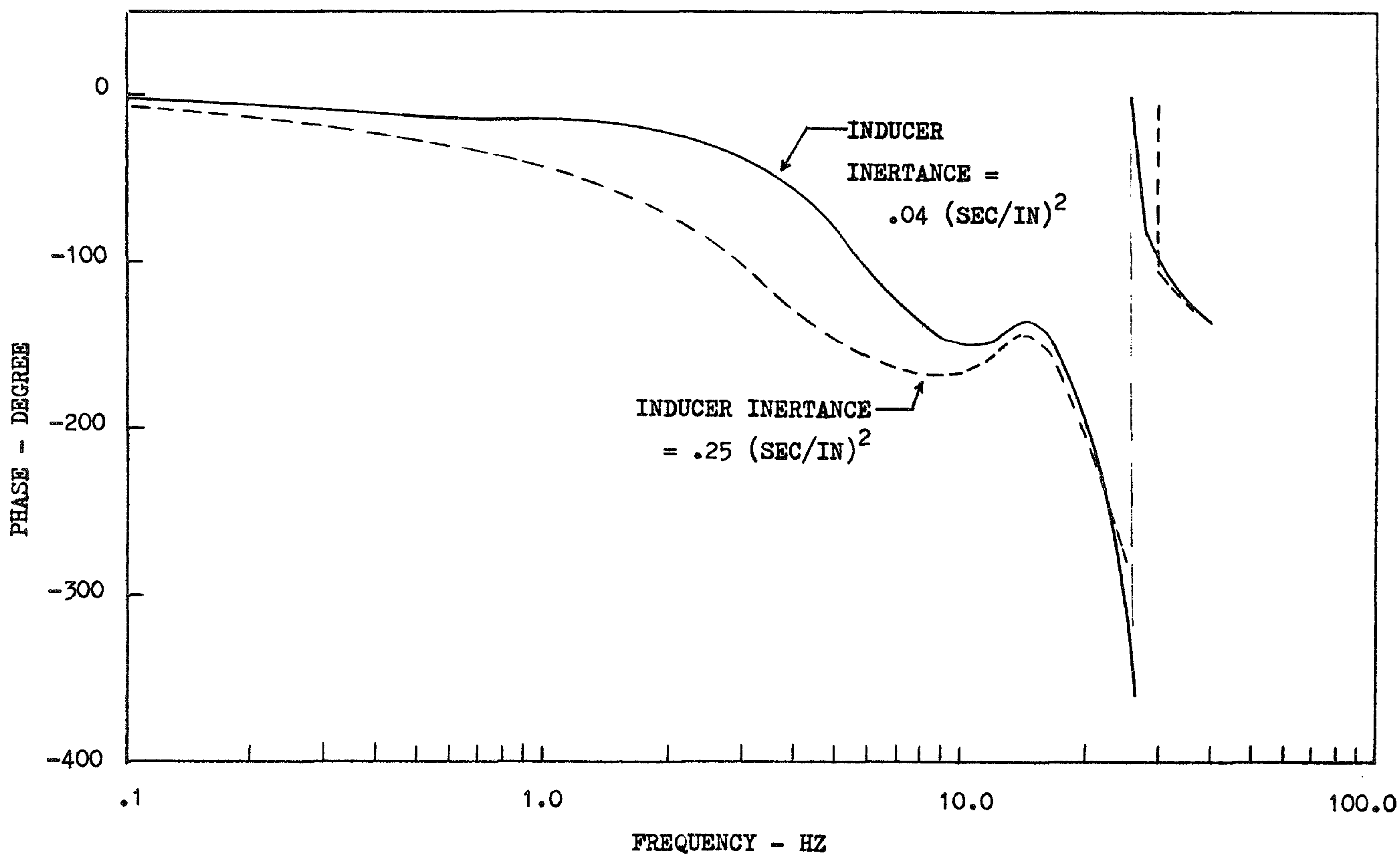

FIGURE 44. EFFECT OF INDUCER INERTANCE ON PHASE

Flight Acceleration Simulation Effects

The effect of simulated flight acceleration inputs are shown in Figures 45 and 46. In addition to the tank exit pressure oscillations generated by acceleration, pressure oscillations caused by the structural acceleration acting on the respective fluid column heights were included at the inducer and main pump inlets. The only significant effect observed is an increase in gain of approximately 10 db.

Two other inducer parameters were varied and they produced insignificant changes in the system frequency response output. These parameters were, (1) the fluid inertance of the inducer turbine feed line (varied from one-half to twice its reference value of 0.0395 sec^2/in^2) and, (2) the inducer discharge compliance (varied from its reference value of 0.001 in^2 to 0.002 in^2).

Effects of Varying Main Pump Inlet Compliance

In a feed system with a low-speed inducer, the inlet pressure to the main pump would be expected to be high enough to prevent any serious cavitation. As a result, the main pump compliances will be small and probably will not vary with inducer NPSH. The pump inlet compliance curves, determined experimentally for the H-1, F-1, and J-2 turbopumps, are presented in Figure 47. Due to the wide range of inlet compliance values, frequency response data was obtained for variation in this variable over the range of test results. The results, presented in Figures 48 and 49 , show that a softer (larger) main pump inlet compliance reduces the resonant frequency associated with the inducer inertance. This, in turn, reduces the gain above 2 Hz.

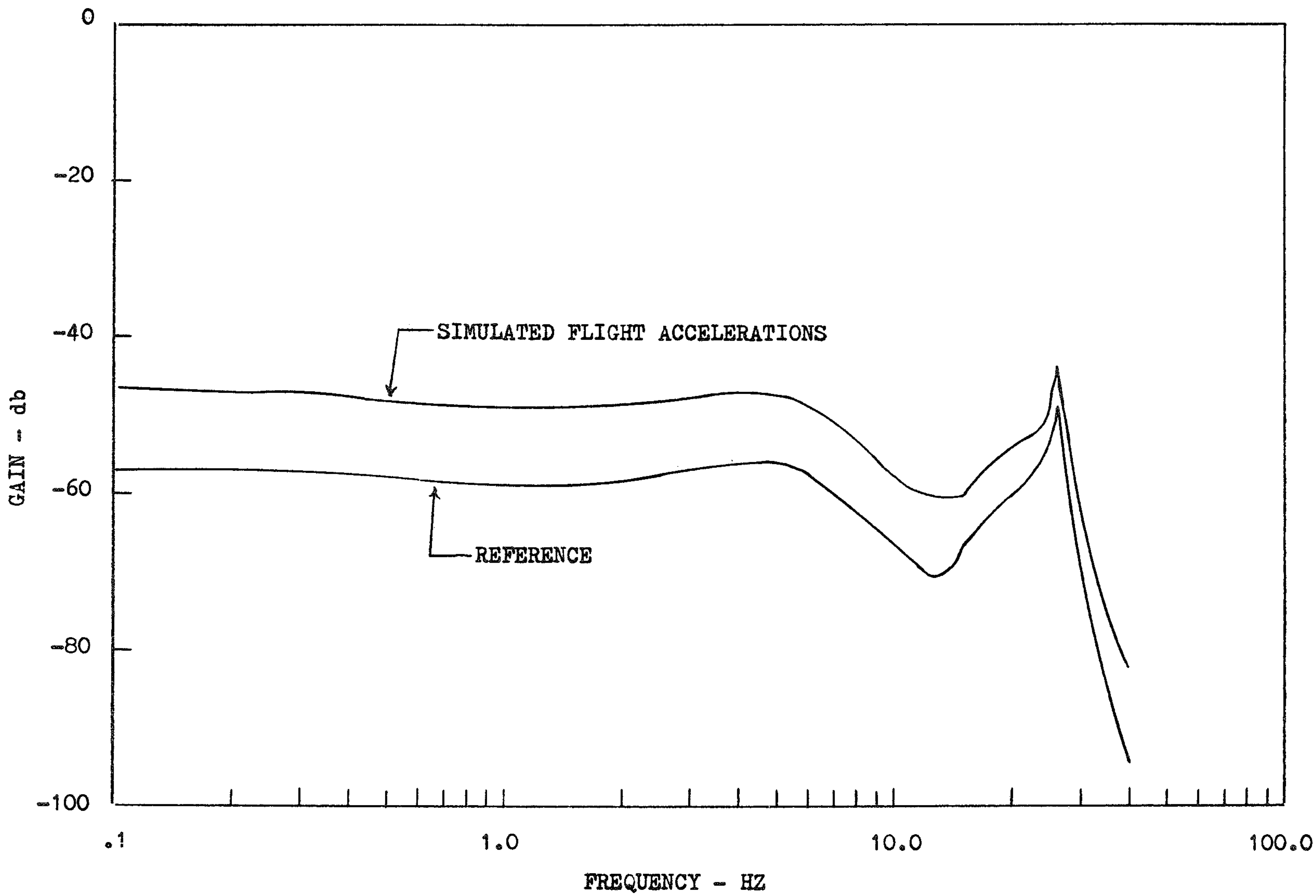

FIGURE 45. EFFECT OF SIMULATED FLIGHT ACCELERATION INPUTS ON GAIN

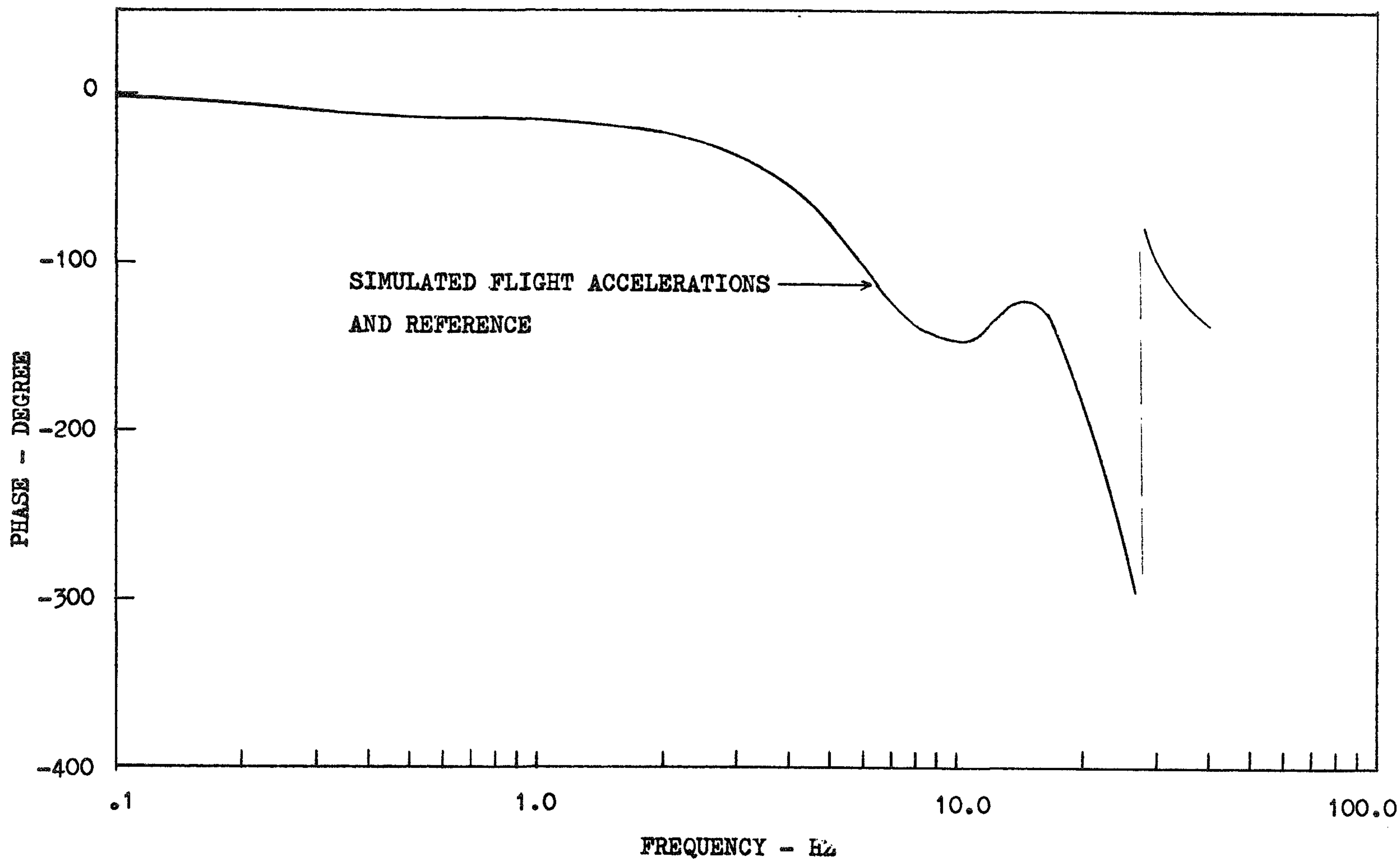

FIGURE 46. EFFECT OF SIMULATED FLIGHT ACCELERATION INPUTS ON PHASE

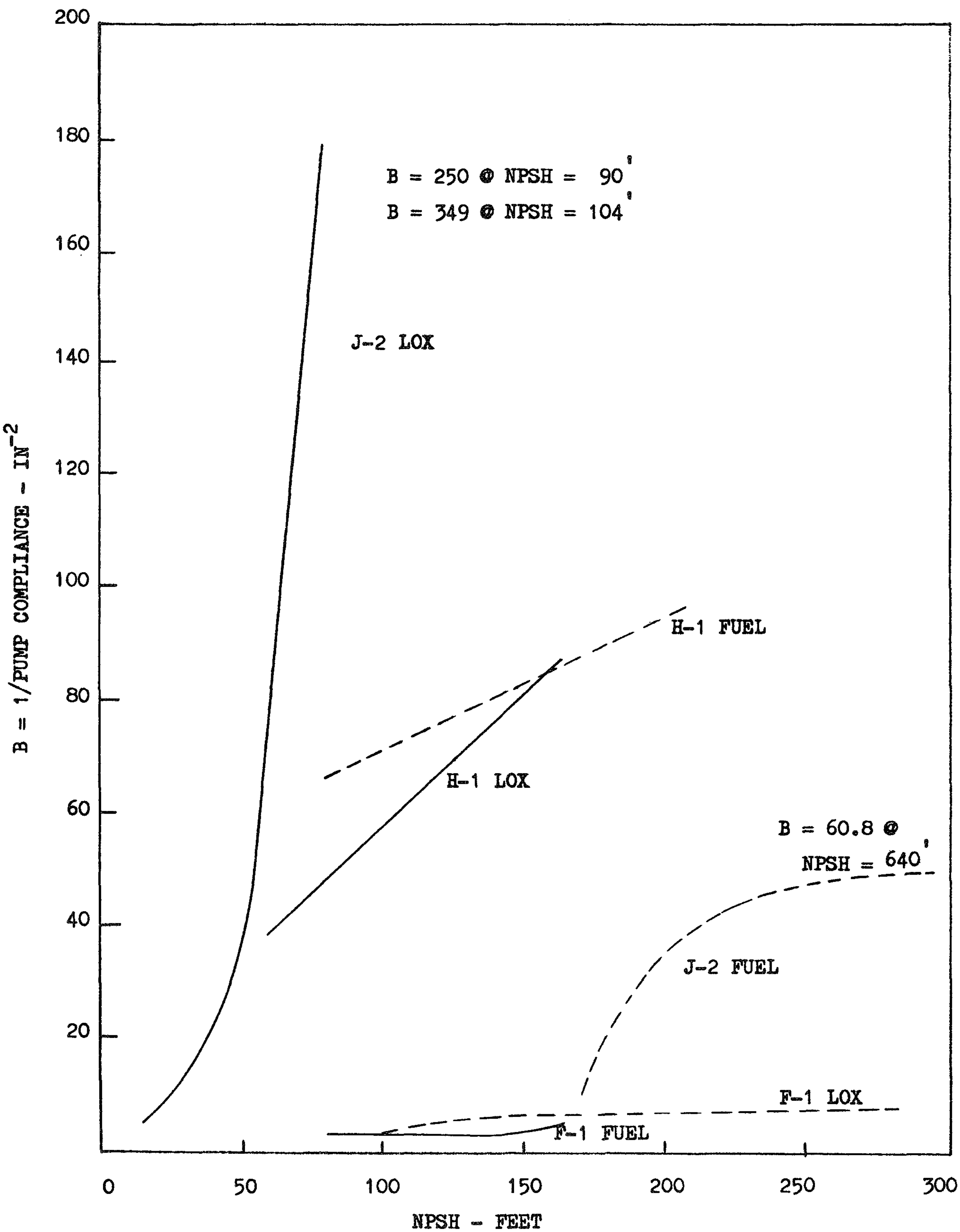

FIGURE 47. TYPICAL PUMP INLET COMPLIANCE VALUES

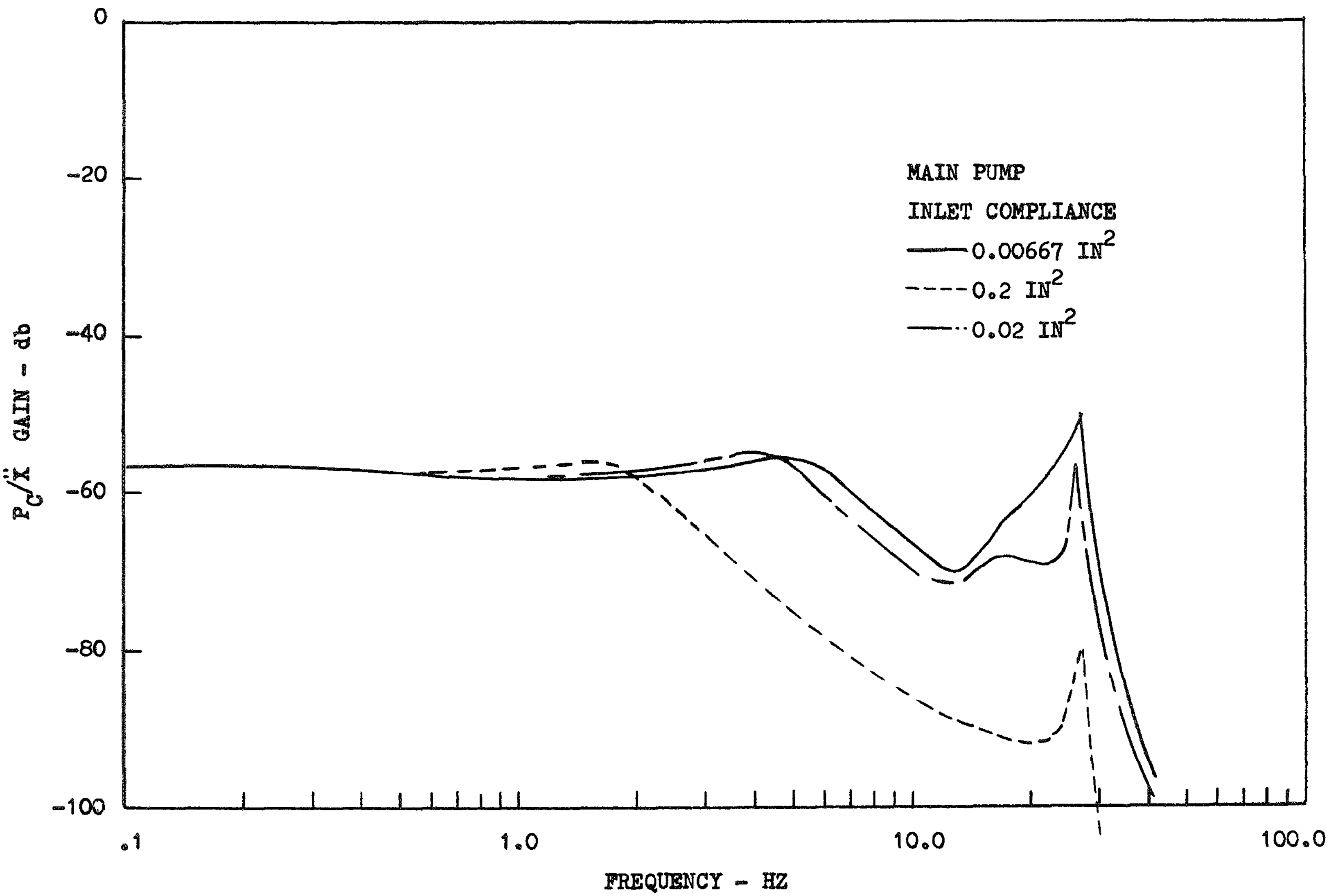

FIGURE 48. EFFECT OF MAIN PUMP INLET COMPLIANCE ON GAIN

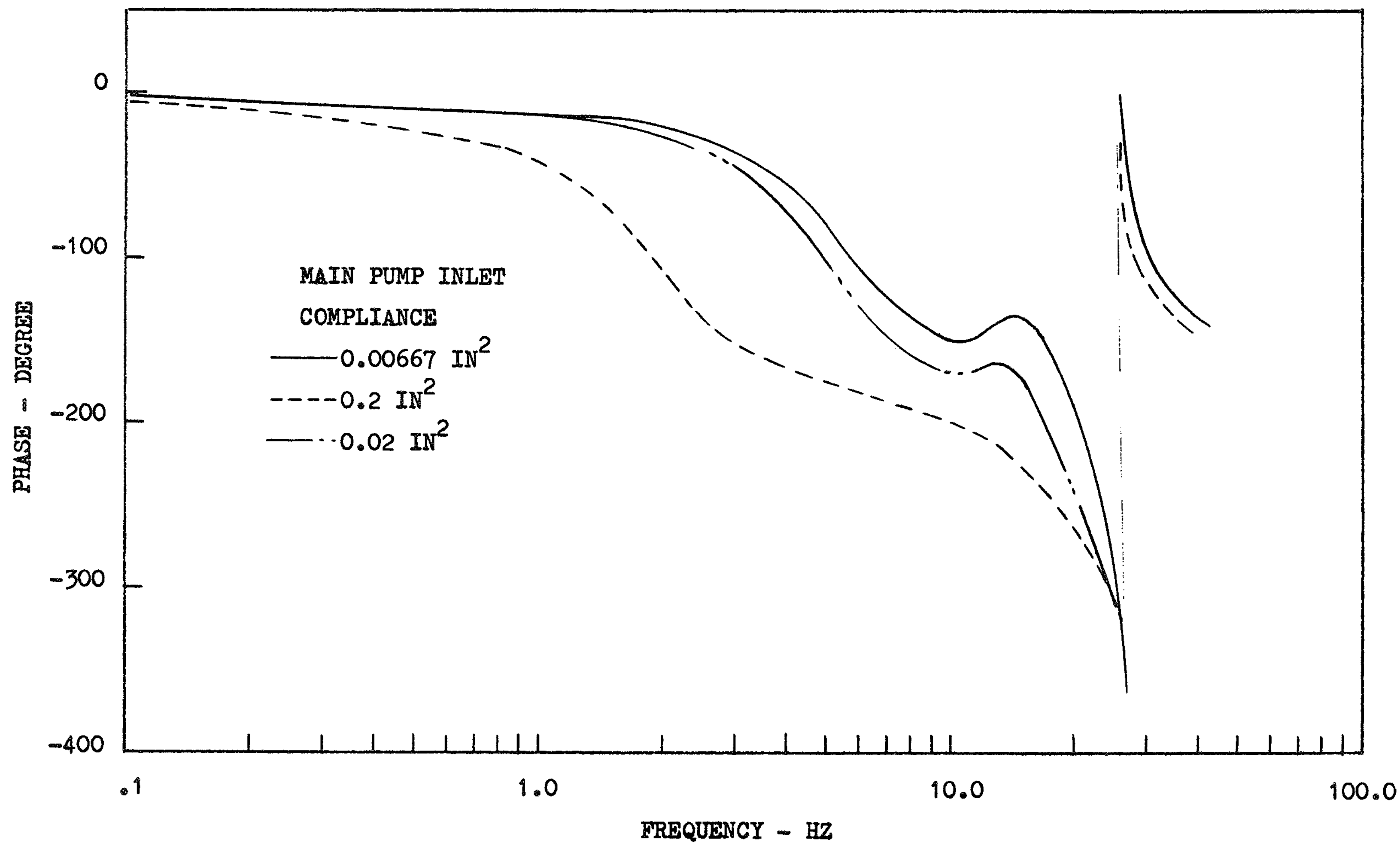

FIGURE 49. EFFECT OF MAIN PUMP INLET COMPLIANCE ON PHASE

CONCLUSIONS

Based on the results of this study, the following conclusions are drawn:

1. The gain and phase of engine thrust to structural acceleration can be significantly altered using a low-speed inducer located in the LOX feed line upstream of the main pump.
2. The fluid inertance associated with the low-speed inducer and the main pump inlet compliance cause a system resonance. If the frequency associated with this resonance is low, a beneficial gain reduction above this frequency is achieved. Therefore the low-speed inducer fluid inertance and the main pump inlet compliance are key parameters.
3. The resonance resulting in the maximum gain is caused by the low-speed inducer inlet line. Therefore the low-speed inducer inlet compliance is the third key parameter.
4. The maximum gain reduction occurs when the low-speed inducer inlet line frequency is low relative to possible structural resonant frequencies. The low NPSP capability of the low-speed inducer provides the potential of reducing inlet line frequency and avoid resonant oscillation with the vehicle structure.

REFERENCES

1. R-7970, Investigation of 17-Hertz Closed-Loop Instability on S-II Stage of Saturn V.

2. R-6813, Engine System Transfer Functions for Support of S-IB Vehicle Longitudinal Stability (POGO)

3. R-6929, Engine System Transfer Functions for Support of S-V Vehicle Longitudinal Stability (POGO) Analysis Program

4. R-7747, NASA CR-73518, The Transient Performance of a Hydraulic-Turbine-Driven Inducer: Computer Predictions and Test Verification

APPENDIX A

ENGINE START MODEL ANALOG COMPUTER DIAGRAMS

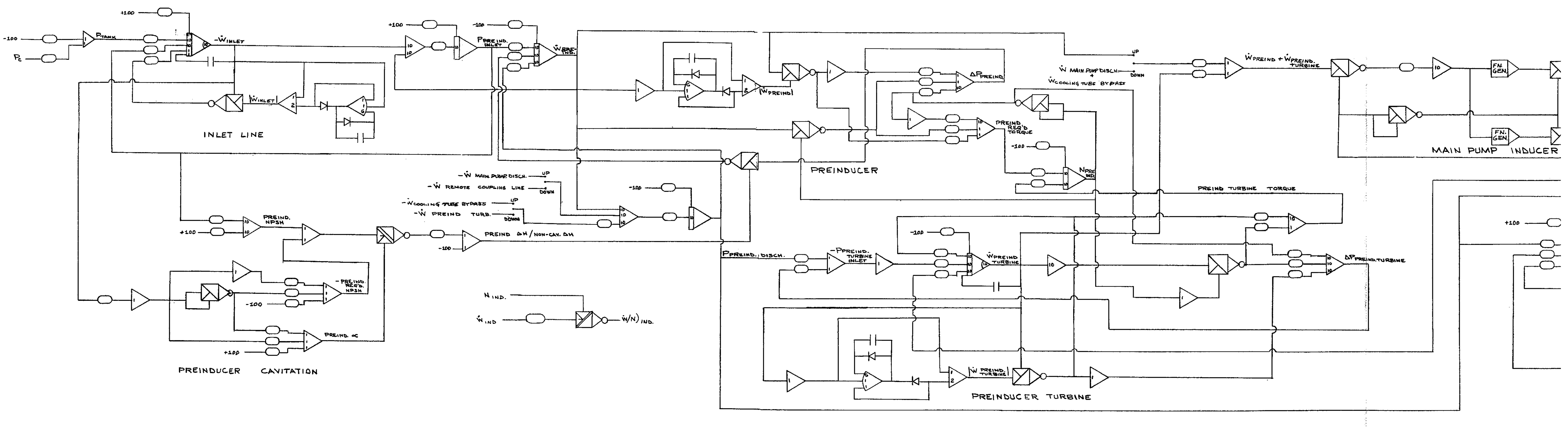
INLET LINE
PREINDUCER
PREINDUCER CAVITATION
PREINDUCER TURBINE
MAIN PUMP INDUCER
PREIND TURBINE TORQUE
PREIND ΔH / NON-CAV. ΔH
-Ẇ MAIN PUMP DISCH.
-Ẇ REMOTE COUPLING LINE
-Ẇ COOLING TUBE BYPASS
-Ẇ PREIND TURB.

2

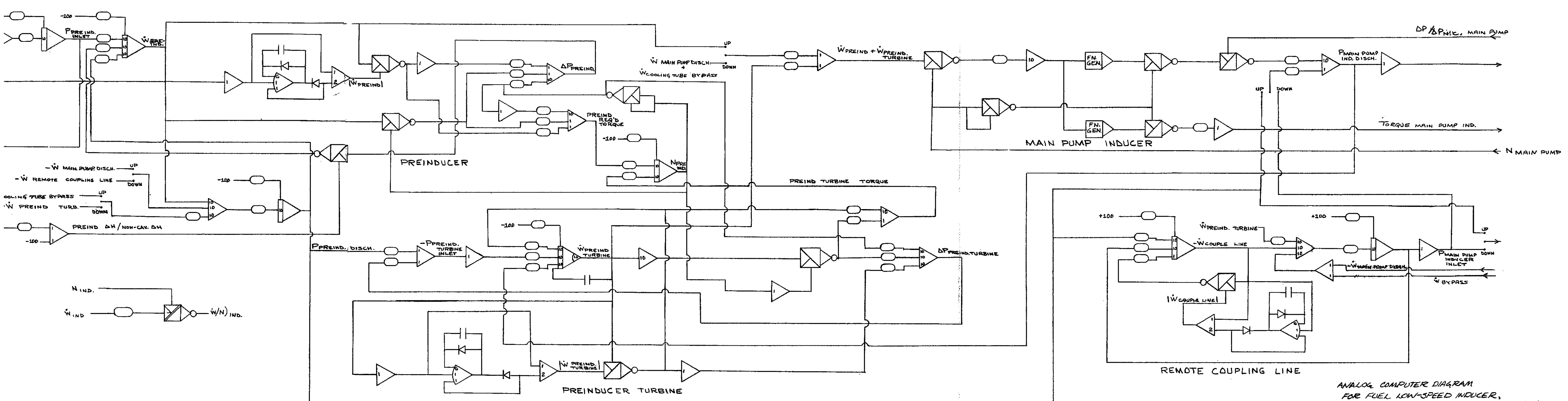

ANALOG COMPUTER DIAGRAM
FOR FUEL LOW-SPEED INDUCER,
MAIN FUEL PUMP INDUCER,
AND CONNECTING LINES

A-1

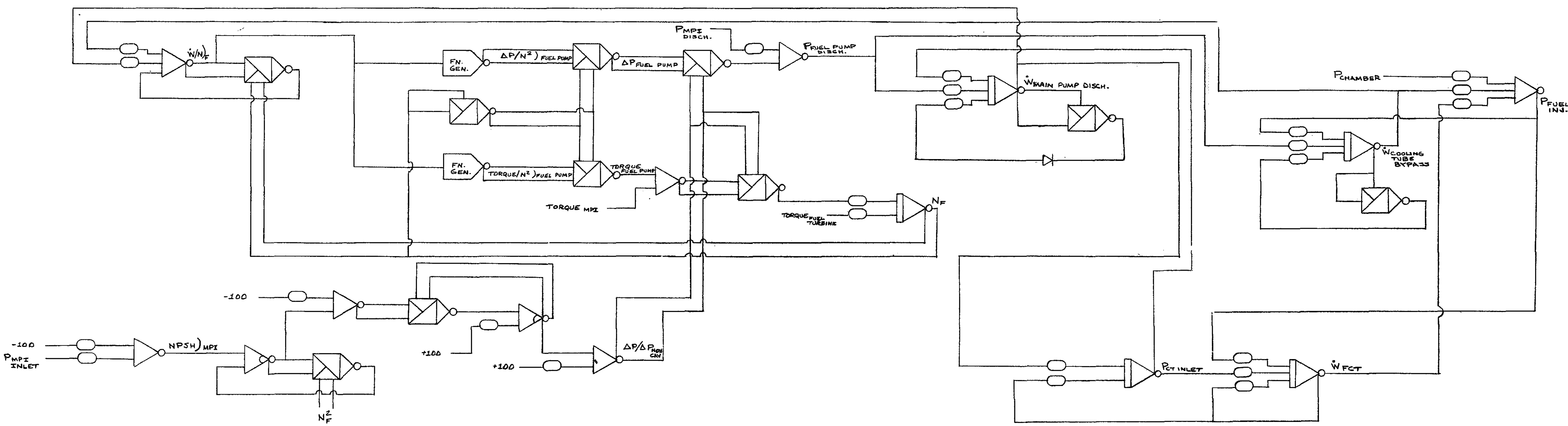

ANALOG COMPUTER DIAGRAM FOR MAIN FUEL PUMP AND HIGH-PRESSURE FUEL LINES

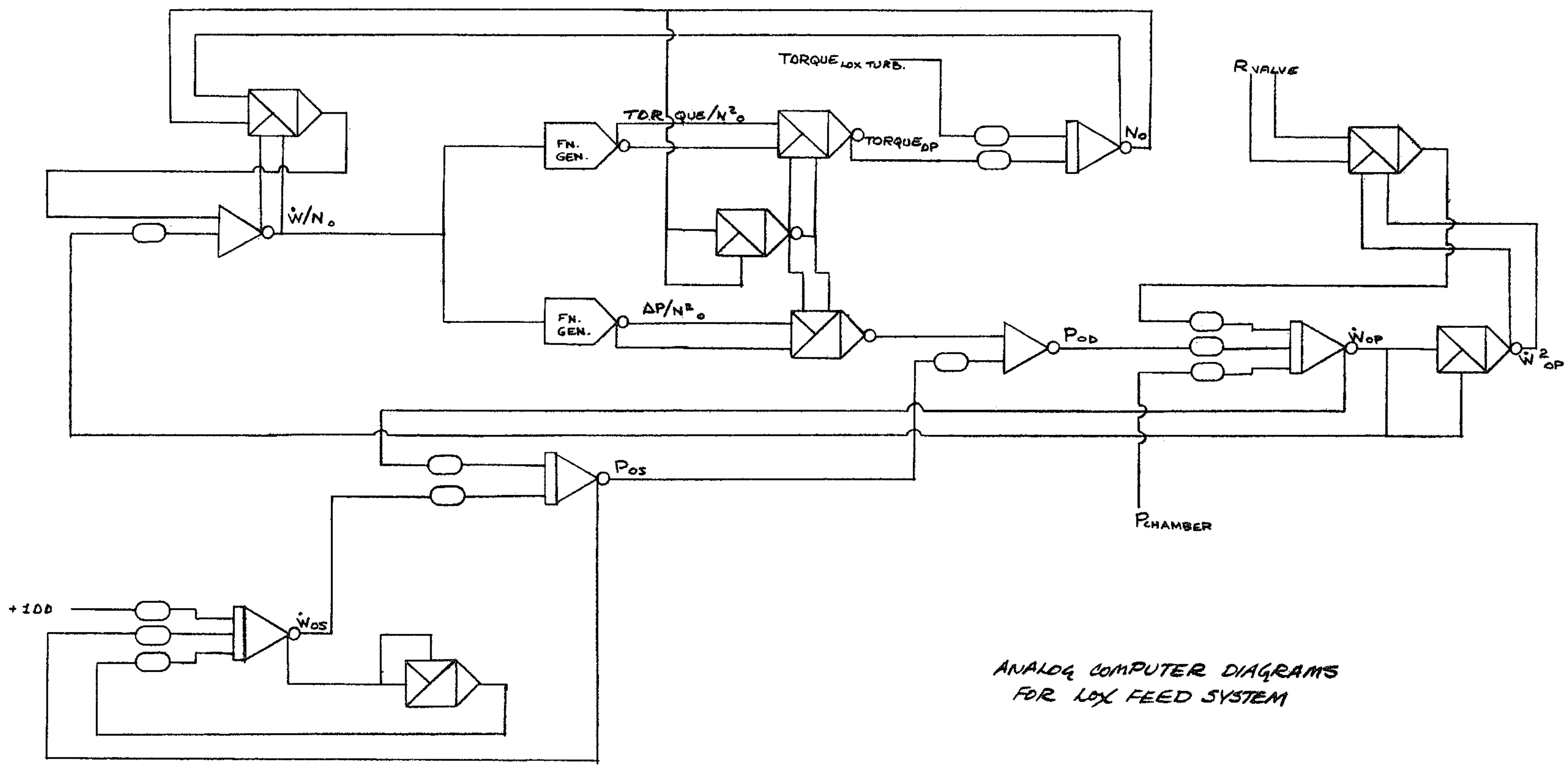

ANALOG COMPUTER DIAGRAMS FOR LOX FEED SYSTEM

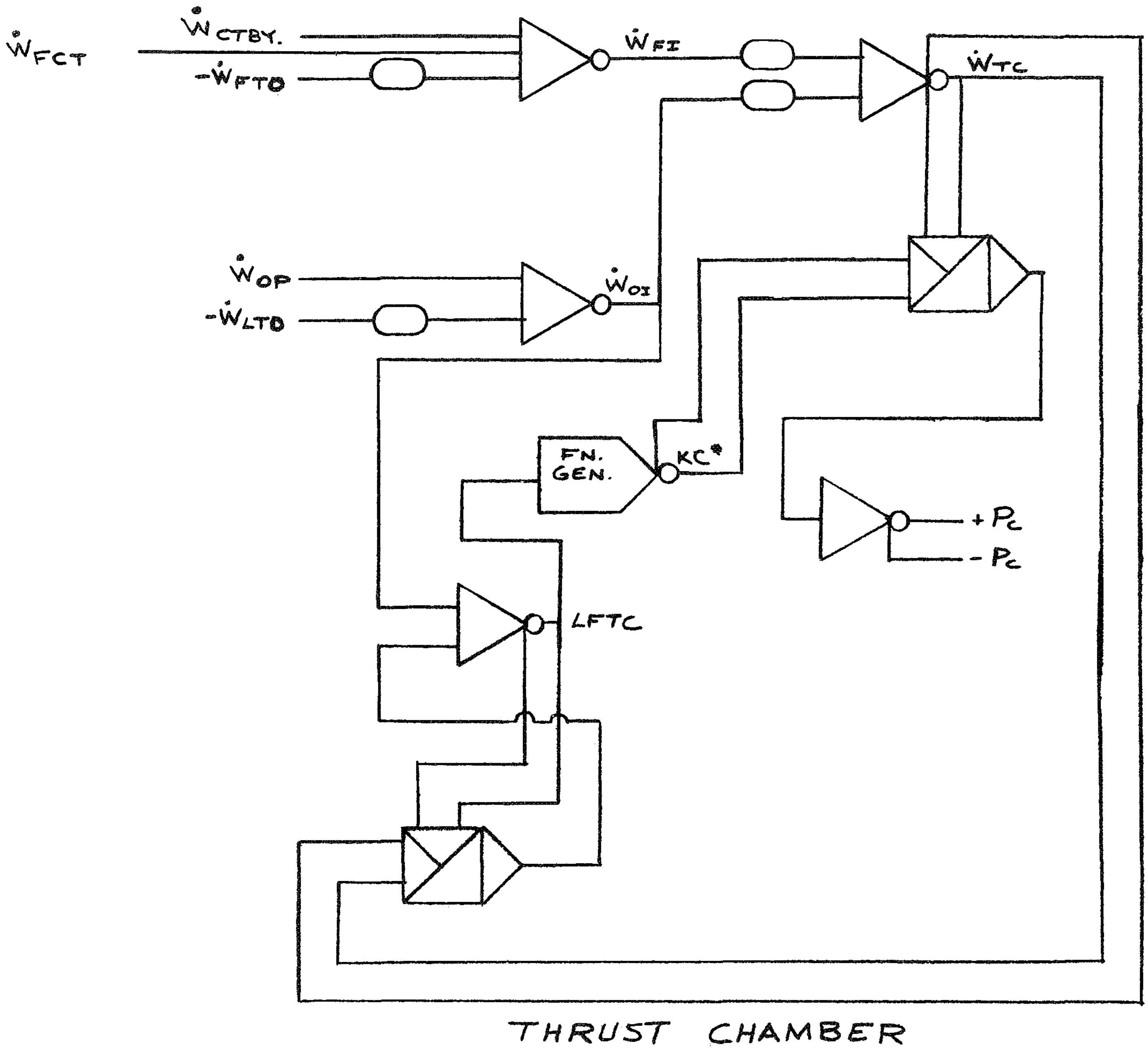

ANALOG COMPUTER DIAGRAM
FOR THRUST CHAMBER

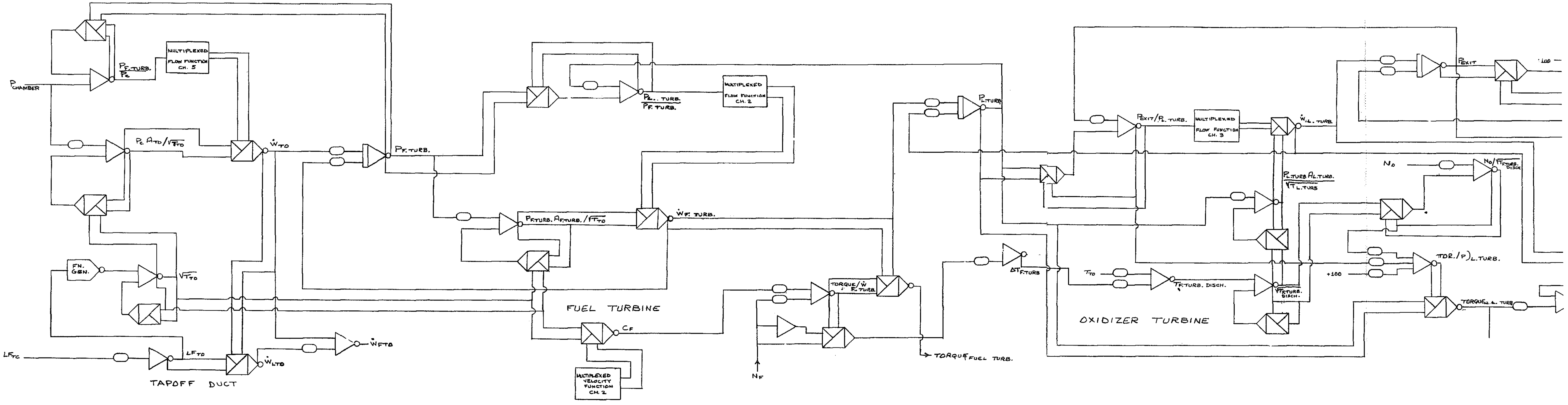

MULTIPLEXED FLOW FUNCTION CH. 5
MULTIPLEXED FLOW FUNCTION CH. 2
MULTIPLEXED FLOW FUNCTION CH. 3
MULTIPLEXED VELOCITY FUNCTION CH. 2
FN. GEN.
FUEL TURBINE
OXIDIZER TURBINE
TAPOFF DUCT
TORQUE FUEL TURB.

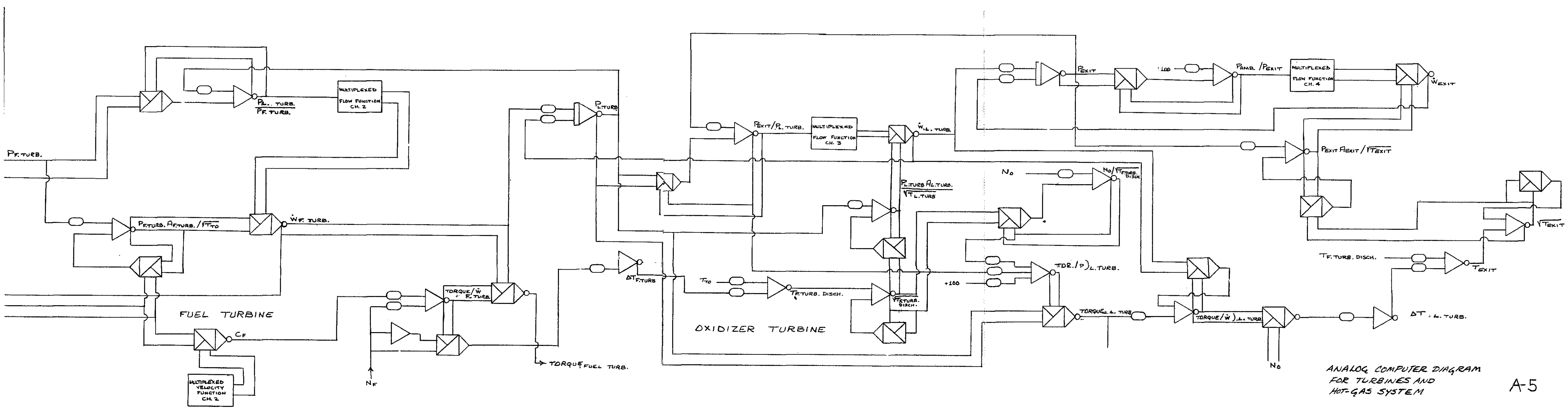

ANALOG COMPUTER DIAGRAM
FOR TURBINES AND
HOT-GAS SYSTEM

A-5

Distribution List for Report on Contract NAS3- 10280

		Copies
National Aeronautics and Space Administration Lewis Research Center 21000 Brookpark Road Cleveland, Ohio 44135		
Attention:	Contracting Officer, MS 500-313	1
	Large Engine Technology Branch, MS 500-203	15
	Technical Report Control Office, MS 5-5	1
	Technology Utilization Office, MS 3-16	1
	AFSC Liaison Office, MS 4-1	2
	Library	2
	H. W. Douglass, MS 500-203	1
	Fluid Systems Components Division, MS 5-3	1
National Aeronautics and Space Administration Washington, D. C. 20546		
Attention:	Code MT	1
	RPX	2
	RPL	2
	SV	1
Scientific and Technical Information Facility P. O. Box 33 College Park, Maryland 20740		
Attention:	NASA Representative Code CRT	6
National Aeronautics and Space Administration Ames Research Center Moffett Field, California 94035		
Attention:	Library	1
	C. A. Syvertson	1
National Aeronautics and Space Administration Flight Research Center P. O. Box 273 Edwards, California 93523		
Attention:	Library	1

	Copies
National Aeronautics and Space Administration Goddard Space Flight Center Greenbelt, Maryland 20771	
Attention: Library	1
National Aeronautics and Space Administration John F. Kennedy Space Center Cocoa Beach, Florida 32931	
Attention: Library	1
National Aeronautics and Space Administration Langley Research Center Langley Station Hampton, Virginia 23365	
Attention: Library	1
National Aeronautics and Space Administration Manned Spacecraft Center Houston, Texas 77001	
Attention: Library	1
National Aeronautics and Space Administration George C. Marshall Space Flight Center Huntsville, Alabama 35812	
Attention: Library	1
Keith Chandler, R-P & VE-PA	1
Loren Gross, R-P & VE-PAC	1
Jet Propulsion Laboratory 4800 Oak Grove Drive Pasadena, California 91103	
Attention: Library	1
Henry Burlage	1
Office of the Director of Defense Research & Engineering Washington, D. C. 20301	
Attention: Office of Assistant Director	1

Copies

Defense Documentation Center
Cameron Station
Alexandria, Virginia 22314 — 1

RTD(RTNP)
Bolling Air Force Base
Washington, D. C. 20332 — 1

Arnold Engineering Development Center
Air Force Systems Command
Tullahoma, Tennessee 37389

Attention: AEOIM — 1

Advanced Research Projects Agency
Washington, D. C. 20525

Attention: D. E. Mock — 1

Aeronautical Systems Division
Air Force Systems Command
Wright-Patterson Air Force Base,
Dayton, Ohio 45433

Attention: D. L. Schmidt,
Code ASRCNC-2 — 1

Air Force Missile Test Center
Patrick Air Force Base, Florida 32925

Attention: L. J. Ullian — 1

Air Force Systems Command (SCLT/Capt. S. W. Bowen)
Andrews Air Force Base
Washington, D. C. 20332 — 1

Air Force Rocket Propulsion Laboratory (RPR)
Edwards, California 93523 — 1

Air Force FTC (FTAT-2)
Edwards Air Force Base, California 93523 — 1

Air Force Office of Scientific Research
Washington, D. C. 20333

Attention: SREP, Dr. J. F. Masi — 1

	Copies
Office of Research Analyses (OAR) Holloman Air Force Base, New Mexico 88330	
Attention: RRRT	1
Major R. E. Brocken, Code MDGRT	1
Commanding Officer U. S. Army Research Office (Durham) Box CM, Duke Station Durham, North Carolina 27706	1
U. S. Army Missile Command Redstone Scientific Information Center Redstone Arsenal, Alabama 35808	
Attention: Chief, Document Section	1
Dr. W. Wharton	1
Bureau of Naval Weapons Department of the Navy Washington, D. C. 20360	
Attention: J. Kay, Code RTMS-41	1
Commander U. S. Naval Missile Center Point Mugu, California 93041	
Attention: Technical Library	1
Commander U. S. Naval Ordnance Test Station China Lake, California 93557	
Attention: Code 45	1
Code 753	1
Commanding Officer Office of Naval Research 1030 E. Green Street Pasadena, California 91101	1

	Copies
Director (Code 6180) U. S. Naval Research Laboratory Washington, D. C. 20390	
Attention: H. W. Carhart	1
Picatinny Arsenal Dover, New Jersey 07801	
Attention: I. Forsten, Chief Liquid Propulsion Laboratory	1
Air Force Aero Propulsion Laboratory Research & Technology Division Air Force Systems Command United States Air Force Wright-Patterson AFB, Ohio 45433	
Attention: APRP (C. M. Donaldson)	1
Aerojet-General Corporation P. O. Box 296 Azusa, California 91703	
Attention: Librarian	1
Aerojet-General Corporation P. O. Box 1947 Sacramento, California 95809	
Attention: Technical Library 2484-2015A	1
Aeronutronic Division of Philco Corporation Ford Road Newport Beach, California 92600	
Attention: Dr. L. H. Linder, Manager	1
Technical Information Department	1

Copies

Aerospace Corporation
P. O. Box 95085
Los Angeles, California 90045

Attention: Library-Documents 1

Arthur D. Little, Inc.
Acorn Park
Cambridge, Massachusetts 02140

Attention: A. C. Tobey 1

ARO, Incorporated
Arnold Engineering Development Center
Arnold AF Station, Tennessee 37389

Attention: Dr. B. H. Goethert
Chief Scientist 1

Battelle Memorial Institute
505 King Avenue
Columbus, Ohio 43201

Attention: Report Library, Room 6A 1

Bell Aerosystems, Inc.
Box 1
Buffalo, New York 14205

Attention: Library 1

The Boeing Company
Aero Space Division
P. O. Box 3707
Seattle, Washington 98124

Attention: Ruth E. Peerenboom (1190) 1

Chemical Propulsion Information Agency
Applied Physics Laboratory
8621 Georgia Avenue
Silver Spring, Maryland 20910 1

Copies

Chrysler Corporation
Space Division
New Orleans, Louisiana 70150

Attention: Librarian 1

Curtiss-Wright Corporation
Wright Aeronautical Division
Woodridge, New Jersey 07075

Attention: G. Kelley 1

University of Denver
Denver Research Institute
P. O. Box 10127
Denver, Colorado 80210

Attention: Security Office 1

Douglas Aircraft Company, Inc.
Santa Monica Division
3000 Ocean Park Blvd.
Santa Monica, California 90405

Attention: Library 1

Fairchild Stratos Corporation
Aircraft Missiles Division
Hagerstown, Maryland 20740

Attention: J. S. Kerr 1

General Dynamics/Astronautics
P. O. Box 1128
San Diego, California 92112

Attention: Library & Information Services (128-00) 1

Convair Division
General Dynamics Corporation
P. O. Box 1128
San Diego, California 92112

Attention: Mr. W. Fenning
Centaur Resident Project Office 1

Copies

General Electric Company
Flight Propulsion Lab. Department
Cincinnati, Ohio 45215

Attention: D. Suichu 1

Grumman Aircraft Engineering Corporation
Bethpage, Long Island
New York 11714

Attention: Joseph Gavin 1

IIT Research Institute
Technology Center
Chicago, Illinois 60616

Attention: Library 1

Kidde Aero Space Division
Walter Kidde & Company, Inc.
675 Main Street
Belleville, New Jersey 07109

Attention: R. J. Hanville,
Director of Research Engineering 1

Lockheed Missiles & Space Company
P. O. Box 504
Sunnyvale, California 94088

Attention: Technical Information Center 1

Lockheed Propulsion Company
P. O. Box 111
Redlands, California 92374

Attention: Miss Belle Berlad, Librarian 1

Lockheed Missiles & Space Company
Propulsion Engineering Division (D. 55-11)
1111 Lockheed Way
Sunnyvale, California 94087 1

	Copies
Marquardt Corporation 16555 Saticoy Street Box 2013 South Annex Van Nuys, California 91404	
Attention: Librarian	1
Purdue University Lafayette, Indiana 47907	
Attention: Technical Librarian	1
Rocketdyne, A Division of North American Rockwell Corporation 6633 Canoga Avenue Canoga Park, California 91304	
Attention: Library, Department 596-306	1
Stanford Research Institute 333 Ravenswood Avenue Menlo Park, California 94025	
Attention: Thor Smith	1
TRW Systems, Incorporated One Space Park Redondo Beach, California 90200	
Attention: G. W. Elverum	1
STL Tech. Lib. Doc. Acquisitions	1
TRW, Incorporated TAPCO Division 23555 Euclid Avenue Cleveland, Ohio 44117	
Attention: P. T. Angell	
United Aircraft Corporation Corporation Library 400 Main Street East Hartford, Connecticut 06118	
Attention: Library	1
Frank Owen	1
W. E. Taylor	1

Copies

United Aircraft Corporation
Pratt and Whitney Division
Florida Research and Development Center
P. O. Box 2691
West Palm Beach, Florida 33402

Attention: Library 1

California Institute of Technology
Pasadena, California 91109

Attention: Dr. A. Acosta 1
Prof. M. S. Plesset 1

The Pennsylvania State University
Ordnance Research Laboratory
P. O. Box 30
State College, Pennsylvania 16801

Attention: Prof. G. F. Wislicenus 1
Dr. J. W. Holl 1

Hydronautics, Incorporated
Pendell School Road
Howard County
Laurel, Maryland 20810

Attention: Dr. Philip Eisenberg 1

Pesco Products
24700 N. Miles Road
Bedford, Ohio 44014

Attention: Mr. J. F. DiStefano 1

TRW Systems, Incorporated
Bldg. 01, Room 1070F
One Space Park
Redondo Beach, California 90278 1